COLLEGE OF SCIENCE AND TECHNOLOGY
SCHOOL OF ENGINEERING
DEPARTMENT OF CIVIL, ENVIRONMENTAL AND GEOMATIC ENGINEERING
P.O. Box: 3900 Kigali, Rwanda.

ADSORPTION OF METHYLENE BLUE FROM AQUEOUS SOLUTION USING SAGO SEED ACTIVATED CARBON

A MASTER DISSERTATION

Submitted to the department of civil, environmental and geomatic engineering, school of engineering, college of science and technology, university of Rwanda in partial fulfillment of the requirements for the degree of

MASTER OF SCIENCE IN WATER RESOURCES AND ENVIRONMENTAL MANAGEMENT

Submitted by

SAID IBRAHIMA (REG.N: 221031987)

Under the Guidance of

Zubeda UKUNDIMANA (PH. D)

August 2024

BONAFIDE CERTIFICATE

This is to certify that the master's thesis entitled **"Adsorption of methylene blue from aqueous solution using Sago Seed Activated carbon"** *is a record of original bonafide work done by Said Ibrahima (Reg.No. 221031987) in partial fulfillment of the requirement for the award of master's of science in Water resources and environmental management of University of Rwanda, College of Science and Technology during the Academic Year 2023-2024.*

Doctor Zubeda UKUNDIMANA (Main supervisor,UR- CST)

Submitted for the final year project examination evaluation held at college of science and technology, on..... August 2024

CERTIFICATION

This research thesis has been submitted for examination with my approval as university supervisor.

Approved by

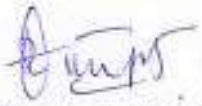

Dr. Zubeda UKUNDIMANA

Senior Lecturer

UR- CST

Nyarugenge Campus

DECLARATION

I **SAID IBRAHIMA** declare that this dissertation entitled: '**Adsorption of methylene blue from aqueous solution using Sago Seed Activated carbon**' is the result of my own work and has not been submitted for any other degree at the University of Rwanda or any other institution.

SAID IBRAHIMA _____ 29/08/2024

Signature date

Abstract

Untreated industrial wastewater discharged into the environment has a detrimental impact on human health and the ecosystem. Textile manufacturing is one industry that produces a substantial amount of wastewater. The effluent from this sector contains a variety of toxins that must be treated before being released into the environment. Methylene blue, a major compound commonly used in textile manufacturing, is present in high concentrations in textile factory effluent and poses a significant hazard as it is highly toxic and carcinogenic. Wastewater treatment is also costly for the industry. This study aims to remove methylene blue from synthetic wastewater using activated carbon derived from the low-cost plant Cycas thouarsii (Sago) seeds through batch mode investigations. The adsorbent was activated using chemical and thermal procedures and characterized using FTIR and XRF analysis. The adsorption isotherm and kinetics were also examined. The experimental design encompassed five factors with six levels each: pH (2, 4, 6, 8, 10, and 12), initial MB concentration (40, 65, 90, 115, 140, and 165 mg/L), adsorbent dosage (0.01, 0.05, 0.1, 0.15, 0.20, and 0.25 mg/100 mL), contact time (30, 40, 50, 60, 70, and 80 min), and agitation speed (25, 50, 75, and 120 rpm). For optimization purposes, synthetic wastewater was created in the laboratory, and the optimal parameters for complete dye removal were determined to be starting concentration: 115 ppm, contact time: 50 min, adsorbent dose: 0.2 g/L, pH: 8, and agitation speed: 75 rpm. Among the three adsorption isotherm models, the Langmuir isotherm model exhibited the best fit with an experimental value of $R^2 = 0.99$, indicating a homogeneous and monolayer adsorption process. The kinetics study also demonstrated a good fit with the pseudo-second-order model at $R^2 = 0.99$, suggesting that the adsorption mechanism involves chemisorption, with the rate-limiting step potentially being the sharing or exchange of electrons between the adsorbate and adsorbent. Overall, this adsorption technique shows great promise for industrial-scale application.

Keywords: Activated carbon, Methylene blue, Sago seed, Adsorption

Tables Contents

Abbreviations

SSAC: Sago seed activated carbon

SSRW: Sago seed raw material

IUCN: International Union for Conservation of Nature

IUPAC: International Union of Pure and Applied Chemistry

MB: Methylene blue

SSRW: Sago seed raw material

PAC: Powdered activated carbon

GAC: Granular activated carbon

EAC: Extruded activated carbon

VOC: Volatile organic compound

Lists of figures

Lists of Tables

Acknowledgements

I am very grateful to express my sincere thanks to my supervisor Zubeda UKUNDIMANA (PhD) for her intellectual inspiration, invaluable help, constant suggestions and comments which proved to be helpful in ensuring the successful completion of this paper; may you receive my special gratitude for your academic guidance and endless support. Secondly, I express my gratitude to my parents for their support through my journey. Furthermore, special thanks to Mr. Valence and chemistry department laboratory technicians for the cooperation during laboratory work and material support as well.

DEDICATION

To the Almighty God,

To my brothers and sister,

To my relatives and friends

CHAPITER1: INTRODUCTION

Due to the global population growth and the advancement of industrial practices, environmental pollution has become a critical concern, with a particular emphasis on the issue of wastewater pollution [1]. Among various pollutants, wastewater from industrial activities poses significant challenges, especially in terms of contamination and toxicity [2]. Industries such as textiles, paper production, cosmetics, food processing, and leather manufacturing discharge vast quantities of wastewater into natural water bodies [3]. The textile industry plays a critical role in water pollution, primarily attributable to its substantial water consumption and utilization of diverse dyes and chemicals throughout the manufacturing process. The resultant wastewater derived from this industry frequently contains suspended solids, toxic compounds, and dyes. The presence of these contaminants poses a significant concern, as they exhibit persistence in the environment and possess the capacity to inflict harm upon aquatic organisms and human well-being [4]. Wastewater poses a global challenge, affecting regions worldwide, including Europe, Asia, Africa, and specific countries like Rwanda. In Europe, industrial activities, urbanization, and agriculture contribute to critical wastewater management issues, necessitating stringent regulations such as the urban wastewater treatment directive to safeguard aquatic ecosystems and public health [5]. In Asia, rapid industrialization and population growth exacerbate challenges, with inadequate infrastructure and poor treatment practices leading to water pollution, especially from textile and pharmaceutical contamination in countries like China and India [6]. Similarly, in Africa, urbanization outpacing infrastructure development results in untreated sewage and industrial effluents discharge, leading to waterborne diseases and environmental degradation. Common treatment methods in countries like Egypt, Ethiopia, and Malawi include lagoons and drying beds [7]. Pit latrines and septic tanks are commonly used decentralized sanitation solutions that primarily aim to decrease the amount of silt, rather than eliminating dangerous chemicals and microorganisms. Therefore, (Ravina et al., 2021) suggest that centralized wastewater treatment plants need to be designed for future expansion to accommodate higher flow rates [7]. Malfunctions in sewer systems, breakdowns, blockages, and improper design contribute to challenges in wastewater management. Rwanda faces similar challenges, A survey of industries in Rwanda revealed that more than 30% of industries did not treat their wastewater due to capacity limitations or lack of treatment requirements [8]. The absence of treatment leads to increased levels of organic matter, as indicated by higher concentrations of biochemical oxygen demand (BOD) and chemical oxygen demand (COD). These levels exceed effluent standards and give rise to

concerns regarding pollution. In 2007, the British Medical Journal stated that the provision of clean water and wastewater disposal is widely recognized as one of the most significant contributions to public health in the last 150 years [9]. This statement underscores the longstanding objective of wastewater treatment, which is to eliminate pollutants and pathogens, therefore guaranteeing the safeguarding of human health and the preservation of the environment. This task is a crucial component of Sustainable Development Goal number 6 [10], and still is a pillar of wastewater treatment. However, other challenges and opportunities are now rising. Emerging contaminants is a broad definition for many substances. They are called "emerging" because the level of risk they pose is not yet ascertained [11]. Dyes are frequently employed in diverse industries for the purpose of imbuing materials with coloration. These dyes can be categorized into distinct groups, namely non-ionic, cationic (basic), and anionic (reactive, acid, direct) dyes [12]. Among the multitude of dyes available, methylene blue (MB) stands out as a frequently employed cationic dye with applications in paper coloring, textile dyeing (specifically cotton, wool, and silk), and paper stock coating [13]. Nevertheless, it is imperative to acknowledge the substantial health hazards associated with MB. Notably, the dye has the potential to inflict severe eye burns, leading to permanent harm in both humans and aquatic organisms. Moreover, exposure to MB may give rise to an array of symptoms, encompassing an accelerated heart rate, vomiting, diarrhea, nausea, shock, and mental disorientation [14]. Given the high toxicity levels of cationic dyes like MB, their removal from industrial effluents is a major environmental concern [15]. Physical techniques are frequently employed for the treatment of industrial wastewater and the elimination of methylene blue dye [16]. These approaches encompass a range of filtration procedures, including membrane filtration [17], nanofiltration [18], ultrafiltration [19], microfiltration [20], and reverse osmosis [21]. These methods entail the passage of wastewater across a discerning membrane that segregates the dye particles from the liquid [14]. Although these procedures are highly efficient in eliminating methylene blue, they do have certain limits. These factors include high operational and maintenance expenses, the possibility of membrane fouling, and the requirement for periodic membrane replacement or cleaning. In addition, the disposal of the concentrated dye waste that is retained by the membranes can present environmental challenges [22]. Coagulation-flocculation is a frequently employed chemical technique in which coagulants such as iron or aluminum salts are introduced into the wastewater. These coagulants facilitate the formation of bigger dye clumps known as flocs, which may be readily removed from the water [23]. Although coagulation-flocculation is successful in lowering dye concentration, it has certain disadvantages. These activities involve producing a substantial

quantity of sludge that necessitates additional processing and disposal. Additionally, it has the potential to elevate the sodium concentration in the processed water, which could provide challenges for companies that aim to recycle water. Adsorption is a proven physical technique for eliminating methylene blue. It is preferred due to its affordability, simplicity in design and operation, wide range of available adsorbent materials, and capacity to withstand exposure to dangerous chemicals. This approach is highly efficient in eliminating diverse chemical compounds from water. Activated carbon is a highly popular adsorbent because of its extensive surface area and porous structure, which enable effective adsorption of pollutants such as methylene blue. Utilizing alternative source materials, such as agricultural wastes like rice husk [24], cashew nut shells [25], and pomegranate peel biochar [26], can be employed to make activated carbon. These alternate sources not only save manufacturing expenses but also aid in waste management. Extensive study has been conducted on the efficacy of activated carbon in adsorbing methylene blue, establishing it as a feasible choice for the treatment of industrial wastewater. Nevertheless, there are downsides associated with the utilization of activated carbon. Commercial activated carbon can be expensive, and regenerating or disposing of it after it becomes saturated with contaminants can be challenging. The regeneration process itself can be expensive and energy-intensive, and improper disposal can lead to environmental issues [27]. Additionally, some adsorption processes require electricity, which may not be readily available in developing regions, limiting the applicability of the technology in those areas. To address these challenges, researchers are continually exploring new materials and methods to improve the efficiency and affordability of adsorption processes [28]. For example, zeolites and kaolin have been extensively investigated as low-cost and effective adsorbents for dye removal. Zeolites possess microporous and crystalline structures, a large surface area, and ion exchange capabilities, making them suitable for capturing dye molecules from water [29]. Similarly, kaolin, a naturally abundant clay, has shown promise in adsorbing basic dyes like methylene blue due to its wide micropores and ion exchange properties [30]. Using activated carbon to adsorb methylene blue from water represents a promising approach to reducing water pollution caused by industrial effluents. Although challenges related to cost and regeneration exist, ongoing research into alternative adsorbent materials such as sago seed aims to overcome these limitations. The pursuit of more efficient, cost-effective, and environmentally friendly solutions is crucial to protecting natural water resources and ensuring a sustainable future.

CHAPTER2: Research problem

The textile industry is widely recognized as one of the most environmentally damaging sectors [31]. In order to convert animal skin into leather, nearly every textile factory relies heavily on the use of various chemicals [32]. Among these chemicals, methylene blue stands out as one of the most commonly employed textile dyes [14]. Conventional methods for treating such wastewater require significant investments in terms of finances, time, and human resources. Given their focus on profitability, industries often hesitate to allocate resources to waste treatment, resulting in the immediate release of untreated effluent into the environment. This practice is particularly prevalent in developing countries like Rwanda [33], where rapid industrial and urban growth has led to the release of liquid waste with high concentrations of toxic elements from both new and old factories into water bodies without proper treatment. Consequently, these practices are among the primary causes of soil and water contamination, thereby posing significant public health concerns [31]. Hence, the development of a low-cost wastewater treatment approach that utilizes locally available materials and exhibits high pollutant removal efficiency is crucial. One such method is adsorption. The expansion of textile factories in developing countries like Rwanda, coupled with the discharge of untreated or partially treated textile wastewater into water bodies, poses substantial health risks for downstream users and causes ecological deterioration in these aquatic systems [33]. Many individuals residing near rivers where textile industries are situated heavily rely on lake and river water for various purposes, including drinking, fishing, livestock watering, irrigation, and recreational activities. Nonetheless, the complex composition of textile industry wastewater makes it challenging to implement adequate treatment measures to meet the discharge limits established by the Rwanda Environment Management Authority (REMA). Effluents from existing treatment systems often contain residual contaminants that surpass Rwanda standard board permissible discharge limits [34]. Consequently, the Rwandan government has established discharge limit standards that necessitate the treatment of wastewater by industries [35]. Furthermore, industry owners are obligated to construct treatment systems capable of meeting the prescribed limits for pollutant removal. This situation calls for the development of efficient and integrated treatment methods. Notably, in Kigali City, there is currently a lack of a centralized sewage treatment plant and sewer system. The existing semi-centralized sewers are primarily owned by hospitals, hotels, government institutions, real estate developers, and large commercial buildings [36].

2.1 Research objective

2.1.1 General Objective

To investigate the efficiency of the activated carbon, derived from Cycas thouarsii (Sago) seed powder, as adsorbent for the removal of methylene blue (MB) from synthesized wastewater.

2.1.2 Specific Objectives

The specific objectives of the study include:

1. Preparation of synthetic wastewater and adsorbent
2. To analyze the structural properties and chemical composition of the adsorbent using Fourier transform infrared spectrometry (FTIR) and X- ray fluorescence (XRF)
3. To determine the effects of different parameters such as pH, contact time, agitation speed, adsorbent dosage, and initial dye concentration on the adsorption process.
4. To study the adsorption isotherms and kinetics, specifically fitting the experimental data to Freundlich, Langmuir, Temkin isotherm models, as well as pseudo-first order, pseudo-second order and Elovich kinetic models

2.2 Research Questions

1) What are the characteristics of activated carbon prepared from Sago seed?
2) What is the effectiveness of Sago seed activated carbon in removing emerging contaminants, such as methylene blue from synthetized wastewater?
3) How do various factors, such as pH modification and specific adsorbent properties, impact the adsorption capacity and the removal efficiency of methylene blue from wastewater?
4) What are the advantages and limitations of using activated carbon adsorbent derived from Sago seed, in the context of removing methylene blue from wastewater?

2.3 Scope and limitation of the study

This study was based on laboratory experiment to remove methylene blue from synthetic wastewater using activated carbon prepared from Sago seed. The optimization of the treatment system was done using four independent variables; contact time, pH, adsorbent dose, and methylene blue concentration while the removal efficiency of adsorbent was dependent variable. This study focuses on the process of producing and evaluating an adsorbent material derived from Sago seeds. Additionally, it involves the creation of synthetic wastewater in a controlled laboratory setting. The study was centered on the elimination of methylene blue from synthetic wastewater. Ultimately, the synthetic wastewater was thoroughly analyzed to determine its properties, and the effectiveness of the adsorbent in removing contaminants was assessed based on the highest recorded removal rates of various factors.

2.4 Signification of the study

This work can provide a significant benefit for developing countries with few resources and limited access to advanced technologies in the removal of dyes from industrial effluent. They are concerned about using inexpensive locally sourced materials to effectively remove methylene blue from wastewater and ensure that the wastewater meets the required standards for release into the environment. Specifically, in tropical and sub - tropical regions where Sago seeds are plentiful, they provide valuable data that can be used as input for future research to develop technology for removing methylene blue from wastewater. Developing nations seeing rapid economic expansion and the establishment of industrial areas. These industries produce a substantial volume of wastewater. This research provides a solution for utilizing locally accessible activated carbon derived from Sago seeds to effectively remove total methylene blue from wastewater.

CHAPTER3: LITERATURE REVIEW

3.1 Wastewater treatment overview

(Mittal, 2010) defined wastewater treatment as an extensive procedure that aims to remove pollutants from wastewater and convert it into a treated effluent that has minimal adverse effects on the environment when reintroduced into the water cycle or can be directly reused [37]. This treatment course occurs within a wastewater treatment plant (WWTP), also known as a Water Resource Recovery Facility (WRRF) or a Sewage Treatment Plant (STP).

The effluent treatment process starts with the so-called “pre-treatments”. Screens are intended to remove coarse solids (wood, rags, cans, bottles) [38]. Sieves retain smaller size solids (ear tips, toilet paper, wet wipes, etc.). Screenings and residues of sieving can be handled as urban wastes, but some can be used to extract cellulosic materials. Degritting and de-oiling units remove sandy sediments and floating greasy matter, but not settleable organics. Settleable sediments are removed in primary settling tanks, and are collected as primary sludge [39]. But the core of the wastewater treatment plant is the biological section, where bacterial biomass grows and perform several tasks, such as:

- oxidize biodegradable organics
- oxidize ammonium to nitrates
- reduce nitrates to gaseous nitrogen
- biologically concentrate phosphorus in their cells

Biological systems can be based on: suspended-growth colonies (called flocs) that are dispersed as a suspension in the wastewater. The mixture is called “mixed liquor” and the process is called “activated sludge” [40]. Attached-growth, where bacteria grow in the form of a biological film attached to inert supports, generally made of plastic material. They can be retained in fixed-bed reactors but they can also be freely moving in the wastewater. In this case the biological tank is called “moving bed biofilm reactor” [41]. In hybrid systems suspended-growth and attached-growth are in the same tank (for example in the IFAS process: integrated fixed-film and activated sludge) [42]. Whatever the type of process, bacteria need oxygen to perform most of their bio-reactions [43]. To provide oxygen, aeration systems are essential. Separation of bacterial colonies from treated wastewater takes place in secondary settling tanks. Since a couple of decades ago, micro and ultrafiltration membranes have been installed in many plants. The combination of activated sludge process and membranes is called Membrane

Bioreactor (MBR) [44]. This combination provides a far more efficient solid/liquid separation. If solid/liquid separation is performed through settling tanks, filtration and disinfection are often required to meet stringent quality standards. In both cases sludge is recycled back to the biological reactor, while a fraction is discharged as "excess biological sludge". But all this may not be enough. Surfactants and trace contaminants such as metabolites of pharmaceuticals or other contaminants of emerging concern may be removed by adding advanced chemical oxidation processes and/or adsorption on activated carbon [45]. The purified effluent can be further refined in constructed wetlands for Phyto depuration. After that, the sludge must properly be treated, the by-product extracted from primary and biological treatments. Sludge is a slurry, with a flow rate two orders of magnitude lower than the incoming wastewater. Nevertheless, it has a water content of 97 to 99% and is rich in biodegradable and unbiodegradable organic compounds.

Sludge treatments have two aims:

- First, reducing the amount of biodegradable compounds; this process is called "biological stabilization". This step is essential to reduce the risk of unwanted fermentation and putrefaction processes, which produce bad smelling compounds and favor the development of microbiological contamination. Anaerobic digestion is an effective process that also produces biogas from which we can recover energy.
- Second, reducing the water content, which means reducing its volumetric flowrate. Thickening and dewatering are the treatments that aim at reducing the water content. Belt-presses, centrifuges and filter-presses are the most widely used technologies.

Once sludge is stabilized and dewatered it can be used in agriculture, often after a further treatment, called "hygienization", that will ensure the compliance with microbiological standards.

3.2 Adsorption in Wastewater Treatment

3.2.1 Adsorption

Adsorption is a crucial procedure used in many different industries, most notably in the treatment of wastewater. It is the process of removing molecules, ions, or particles from a gas or liquid phase by accumulating them on the surface of a solid substance called an adsorbent; the substance that has been adsorbed is referred to as the adsorbate [46]. In wastewater treatment, this process is instrumental in purging pollutants from water, employing a variety of adsorbents like activated clays, activated carbons, and molecular sieves, chosen based on their

surface area, typically ranging from 100 to 1200 square meters per gram. An adsorbent's effectiveness is determined by its adsorption capacity, which is expressed in milligrams of pollutants removed per gram of adsorbent; a larger capacity denotes better pollutant removal [47]. Constant research endeavors are directed towards innovating new adsorbent types such as metal organic frameworks and carbon nanotubes to bolster adsorption capabilities for water treatment and gas separation (fig 3.1) [48].

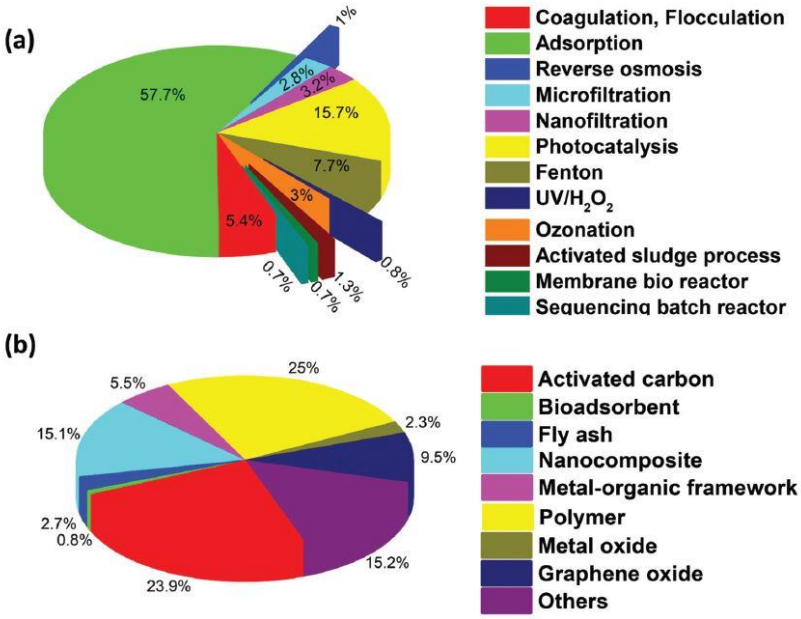

Figure 3.1: Pie-chart illustrating the proportion of accessible literature on dye removal methods for: (a) diverse physicochemical and biological approaches; and (b) adsorption methods employing distinct adsorbents [49].

The meticulous selection of adsorbents, considering factors like pore diameter and structure, is vital for optimizing adsorption processes, with adsorbents classified into oxygen-containing, carbon-based, and polymeric-based compounds, each influencing adsorption performance differently.

3.2.1.1 Adsorbents

Adsorbents are materials used in adsorption processes to attract and retain molecules, ions, or particles from a gas or liquid phase onto their surface [50]. Adsorbents are essential for eliminating impurities and toxins from water sources while treating wastewater. The industry uses a variety of adsorbent kinds, each with special qualities and uses:

- **Activated Carbon-Based Adsorbents**: One of the most widely utilized and widely available adsorbents for treating water and wastewater is activated carbon. It is renowned for being highly successful at removing a variety of contaminants from water sources due to its strong adsorption capability.
- **Non-Conventional Low-Expense Adsorbents**: As substitutes for conventional materials based on activated carbon, these adsorbents are being developed. They can be derived from waste materials from agriculture and industry, natural materials like clays, zeolites, and silica, or bio adsorbents such as biomass and biopolymers. These low-cost adsorbents offer sustainable and cost-effective solutions for water treatment applications.
- **Nanomaterial Adsorbents**: Nanomaterials, including nanocomposite adsorbents, are being developed for various adsorption applications. These materials exhibit unique properties at the nanoscale, making them promising candidates for efficient pollutant removal in water treatment processes.
- **Miscellaneous Adsorbents**: In addition to the categories mentioned above, there are numerous more kinds of adsorbents with unique qualities and uses that are employed in the treatment of water. Activated clays, fuller earth, bauxite or alumina, bone char, molecular sieves, synthetic polymeric adsorbents, and silica gel are a few examples of these adsorbents.

Choosing the right adsorbent is essential to creating efficient adsorption procedures for treating wastewater. Adsorbent efficacy in eliminating contaminants from water sources is influenced by various factors, including compatibility with the targeted pollutants, surface area, pore structure, and adsorption capacity. In order to meet the changing challenges in the treatment of water and wastewater, researchers are still investigating and creating new kinds of adsorbents with improved adsorption capacities.

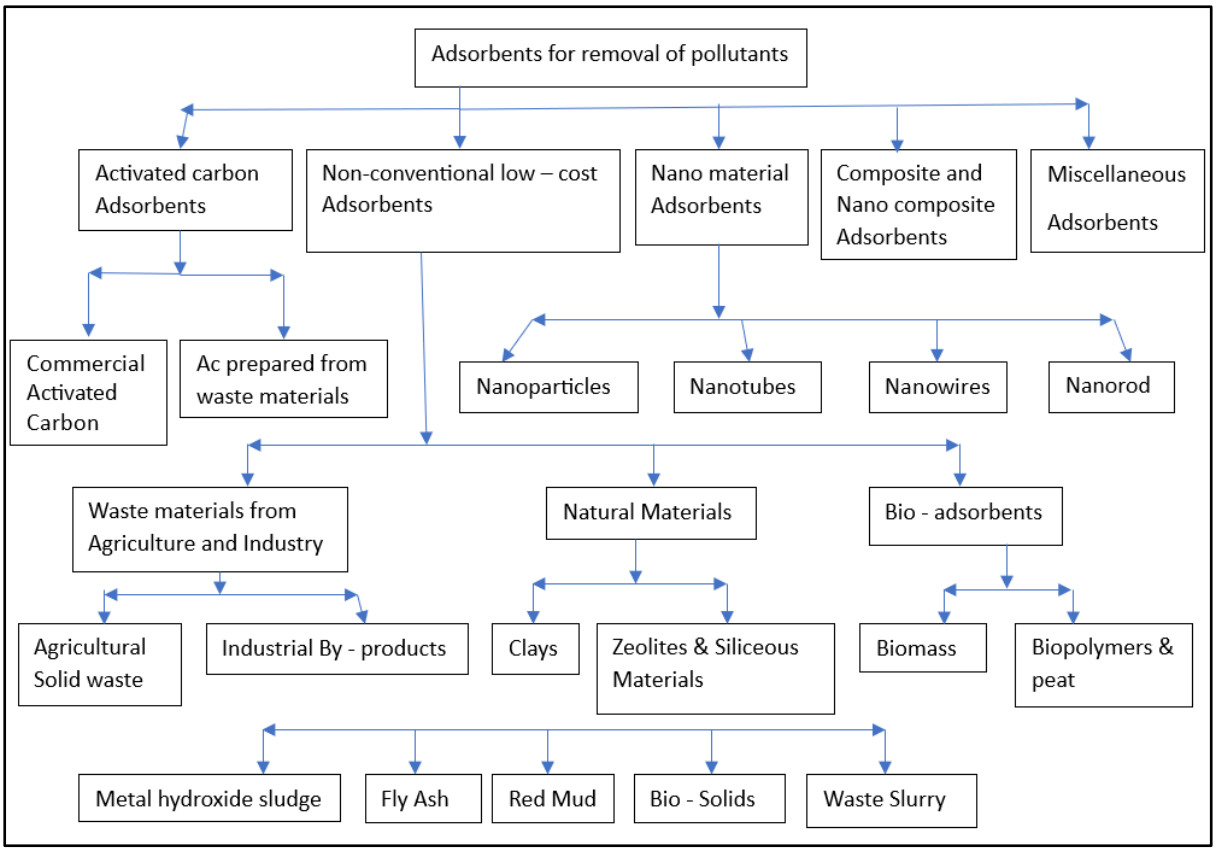

Figure 3.2: Different adsorbents for pollutants removal [51]

3.2.1.2 Comparison of carbon-based, polymer and zeolite adsorbents

Carbon-based, polymer and zeolite adsorbents are commonly used in various industries, including wastewater treatment, due to their unique properties and applications. Here is a comparison of these three types of adsorbents based on their characteristics and suitability for different adsorption processes [46]:

Table 3.1: Activated carbon, zeolite, and polymer adsorbents comparison

Adsorbent	**Characteristics**	**Advantages**	**Disadvantages**
Activated Carbon	• Wide range of pore sizes (2 to 500 angstrom). • High surface area, typically ranging from 100 to 1200 square meters per gram. • Low cost and suitable for removing a variety of pollutants, including volatile organic compounds (VOCs).	• Effective in adsorbing a broad spectrum of pollutants. • Versatile and extensively utilized in water and wastewater treatment applications.	• May have limitations in removing VOCs with high polarity. • Some variations in performance based on specific applications.

Zeolite	• Uniform crystallized structure with uniform pores. • Specific surface area higher than activated carbon. • Ability to design different pore sizes for specific applications.	• Excellent for separating molecules of different sizes due to uniform pore structure. • Suitable for various applications requiring specific pore sizes.	• High surface area and larger pore sizes suitable for diverse adsorption processes. • Can be tailored with specific functional groups for targeted pollutant removal.
Polymer Adsorbents	• Greater surface area and bigger pore diameters are found in crosslinked polymers as opposed to zeolite and activated carbon. • Pores in the range of mesopores, offering wider application possibilities.	• Limited initial cost compared to activated carbon. • May have constraints in certain applications due to pore size limitations.	• Higher initial cost compared to traditional adsorbents. • Regeneration temperature requirements may vary based on the polymer type.

Activated carbon is widely used for its versatility and cost-effectiveness, zeolites excel in applications requiring precise pore sizes, and polymer adsorbents offer tailored solutions with specific functional groups for targeted pollutant removal. The choice of the most appropriate adsorbent relies on the particular demands of the adsorption procedure and the contaminants targeted for elimination in applications related to wastewater treatment.

3.2.1.3 Characteristics and general requirements of Adsorbents

Adsorbents have a pivotal role in adsorption processes employed for the purpose of eliminating pollutants from water and wastewater. Therefore, it is imperative to carefully evaluate the characteristics and overall requirements of adsorbents when selecting the optimal material for efficient pollutant removal [52]. The following are some key characteristics and general requirements of adsorbents:

a) Surface Area:

Having a high surface area is crucial for adsorbents as it directly influences the adsorption capacity. Commercial adsorbents typically have surface areas ranging from 100 to 1200 square meters per gram. Larger surface area allows for more adsorption sites, leading to increased pollutant removal efficiency [53].

b) Pore Structure and Distribution:

Pore size and structure of adsorbents play a crucial role in the transportation of pollutants as well as the diffusion limitations associated with them. By tailoring the pore size, adsorbents can be specifically designed for particular applications, thereby facilitating the effective separation of molecules based on their size. Zeolites, with their uniform pore structure, exhibit remarkable capabilities for precisely separating molecules with varying sizes. Furthermore, the pore size and distribution significantly influence the adsorption kinetics and selectivity of the adsorbent [54].

c) Selectivity:

Selectivity refers to the ability of an adsorbent to preferentially adsorb certain pollutants over others. Adsorbents with high selectivity can target specific contaminants in water for efficient removal [55].

d) Kinetics:

Adsorption kinetics determine the rate at which pollutants are adsorbed onto the adsorbent surface. Faster kinetics indicate rapid pollutant removal, which is desirable for efficient water treatment processes [56].

e) Adsorption Capacity:

The adsorption capacity of an adsorbent refers to the amount of pollutant it can adsorb per unit mass. Higher adsorption capacity indicates better performance in pollutant removal and is a key factor in selecting an adsorbent [47].

f) Regeneration:

The ability to regenerate and reuse adsorbents is important for cost-effectiveness and sustainability in adsorption processes. Regeneration temperature requirements may vary based on the type of adsorbent, such as polymer adsorbents [57].

g) Chemical Stability:

Adsorbents should exhibit chemical stability to withstand the conditions of the adsorption process, especially in the presence of acidic or basic pollutants. Chemical stability ensures the longevity and effectiveness of the adsorbent in pollutant removal applications [58].

h) Abrasion Resistance:

Adsorbents should have high abrasion resistance, particularly in applications where the water may contain abrasive particles or high acidity. Abrasion resistance ensures the durability and longevity of the adsorbent in water treatment processes [59].

i) Cost:

The cost of the adsorbent, including initial investment and regeneration costs, is a significant factor in selecting an adsorbent for water treatment. Cost-effective adsorbents that offer efficient pollutant removal are preferred for large-scale water treatment applications [60].

j) Environmental Impact:

Consideration of the environmental impact of the adsorbent and its disposal after use is important for sustainable water treatment practices. Therefore, selecting an adsorbent that meets these requirements is essential for achieving efficient and sustainable pollutant removal [61].

3.2.1.4 Concepts of porosity: Open vs. Closed pores

In the context of adsorption, porosity refers to the presence of pores in an adsorbent material that allow for the movement of adsorbate molecules within them. There are different types of pores, including open and closed pores. Open pores are accessible to the adsorbate molecules, meaning they provide a pathway for the adsorbate to enter and interact with the adsorbent material. On the other hand, closed pores are not accessible to the adsorbate molecules as they are blocked at one end [62].

It is important to note that the presence of open pores is crucial for effective adsorption, as they allow for greater surface area and more interaction points for adsorption to occur. Closed pores, due to their limited accessibility, may not contribute significantly to the adsorption process. Therefore, highly porous adsorbents with open pores are desirable to maximize the adsorption capacity [63].

3.2.2 Adsorption steps/mechanism

Adsorption involves several steps or mechanisms for the movement of the adsorbate within the adsorbent and its subsequent adsorption. The following are the main adsorption steps [64]:

- Transport of adsorbate from the bulk solution to the exterior film surrounding the adsorbent particle. The adsorbent particle is always surrounded by a liquid film that moves along with it.
- Movement of adsorbate across the external film to the external surface site on the adsorbent particle. This step is known as film diffusion, and the adsorbate must traverse the film to reach the external surface of the adsorbent particle.
- Migration of adsorbate within the pores of the adsorbent, also known as intraparticle diffusion or pore diffusion. The adsorbate moves inside the pores of the adsorbent, allowing it to penetrate deeper into the adsorbent particle.
- Adsorption of the adsorbate at the internal surface site of the adsorbent particle. This step involves the adsorbate attaching or bonding to the internal surface of the adsorbent particle.

These steps collectively describe how the adsorbate moves from the bulk solution to the adsorbent particle and becomes adsorbed onto its surface. The efficiency and speed of the adsorption process can be improved by optimizing these steps. The mechanisms of adsorption can occur through physical adsorption via van der Waals forces or chemical adsorption through chemical bonding.

3.2.3 Factors controlling Adsorption

The factors that control adsorption can be classified into three categories:

- Adsorbent properties
- Adsorbate properties
- Solution properties

The adsorbent properties include the nature of the adsorbent, such as its surface area, pore size, and presence of functional groups. Surface area is a critical parameter, where highly porous adsorbents are preferred to allow for the movement of adsorbate molecules within the pores. The pore size also affects adsorption, where average pore size becomes an important property [65]. Additionally, the presence of functional groups on the adsorbent surface affects the adsorption process.

The adsorbate properties, including its polarity and acidity/basicity, also play a significant role in determining whether adsorption will occur. The nature of the adsorbate affects the affinity between the adsorbate and adsorbent. For example, in chemisorption, adsorption occurs

through chemical bonding, while in physical adsorption, it occurs through van der Waals forces of attraction.

The solution properties, such as acidity, basicity, and phase (gas phase-liquid phase), also influence adsorption. Changing the operating parameters like temperature can significantly impact adsorption. Higher or lower temperatures may result in more significant adsorption.

Other factors that affect the adsorption process may include contact time, concentration of the adsorbate, and pH of the solution [66] [67].

3.2.3.1 Nature of Adsorbent

The nature of the adsorbent in wastewater treatment plays a significant role in the adsorption process. Important properties of an effective adsorbent include surface area, pore size, and functional groups [68]. The specific surface area of an adsorbent can vary, with some commercial adsorbents having high surface areas like metal organic frameworks with up to 78000 square meters per gram, while simple charcoal may have a surface area of only 100 square meters per gram. Highly porous adsorbents are desirable to allow for the movement of adsorbate molecules within the pores. Different types of pores such as open pores that are accessible to the adsorbate and closed pores that are not. The nature of the adsorbent and its affinity for the adsorbate are crucial factors in determining the effectiveness of adsorption.

3.2.3.2 Shapes of pores

Different shapes of pores can be found in adsorbents. Some common types include cylindrical pores, slit-shaped pores, conical pores, ink bottle-type pores, and interstices between particles. Open pores are accessible to the adsorbate, while closed pores are not. Pores can also be classified based on their sizes. According to the International Union of Pure and Applied Chemistry (IUPAC), micro pores have a diameter less than 2 nanometers, meso-pores have a diameter in the range of 2 to 20 angstroms, and macro pores have a diameter greater than 20 angstroms [69].

3.2.3.3 pH of solution

The pH of the solution is an important factor that affects the adsorption process in wastewater treatment. The surface charges and degree of ionization of the adsorbate are influenced by the pH of the solution. The pH can determine whether a molecule will be ionized and what type of

charge it will have. The adsorption of other molecules and ions is also influenced by the pH. Furthermore, it has been observed that the surface tends to adsorb anions favorably at low pH and cations at high pH. The selectivity of the adsorbent to different pollutants may also depend on the pH, and in some cases, a multi-stage removal process may be necessary to effectively remove all pollutants. Understanding the pH of the solution is essential in optimizing the adsorption process for wastewater treatment, as it influences the surface charges, ionization of pollutants, and the overall efficiency of pollutant removal [30].

3.2.3.4 Contact time

Contact time refers to the duration of contact between the adsorbate (pollutant) and the adsorbent surface during the adsorption process. It plays a crucial role in determining the efficiency of adsorption. In the case of physisorption or van der Waals forces of attraction, a shorter contact time is generally sufficient for the adsorbate to attach to the adsorbent surface. On the other hand, for chemisorption or chemical bonding to occur, a larger contact time is required for the adsorbate to bond with the adsorbent surface site and achieve equilibrium.

During the initial stages of contact, the rate of adsorption is higher, and the driving force is greater, resulting in rapid uptake of the adsorbate. However, as the available vacant sites on the adsorbent surface decrease and the concentration of the adsorbate in the solution decreases, the driving force and the rate of removal of the pollutant via adsorption decrease. Therefore, the concentration of the adsorbate in the solution and the rate of adsorption are influenced by the contact time.

It is important to note that different adsorption processes have varying contact time requirements, depending on the type of forces involved in adsorption. Additionally, the relationship between contact time and adsorption is complex and can be influenced by factors such as the concentration of adsorbate, available vacant sites, and the nature of the adsorbent itself [70].

3.2.3.5 Initial concentration of Adsorbate

The initial concentration of the adsorbate in a solution plays a crucial role in the adsorption process. When the concentration of the adsorbate is very high, the adsorbent can get exhausted quickly. As the concentration of the adsorbate increases, the amount adsorbed generally decreases due to the resistance to the uptake of the solute increasing with higher solute

concentration. Moreover, the rate of adsorption is higher in the initial stages of contact when the concentration of adsorbate is high. However, it takes some time for the process to reach equilibrium, and the percentage removal generally decreases with an increase in the concentration of adsorbate. As time progresses, the rate of adsorption slows down due to the decrease in available vacant sites and the repulsion between the solid and adsorbate molecules on the adsorbent surface [71].

3.2.3.6 Temperature

Temperature plays a significant role in the process of adsorption for wastewater treatment. The effect of temperature on the adsorption rate and equilibrium adsorption capacity is complex. Generally, adsorption processes are exothermic, meaning they release heat. However, the rate of adsorption usually decreases with an increase in temperature.

The relationship between temperature and adsorption can vary based on factors such as pore size and diffusion control. For instance, if pore diffusion is the controlling step due to small pore size, the increase in temperature can enhance the rate of adsorption. In cases where adsorption processes are diffusion-controlled, the overall process may become endothermic with increasing temperature, leading to an increase in adsorption capacity.

It is important to note that the temperature dependency of adsorption can be intricate, with some scenarios showing an increase in adsorption with temperature while others exhibit a decrease. Hence, understanding the impact of temperature on adsorption processes is crucial for optimizing wastewater treatment efficiency [72].

3.2.3.7 Adsorption Kinetics

Adsorption kinetics is crucial for understanding the rate at which adsorption occurs and how pollutants are removed from a solution. It primarily involves studying how the concentration of adsorbate changes over time, providing insights into the rate of adsorption [47].

3.2.3.7.1 Pseudo – first – order

In the context of wastewater treatment, the pseudo-first-order kinetic model is a common model used to describe the kinetics of adsorption processes:

1. **Reversible Process**: The pseudo-first-order model assumes that the adsorption of the adsorbate from the solution onto the adsorbent surface is a reversible process, with equilibrium eventually being established between the solution and the adsorbate.

2. **Non-Dissociating Molecular Adsorption**: This model assumes non-dissociating molecular adsorption of adsorbate molecules onto the adsorbent surface. It describes the adsorption process as a diffusion-controlled process using first-order kinetics.

3. **Rate Equation**: The pseudo-first-order model is based on the assumption that the rate of adsorption is directly proportional to the difference between the equilibrium adsorption capacity and the amount of adsorbate adsorbed at any given time.

4. **Mathematical Representation**: The pseudo-first-order kinetic model equation is typically expressed as [73]:

   $$\frac{dq}{dt} = k_1(q_e - q_t) \qquad \text{(eq 3.1)}$$

   where q represents the amount of adsorbate adsorbed at time t, q_e is the amount of adsorbate adsorbed at equilibrium, k_1 is the rate constant of the pseudo-first-order model, and t is time.

5. **Linearization**: The equation of the pseudo-first-order kinetic model can be linearized as follows [74]:

   $$\ln (q_e - q_t) = \ln (q_e) - K_1 t \qquad \text{(eq 3.2)}$$

   where q_e is the equilibrium adsorption capacity, qt is the adsorption capacity at time t, and K_1 is the rate constant of the pseudo first order adsorption. This linear form equation enables a more convenient analysis and determination of the parameters of the pseudo-first-order kinetic model.

6. **Model Fitting**: Experimental adsorption data can be fitted to the pseudo-first-order kinetic model to determine the rate constant k_1 and to assess how well the model describes the adsorption process. It's essential to acquire kinetic data for analysis, as it helps in understanding the adsorption process. This data can be obtained by conducting tests in beakers and plotting $\ln (q_e - q_t)$ versus t to observe the adsorption rates over time

7. **Limitations**: While the pseudo-first-order model is widely used, it has limitations, especially when the adsorption process does not follow first-order kinetics or when the experimental data deviates significantly from the model predictions.

The pseudo-first-order kinetic model provides a simple and widely used approach to describe the adsorption kinetics of pollutants onto adsorbent surfaces. It serves as a valuable tool for understanding and predicting the rate of adsorption in various environmental and industrial applications.

3.2.3.7.2 Pseudo – second – order

The pseudo-second-order kinetic model is another commonly employed approach to describe the adsorption kinetics of pollutants onto adsorbent surfaces:

1. **Rate Equation**: The pseudo-second-order model is based on the assumption that the rate of adsorption is directly proportional to the square of the difference between the equilibrium adsorption capacity and the amount of adsorbate adsorbed at any given time.

   Mathematical Representation: The pseudo-second-order kinetic model equation is typically expressed as [75]:

   $$\frac{dq}{dt} = k_2(q_e - q_t)^2 \qquad \text{(eq 3.3)}$$

   where q represents the amount of adsorbate adsorbed at time t, q_e is the amount of adsorbate adsorbed at equilibrium, k_2 is the rate constant of the pseudo-second-order model, and t is time.

2. **Linearization**: The equation of the pseudo- second -order kinetic model can be in the following manner [76]:

   $$\frac{t}{q_e} = \frac{1}{K_2 q_e 2} + \frac{1}{q_e} \qquad \text{(eq 3.4)}$$

3. Here, t represents time, q_e is the amount of adsorbate at equilibrium, and K_2 is the rate constant of the pseudo-second-order adsorption.

4. **Initial Sorption Rate**: In the pseudo-second-order model, the term $k_2 q_e^2$ represents the initial sorption rate, indicating how much adsorption occurs per unit time per unit mass of adsorbent.

5. **Model Fitting**: Experimental adsorption data can be fitted to the pseudo-second-order kinetic model to determine the rate constant k_2 and to assess how well the model describes the adsorption process. This model is particularly useful when the adsorption process follows second-order kinetics.
6. **Comparison with Pseudo-First-Order**: The pseudo-second-order model is often preferred over the pseudo-first-order model for adsorption systems that exhibit chemisorption or when the experimental data better align with second-order kinetics. It provides a more accurate description of the adsorption process in such cases.
7. **Intraparticle Diffusion Model**: In addition to the pseudo-first-order and pseudo-second-order models, the intraparticle diffusion model, also known as the Weber Morris model, can be used to explore the possibility of intraparticle diffusion as a rate-controlling step in the adsorption process.

The pseudo-second-order kinetic model offers a valuable tool for understanding and predicting the adsorption kinetics of pollutants onto adsorbent surfaces. It is particularly useful for systems where chemisorption or second-order kinetics play a significant role in the adsorption process.

3.2.3.8 Adsorption isotherms model

Adsorption isotherm models are essential for understanding the equilibrium data in the process of wastewater treatment. The two most commonly used adsorption isotherm models are the Langmuir and Freundlich models. Both models provide valuable insights into the relationship between the quantity of pollutants adsorbed and the concentration of the system.

The Langmuir adsorption model is applicable for monolayer adsorption onto a homogeneous surface when there is no interaction between the adsorbed species. The Langmuir isotherm assumes linear adsorption at low densities and predicts a maximum surface coverage at higher concentrations of the metal or solute in the system. It primarily applies to chemisorption systems, where monolayer adsorption is assumed to occur.

On the other hand, the Freundlich adsorption model is based on the assumption of a heterogeneous surface with a non-uniform distribution of heat of adsorption over the surface. The Freundlich isotherm describes the variation in the quantity of pollutants adsorbed by a unit

mass of solid adsorbent in relation to changes in pressure or concentration of the system at a given temperature.

Both the Langmuir and Freundlich isotherm models are characterized by two parameter values, making them relatively simple and commonly used in adsorption studies. The Langmuir model involves the equilibrium adsorption capacity (q_m), equilibrium concentration of the solution (Ce), and Langmuir adsorption constant (K_L). On the other hand, the Freundlich model includes the equilibrium adsorption capacity (q_e), equilibrium concentration of the solution (Ce), relative adsorption capacity (K_f), and the Freundlich constant (1/n).

In the context of designing a system for wastewater treatment, it is crucial to determine the equilibrium data and select the most appropriate isotherm model for representing the adsorption behavior of the pollutants in the system. By utilizing these isotherm equations, such as the Freundlich and Langmuir models, researchers can optimize the design of adsorption systems and determine the parameters essential for effective treatment processes.

1. **Other Isotherm Models**:
    - **Temkin Isotherm**: Accounts for the indirect interaction between adsorbate molecules on the surface.
    - **Redlich-Peterson Isotherm**: A three-parameter model that considers the non-ideal behavior of adsorption.
    - **BET Isotherm**: Used for multilayer adsorption on solid surfaces.

3.2.3.8.1 Freundlich isotherm

The Freundlich isotherm is a widely used model for describing adsorption onto heterogeneous surfaces with a non-uniform distribution of heat of adsorption:

1. **Equation**:

- The Freundlich isotherm equation is given by [73]:

$$q_e = K_f * Ce^{1/n} \qquad \text{(eq 3.5)}$$

where:

q_e is the equilibrium adsorption capacity,

Ce is the equilibrium concentration of the solution,

K_f is the relative adsorption capacity, and

1/*n* is the Freundlich constant.

2. **Assumptions**:

- Assumes a heterogeneous surface with a non-uniform distribution of heat of adsorption over the surface.
- Describes the variation in the quantity of adsorbate adsorbed by a unit mass of solid adsorbent with changes in concentration.

3. **Linearization**:

The Freundlich isotherm equation can be linearized as [76]:

$$\log q_e = \log K_f + \frac{1}{n}\log C_e \qquad \text{(eq 3.6)}$$

This linear form allows for easier analysis and determination of the Freundlich constant K_f and the parameter 1/*n*.

4. **Interpretation**:

- The Freundlich isotherm is particularly useful for understanding the adsorption behavior of adsorbates on surfaces with varying affinities for adsorption.
- It provides insights into the relationship between adsorbate concentration and adsorption capacity.

5. **Applications**:

- Widely applied in studying adsorption processes in various fields, including wastewater treatment, environmental remediation, and material science.
- Helps in determining the adsorption capacity of the adsorbent under different equilibrium conditions.

3.2.3.8.2 Langmuir isotherm

The Langmuir isotherm model is commonly used to describe monolayer adsorption onto a homogeneous surface where there is no interaction between the adsorbed species. Here are some key points about the Langmuir isotherm:

1. **Equation**:
    - The Langmuir isotherm equation is given by [73]:

$$q_e = \frac{q_m.K_L.Ce}{1+K_L.Ce} \quad \text{(eq 3.7)}$$

where:

- q_e is the equilibrium adsorption capacity,
- Ce is the equilibrium concentration of the solution,
- q_m is the maximum adsorption capacity (monolayer coverage), and
- K_L is the Langmuir adsorption constant.

2. **Assumptions**:
    - Applicable for monolayer adsorption on a homogeneous surface without interactions between adsorbed species.
    - Predicts linear adsorption at low densities and a maximum surface coverage at higher concentrations.

3. **Linearization**:
    - The Langmuir isotherm equation can be linearized as [76]:

$$\frac{1}{q_e} = \frac{1}{K_L * q_{max}} * \frac{1}{C_e} + \frac{1}{q_{max}} \quad \text{(eq 3.8)}$$

This linear form allows for easier analysis and determination of the Langmuir adsorption constant K_L and the maximum adsorption capacity q_m.

4. **Interpretation**:
    - The Langmuir isotherm model helps in understanding the adsorption behavior of adsorbates forming a monolayer on the adsorbent surface.

- It provides insights into the maximum adsorption capacity of the adsorbent and the affinity of the adsorbate for the adsorbent surface.

5. **Applications**:
    - Widely used in studying adsorption processes in various fields, including wastewater treatment, surface chemistry, and catalysis.
    - Helps in predicting the adsorption behavior of pollutants and optimizing adsorption systems for efficient pollutant removal.

3.2.4 Activated carbon

3.2.4.1 Definition of activated carbon

Activated carbon, also known as activated charcoal, is a highly porous form of carbon with a large surface area, making it an effective adsorbent for a wide range of substances [59]. It is produced by heating carbonaceous materials, such as coal, wood, coconut shells, or agricultural wastes, at high temperatures in the absence of oxygen. This process creates a network of pores and a vast surface area that can adsorb molecules and ions from gases or liquids through physical or chemical bonding [77].

3.2.4.2 History of activated carbon

From Ancient Egypt to modern-day applications in air and water purification systems, activated carbon has a long and rich history steeped in practicality [78]. Around 1500 B.C., Egyptian papyri provide the earliest evidence of the use of carbon for medicinal purposes [79] [80]. Ancient Hindus and Phoenicians began using activated carbon to filter water around 400 B.C. after learning about its therapeutic benefits. The earliest form of activated carbon was discovered around 3750 B.C. when people living around the Indus Valley began burning sugary cane to reduce its odor. Soon after this breakthrough, people began experimenting with different raw materials such as coal, wood, and coconut shells to make activated carbon – many of which are still used in industrial processes today. Charcoal-based carbon has been used for centuries to oxidize and filter odors. During World War II, activated carbon was first artificially created when scientist Walter A. Cobbold developed the process of steam activation [78]. Through further innovations and technological developments, activated carbon became a key component in treating many industrial pollutants in the 1950s. It is now commonly used to treat

a variety of liquids, gases, and other chemical pollutants like toxins. Activated charcoal remains incredibly effective today, not only as a filtering tool but also as an odor eliminator.

The use of activated carbon in wastewater treatment, gas purification, and air filtration is energizing the modern world. Due to its high porosity, customizability, and selectivity, activated carbon is becoming increasingly popular among communities and industries. Its ability to absorb a wide range of contaminants makes it a powerful natural purifier. Modern technological advancements have enabled the production of activated carbon with greater surface areas, improved pore sizes, and broader chemical profiles to meet diverse needs. These improvements provide economical solutions for removing toxins from water sources and gaseous emissions. Activated carbon has a multifaceted history with an enchanting discovery story. Not only was it integral to early civilizations, but it has also benefitted both people and the planet in numerous ways since. Recent studies suggest that activated carbon possesses many advantageous properties that could positively impact our society's current environmental challenges [81].

3.2.4.3 Structure of activated carbon

Activated carbon, also known as activated charcoal, has a rough and imperfectly structured composition similar to graphite [59]. It consists of a wide spectrum of pores of varying sizes, ranging from visible fractures and fissures to molecular dimensions. The significant surface area of activated carbon is due to these pores, which enhance its ability to adsorb impurities from air and water [82]. The structure of activated carbon is composed of fused hexagonal layers, similar to the structure of pure graphite, with weak van der Waals forces holding the layers together [83]. The distance between layers in activated carbon is slightly larger than that in graphite, with an interlayer spacing of 0.34 to 0.35 nm in activated carbon compared to 0.33 nm in graphite [59].

Table 3.2: Classification of pore

Type of Pore Width	**Width**
Micro	< 2 nm
Meso	2-50 nm
Macro	> 50 nm

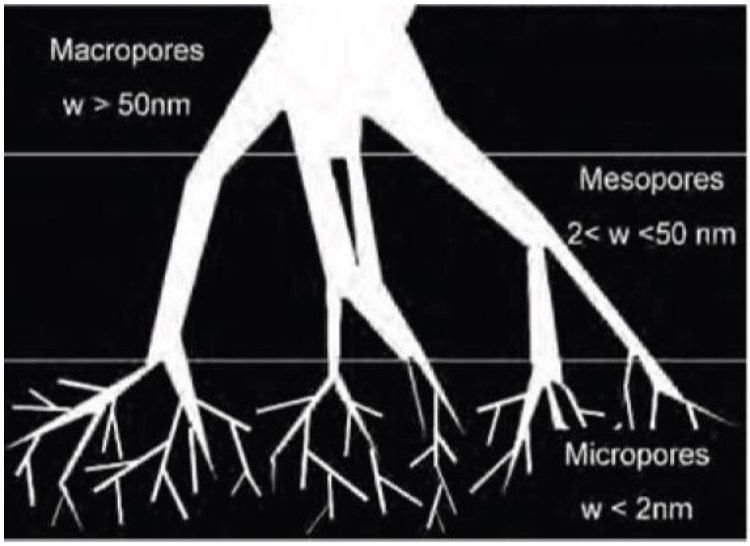

Figure 3.3: Graphical representation of pore structure on activated [84]

3.2.4.4 Classification of activated carbon

Activated carbons are complex materials that cannot be easily classified due to the diverse manufacturing techniques employed in their production, as well as their distinct behavior and surface properties [85]. Currently, the market provides three primary forms of activated carbon: powder, granular, and pellet. These forms are differentiated based on their particle sizes and shapes, each serving a specific purpose. However, there is also a broader classification based on their physical characteristics, which renders them suitable for more general applications.

3.2.4.4.1 Powdered activated carbon (PAC)

Powdered activated carbon (PAC) possesses an average diameter ranging from 15 to 25 μm, making it smaller than 100 μm [86]. Consequently, PAC exhibits a substantial internal surface area and a minimal diffusion distance. Consisting of crushed or ground carbon particles, PAC allows for the passage of 95-100% of its particles through a specific mesh sieve. Powdered activated carbons primarily find application in liquid phase adsorption and flue gas treatment [87]. In the context of wastewater treatment, PAC is commonly employed in a secondary treatment process known as powdered activated carbon treatment. Given the potential for significant head loss, PAC is typically not utilized in a dedicated vessel. Instead, it is frequently added directly to other process units, including raw water intakes, rapid mix basins, clarifiers, and gravity filters [88].

3.2.4.4.2 Granular activated carbon (GAC)

Granular activated carbon (GAC) is distinguished by its larger particle size in comparison to powdered activated carbon, leading to a reduced external surface area [89]. The diffusion of the adsorbate plays a critical role in GAC, making it a preferred option for the adsorption of gases and vapours due to its enhanced diffusion rate. GAC finds widespread application in water treatment, deodorization, and component separation in flow systems [90]. It is available in granular or extruded form, with specific sizes designated as 8×20, 20×40, or 8×30 for liquid phase applications, and 4×6, 4×8, or 4×10 for vapour phase applications.

3.2.4.4.3 Extruded activated carbon (EAC)

The process of extruding activated carbon entails the amalgamation of powdered carbon with a binder. This amalgamation yields a cylindrical block of activated carbon, with a diameter that can range from 0.8 to 130 mm [91]. These blocks find primary application in gas phase contexts owing to their favorable attributes, namely, low pressure drop, high mechanical strength, and low dust content.

3.2.4.4.4 Impregnated carbon

Porous carbons, which are impregnated with various substances such as iodine, silver, and cations like Al, Mn, Zn, Fe, Li, and Ca, have been developed for specific applications in air pollution control, particularly in the preservation of artifacts in museums and galleries. One notable application of silver-loaded activated carbon is its use as an adsorbent for purifying drinking water [92]. In order to obtain potable water from natural sources, the natural water can be treated with a combination of activated carbon and $Al(OH)_3$, which serves as a flocculating agent. Impregnated carbons are also employed for the adsorption of H_2S and thiols. It has been reported that the adsorption rates for H_2S can reach as high as 50% by weight

[93] .

3.2.4.4.5 Polymer coated carbon

This technique is capable of coating a porous carbon material with a biocompatible polymer, thereby creating a smooth and permeable layer that does not obstruct the pores [94]. The resulting carbon material is particularly beneficial for the application of hemoperfusion [86],

which is a treatment method involving the circulation of large volumes of the patient's blood over an adsorbent substance to remove toxic substances from the bloodstream.

3.2.4.5 Applications of activated carbon

Activated carbon is utilized in various fields, encompassing gas purification, gold purification, metal extraction, water purification, medicine, sewage treatment, and air filtration in gas masks and respirators, among others [95]. Additionally, activated carbon filters have experienced a surge in demand among recreational cannabis and herb smokers due to their remarkable capacity to efficiently eliminate "Tar" from smoke [96]. Furthermore, activated carbon exhibits numerous specific applications, such as:

3.2.4.5.1 Metal finishing field

This is an important industrial application of activated carbon in the field of metal finishing. It is widely utilized for the purification of electroplating solutions, specifically for the elimination of organic contaminants from bright nickel plating solutions [97]. Plating solutions often contain various organic chemicals that enhance the qualities and properties of deposits, such as brightness, smoothness, and ductility. However, these organic additives can generate undesired breakdown products in the solution during the electroplating process, due to the flow of direct current and the occurrence of anodic oxidation and cathodic reduction electrolytic reactions. If these breakdown products accumulate excessively, they can have a negative impact on the quality of the plating and the physical properties of the deposited metal. Activated carbon treatment effectively eliminates these impurities and restores the plating performance to the desired level. Additionally, activated carbon is also employed as a stationary phase, in combination with celite, in the analytical or preparative separation of carbohydrates using ethanol solutions (5–50%) as the mobile phase [98].

3.2.4.5.2 Environmental field

Here, activated carbon adsorption is extensively employed in diverse industrial and field applications. These applications encompass spill cleanup, groundwater remediation, drinking water filtration, air purification, and the elimination of volatile organic compounds from processes such as paint, dry cleaning, and gasoline dispensing [59].

3.2.4.5.3 Medical application

In medical applications, activated carbon is utilized for the treatment of poisonings and overdoses that occur as a result of oral ingestion [99]. It is believed that activated carbon binds to the toxic substance, thereby preventing its absorption by the gastrointestinal tract. In instances where poisoning is suspected, medical personnel administer activated charcoal either at the scene or in the emergency department of a hospital [100]. The dosage is typically determined through empirical means, at a rate of 1 gram per kilogram of body weight (equivalent to 50-100 grams for adolescents or adults), and is generally administered only once. However, depending on the specific drug involved, multiple administrations may be necessary [101]. In exceptional cases, activated charcoal is employed in Intensive Care Units to eliminate harmful drugs from the bloodstream of poisoned patients. Activated charcoal has emerged as the preferred treatment for numerous poisonings, rendering other decontamination methods such as ipecac-induced emesis or gastric lavage increasingly uncommon [102].

3.2.4.5.4 Gold Recovery

Activated carbon serves as a sorbent for aurocyanide and various other complex ions when they are in a dissolved state [103]. In the gold extraction process, carbon particles that are notably larger than the size of the ore particles may be combined with both the ore and the cyanide solution. The gold cyanide complex adheres to the carbon until it reaches a state of equilibrium with the gold solution [104]. Owing to their larger dimensions, the carbon particles can be conveniently separated from the slurry by employing a wire mesh for the purpose of screening. The gold is subsequently reactivated and reintroduced into the circuit.

3.2.4.5.5 Alcohol Purification

Activated carbon filters are widely utilized for the removal of organic impurities from alcoholic beverages, specifically vodka and whiskey. The presence of these impurities adversely affects the color, taste, and odor of the beverage, thereby emphasizing the significance of purification [59]. Moreover, activated carbon filters are extensively employed across diverse industries, such as corn and cane sugar refining [105], recovery processes in dry cleaning, elimination of fats and oils, catalyst support, battery electrodes, and supercapacitors [106].

3.2.4.5.6 Water Purification

Activated carbon water filters are commonly employed in residential water purification systems primarily for the purpose of eliminating taste and odor [107]. While taste and odor may be unpleasant, they are generally not seen as detrimental to one's health. Activated carbon filters have been increasingly employed in recent years to eliminate the pollutants found in water supplies. Activated carbon is highly efficient in removing organic pollutants, including volatile organic compounds, insecticides, and benzene [108] [109]. Additionally, it can eliminate some metals [110], as well as chlorine and radon [111]. Like any treatment system, it is incapable of completely eliminating all potential toxins in drinking water. Activated carbon systems have limitations in their ability to effectively remove certain types of substances. Therefore, it is crucial for homeowners to identify the specific water contaminants existing before employing such a system. This necessitates the necessity for water analysis [112].

3.2.5 Activated carbon in the drinking water manufacturing

Activated carbon plays a crucial role in the manufacturing of drinking water due to its outstanding adsorption capabilities [113]. It is a processed form of carbon with a vast number of tiny pores, significantly increasing its surface area and enhancing its ability to adsorb a wide variety of contaminants from water. The material can be derived from multiple sources, including wood, coal, coconut shells, and peat, each source offering different characteristics that make it suitable for specific applications in water purification [114].

The effectiveness of activated carbon in water purification stems from the adsorption process, where contaminants adhere to the surface of the carbon particles. The extensive pore structure of activated carbon provides a large surface area for contaminants to bind, making it highly efficient in trapping impurities such as chlorine, volatile organic compounds (VOCs) [115], and other unwanted substances [116]. This process not only removes harmful contaminants but also improves the taste and odor of the water, making it more palatable.

There are several types of activated carbon filters used in drinking water manufacturing, each designed for specific applications and varying levels of contaminant removal. Granular Activated Carbon (GAC) filters, for instance, use loose granules of activated carbon. These filters are typically employed in high-flow applications such as faucet filters and refrigerator filters, where water passes through the filter media with minimal resistance, maintaining a

higher flow rate [117]. While GAC filters are effective at removing taste and odor impurities, their performance in removing heavy metals and other complex contaminants is somewhat limited compared to other forms [118].

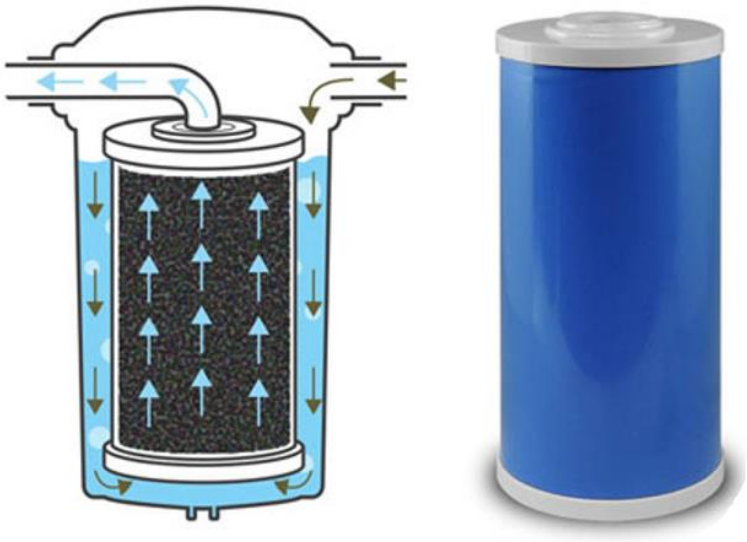

Figure 3.4:Granular activated carbon filter [119]

Carbon block filters, on the other hand, are denser and more efficient than GAC filters. Made from compressed activated carbon, these filters have a significantly larger surface area, allowing for greater contaminant removal capability [120]. The density of the carbon block prevents channeling, a phenomenon where water follows the path of least resistance, ensuring that all water passes through the filter media. Although carbon block filters can reduce water flow rates, their superior filtration capabilities make them ideal for applications where water quality is paramount [121].

Figure 3.5: Carbon block filter [122]

Catalytic carbon filters represent an advanced form of activated carbon. Chemically enhanced to remove specific contaminants such as chloramine, these filters combine adsorptive and reactive properties, providing a higher percentage of contaminant removal [123]. Catalytic carbon is particularly effective at eliminating stubborn impurities like lead and ammonia, making it a valuable component in areas with heavily contaminated water sources [124].

Figure 3.6: Catalytic carbon filter [125]

Activated carbon filters are capable of removing a wide range of contaminants from drinking water. They are particularly effective at removing chlorine and chloramine, substances commonly used in public water systems to disinfect water but which can cause adverse health effects and unpleasant tastes [126]. Additionally, activated carbon filters can remove pesticides and herbicides, which often find their way into water supplies through agricultural runoff.

These substances are associated with long-term health risks, making their removal from drinking water crucial. Pharmaceutical residues, including prescription drugs and over-the-counter medications, have been found in alarming levels in municipal water supplies. Activated carbon filters are effective at reducing up to 95% of these contaminants, safeguarding public health [127]. Similarly, VOCs, which are found in many household products, can migrate into drinking water and cause health issues ranging from asthma to nerve disorders. Carbon filters can significantly reduce the presence of VOCs in water [128].

In terms of heavy metal removal, advanced carbon filters are capable of eliminating substances like lead and mercury, which pose significant health risks, particularly to vulnerable populations such as children and pregnant women [129]. For instance, lead contamination in drinking water has been linked to severe neurological and developmental disorders. Premium activated carbon filters can remove up to 99% of lead, providing a critical line of defense against this dangerous contaminant.

Activated carbon filters are used in various applications within the drinking water manufacturing process. Point-of-entry systems treat all water entering a building, ensuring that every tap delivers purified water. These systems are commonly used in residential and commercial settings where comprehensive water treatment is necessary. Countertop filters and pitcher filters offer simple and cost-effective solutions for individual use, making high-quality water accessible to households without extensive infrastructure. Whole-house filters provide a complete solution for entire households or facilities, addressing all water sources within the premises [130]. Safety and quality considerations are paramount when selecting activated carbon filters. Most filters are made from natural, sustainable materials, and some may contain additional media to enhance filtration. It is essential to choose filters certified by recognized standards such as the National Sanitation Foundation (NSF) to ensure they meet rigorous safety and performance criteria [131]. This certification guarantees that the filters are structurally sound and free from toxic materials that could leach into the drinking water.

Activated carbon remains one of the most effective and economical solutions for water purification in the drinking water manufacturing industry. Its versatility and efficiency in removing a wide range of contaminants ensure that consumers have access to safe, clean, and palatable water. Despite decades of innovation in water filtration technology, activated carbon filters continue to be a cornerstone of effective water treatment systems, proving that comprehensive solutions can come in simple and affordable packages.

3.2.6 Methods of Activation

3.2.6.1 Chemical Activation

Chemical activation is a frequently employed method when wood products are used as source materials. This method integrates pyrolysis and activation into a single step at a lower temperature, without the involvement of oxygen [81]. Phosphoric acid, zinc chloride, and potassium hydroxide are chemical agents that function as dehydrating and stabilizing agents. They improve the formation of a porous structure in activated carbon [132]. The process can be succinctly outlined by the flow chart provided below:

Figure 3.7: The Process of Chemical Activation

Chemical activation is typically avoided in industrial applications because of environmental concerns and the expenses associated with treating materials using chemicals [59]. Chemical activation has multiple benefits as it combines carbonization and activation into a single step, operates at lower temperatures, achieves a significantly higher yield compared to physical activation, and consequently leads to the formation of a superior porous structure. Nevertheless, there are additional drawbacks to consider, like the caustic nature of the process and the cleaning phase.

The thermal treatment process of one-step chemical activation can be illustrated as follows:

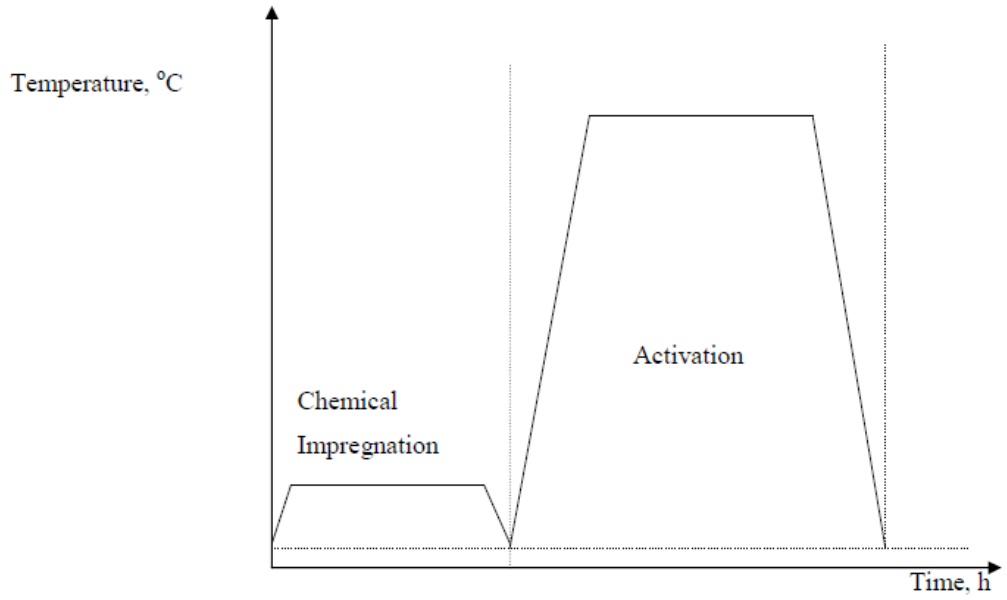

Figure 3.8: Thermal treatment scheme of one-step chemical activation

Chemical activation in the context of adsorption refers to the process of preparing activated carbon by treating a precursor material with a chemical agent to introduce specific functional groups and enhance its adsorption capacity [133]. This process involves heating the precursor material at high temperatures in the presence of steam, oxygen, or CO2 to create activated carbon that is highly porous and has specific functional groups such as COOH and OH. The activated carbon material generated through chemical activation typically has a higher binding capacity for adsorbates due to its unique surface properties and pore structure.

Chemical activation results in the formation of activated carbon that is capable of adsorbing a wide range of contaminants, making it a preferred choice for various applications such as water and wastewater treatment. The nature of the functional groups on the carbon surface, which is influenced by the activation process temperature, determines the adsorption behavior of the activated carbon. Carbon activated at temperatures below 500°C tends to be weakly acidic, while carbon activated at temperatures above 500°C is weakly basic [134].

3.2.6.2 Physical Activation

It is a conventional manufacturing process for activated carbon. The general procedure typically involves two stages: thermal pyrolysis at a relatively moderate temperature (typically 400 - 600^{o}C) in the presence of nitrogen or helium to disrupt the connections between carbon

atoms, followed by activation with an activating gas at 800 -1000ºC to enhance the formation of pores [135]. The features of carbon are significantly affected by the level of activation as well as the type of activating agent (steam or carbon dioxide) and the temperature of the process. In order to increase the level of burn-off, the activation temperature is often set above 900oC to ensure a suitably rapid reaction rate [136].

The diagram below illustrates the heat treatment process for a two-step physical activation:

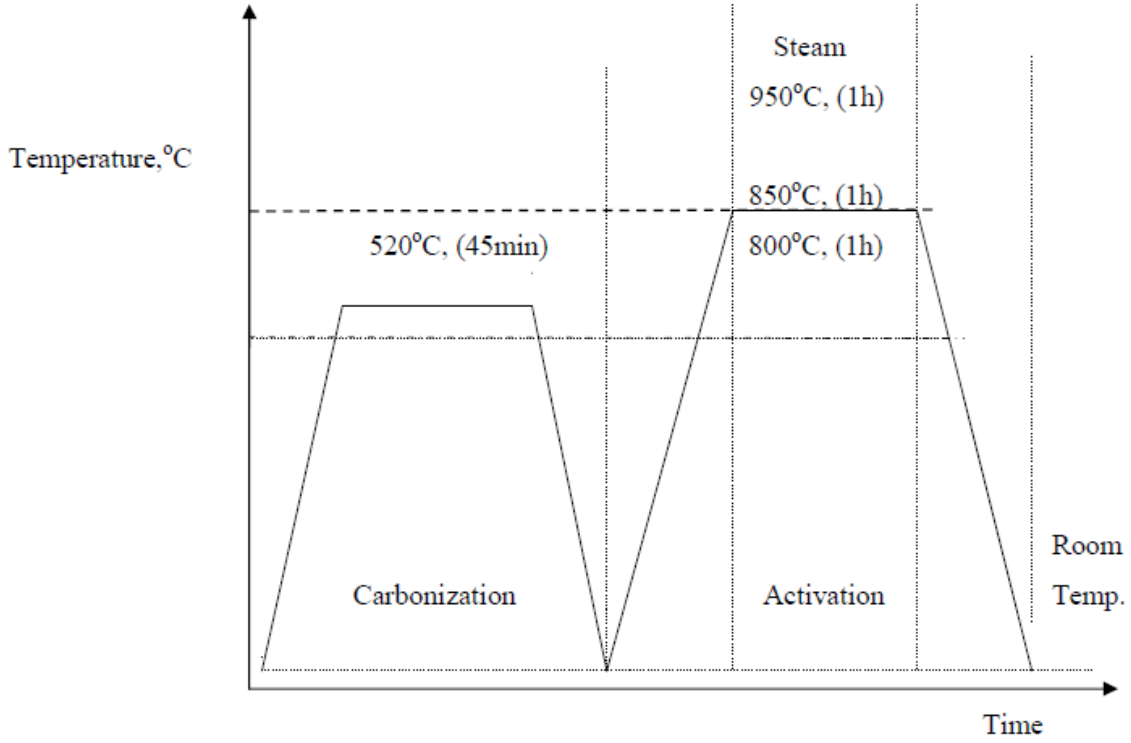

Figure 3.9: Thermal treatment scheme for a two-step physical activation

Given that the overall reaction, which involves converting carbon to carbon dioxide, releases heat energy, it is feasible to harness this energy and achieve a self-sustaining process, as demonstrated by the equations below:

$C + H_2O$ (steam) ---> $CO + H_2$ (-31 Kcal) (eq 3.9)

$CO + ½ O_2$ ---> CO_2 (+67 Kcal) (eq 3.10)

$H_2 + ½ O_2$ ---> H_2O (steam) (+58 Kcal) (eq 3.11)

$C + O_2$ ---> CO_2 (+94 Kcal) (eq 3.12)

The reaction between C and H_2O (in the form of steam) results in: The reaction between carbon monoxide (CO) and hydrogen gas (H_2) releases an energy of -31 kilocalories (Kcal). The chemical equation is written as $CO + ½ O_2$ ---> Carbon dioxide (with an energy content of 67 kilocalories) The chemical equation is as follows: $2H_2 + O_2$ ---> $2H_2O$ (steam) with the release of 58 kilocalories. The chemical reaction between carbon (C) and oxygen (O_2) produces carbon

dioxide (CO_2) along with the release of 94 kilocalories (Kcal). The activation of the process that generates H_2 is hindered due to the significant adsorption of H_2 at the active sites on the carbon surface. Research has demonstrated that steam is a more effective activating agent than CO_2, as it leads to a higher BET surface area [137]. This is due to the water molecules having a tiny Van der Waal radius. The concept of physical activation can be further elucidated through the utilization of the process diagram shown below:

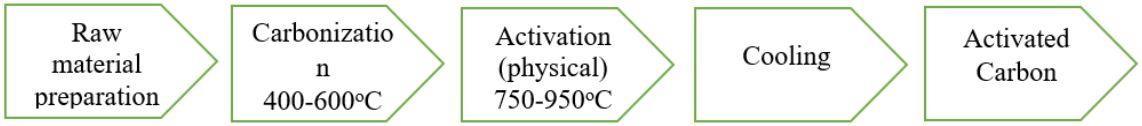

Figure 3.10: The Process of Physical Activation

3.2.6.3 Physical – Chemical Activation

Activated carbon is produced via a two-step chemical activation process. The substance undergoes carbonization in an inert atmosphere, resulting in the production of char. Next, the characters undergo chemical treatment. The mixture is subsequently activated in a furnace reactor system for varying activation durations [138]. The outcome is that the Carbon yield and surface area exhibit a small increase. This indicates that the product quality of two-stage pyrolysis is superior in comparison to single step pyrolysis. The diagram below illustrates the thermal treatment process of the two-step chemical activation approach being utilized:

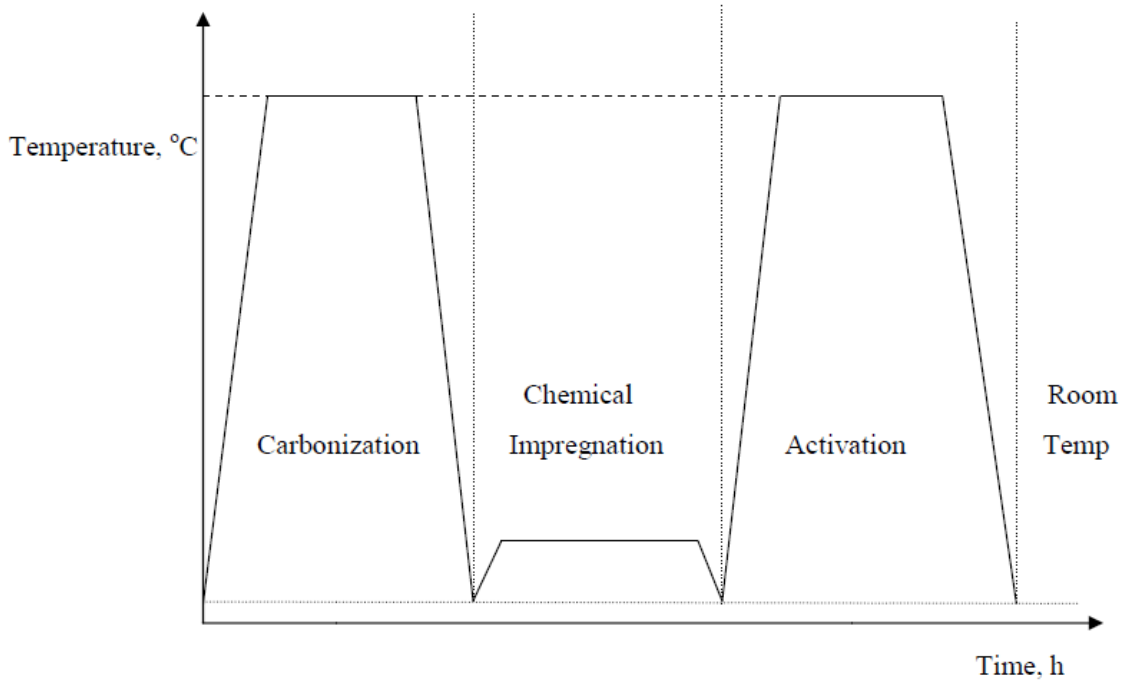

Figure 3.11: Thermal treatment scheme of two-step chemical activation

3.2.7 Cycas thouarsii (Sago)

3.2.7.1 Precursor Details

- Scientific Classification[139]:

  Kingdom: Plantae
  Clade : Tracheophytes
  Clade : Gymnospermae
  Division : Cycadophyta
  Class : Cycadopsida
  Order : Cycadales
  Family : Cycadaceae
  Genus : Cycas
  Species : **C. thouarsii**

- Binomial name: **Cycas thouarsii**

3.2.7.2 Description

- Small palm-like tree, up to 5 m tall and, unusually, 800 mm in diameter; indigenous and cultivated.
- Leaves paripinnate, up to 2 m long.

- Fruits hard, 40 - 60 mm in diameter.

Figure 3.12: Cycas thouarsii (Seeds and palm)

3.2.7.3 Origine and history

Cycas thouarsii, a species of cycad plant, has a rich history that dates back to its initial description in the early 19th century [140]. Commonly known as the Madagascar cycad, is an evergreen arborescent cycad found in various regions including Madagascar, Comoros, Mayotte, the Seychelles, and some African countries [141]. The plant was first recorded by French botanist Louis-Marie Aubert du Petit-Thouars in 1804 under the name C. circinalis. It was later described by French explorer and botanist C. Gaudichaud-Beaupre in 1829, who provided a minimal but valid description and attributed the name to Robert Brown. There have been various taxonomic considerations over the years, including descriptions by Miquel and de Candolle in the mid-19th century and the introduction of the name C. comorensis by French nurseryman G. Bruant in 1888. However, the name C. thouarsii was reinstated by Melville in 1958 and further supported by de Laubenfels in 1972 [142]. Cycas thouarsii is primarily found in near-coastal habitats, particularly in east coast forests with calcareous sand in Madagascar and the Comoro group. Its distinctive features include bluish new leaves with spinescent petioles and stout spines on the microsporophylls. Despite being abundant in some areas, the species is under threat from habitat destruction, leading to its classification as “Lower Risk - conservation dependent” by the IUCN Red List [140].

3.2.7.4 Chemical composition

Commonly known as the Madagascar cycad, it has a complex chemical composition that includes toxic compounds. The seeds of the plant contain cyanotoxins, which are toxins produced by cyanobacteria. Despite being toxic, the seeds are consumed on the Comorian island of Ngazidja after undergoing a process of washing, fermentation, and drying to remove the cyanotoxins. Additionally, the spongy endocarp of the seeds is a characteristic feature of Cycas thouarsii, allowing the seeds to float. This spongy endocarp is essential for the dispersal of seeds in the plant species [139]. In accordance with nutritional evaluations, 89% of the total composition of cycad almond flour is made up of carbs, with starch making up the remaining 73%. Protein and fat make up 5% and 3% of the mixture, respectively, and soluble carbohydrates make up 10%. Because of the little presence of insoluble components including formic acid, cellulosics, and pectic acid, these fruits are categorized as potential sources of starch. Cycad almonds and their flour have been shown through phytochemical research to contain unsaturated alkaloids, triterpenes, and sterols. Fresh almonds have also been shown to possess cyanogenic glycosides. These almonds are more nutritious due to the lack of flavonoids and tannins, which can have anti-nutritional effects [142].

3.2.7.5 Usages

Cycas thouarsii is primarily recognized for its ornamental and horticultural uses. Its distinctive features, such as bluish new leaves with spinescent petioles and stout spines on the microsporophylls, make it highly valued for landscaping purposes. The plant is cultivated in horticulture and can be found in certain botanical gardens and collections. Distributed among enthusiasts, Cycas thouarsii has entered horticulture under various names, particularly from seeds imported into France [140]. In traditional Comorian cuisine, the fruits of Cycas thouarsii are valued for their nutritional benefits and are processed into flour for dishes like porridge. Additionally, Cycas leaves are used for non-food purposes, such as protecting young seedlings from sunlight and decorating public spaces during traditional or religious events. Utilizing Cycas thouarsii fruits for food consumption in the Comoros can enhance the local diet and promote sustainable plant biodiversity management. Incorporating Cycas fruits into the traditional diet may reduce reliance on industrial food products, minimize chemical contamination risks, and generate additional income for local communities [142]. In Ngazidja, ntsambu is a highly symbolic food representing regional identities. Its aroma has been likened to a particularly ripe Camembert cheese. The fermentation process seems adequate to remove

toxins, though boiling the seeds may not eliminate the smell. The cooking process with coconut milk and fish is considered part of Comorian cultural knowledge. Zanzibari Comorians have a long history of eating ntsambu, with its import to Zanzibar dating back to the late 19th century. The plant holds cultural significance among Comorians in Ngazidja and the diaspora [141].

3.2.8 Methylene blue

3.2.8.1 Definition

Methylene blue is a Basic Blue 9 dye with the IUPAC name 3,7-bis (dimethylamine) phenothiazin-5-ium chloride with a deep blue color [29].

Figure 3.13: Methylene blue in a powder form (a), and solution (b)

It is a cationic textile dye highly soluble in water that is commonly used in textile manufacturing processes [4], and also used as a redox indicator in chemistry and as a medication for various medical purposes, including the treatment of methemoglobinemia and cyanide poisoning [143]. However, it poses health hazards such as damage to the nervous system, brain, and liver when ingested, eye burns, fast breathing, profuse sweating, and potential cancer risks [29].

3.2.8.2 Chemical composition

Methylene blue has the chemical formula $C_{16}H_{18}ClN_3S$ and its chemical structure consists of a tricyclic phenothiazine ring system [143].

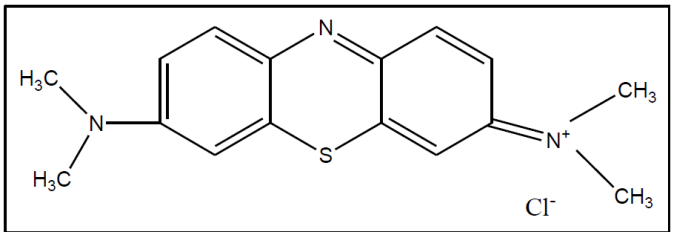

Figure 3.14: Molecular Structure of methylene blue (MB)

This compound has a molecular weight of 319.9 g/mol [4], and appears as a green crystalline powder, which is highly soluble in water, with solubility values reaching up to 40 g/L at 20°C .The chemical composition of methylene blue consists of carbon (C) accounting for 60.08%, hydrogen (H) for 5.67%, nitrogen (N) for 13.14%, sulfur (S) for 10.03%, and chlorine (Cl) for 11.08%. This complex composition allows the dye to exhibit a maximum absorbance at the wavelength of 665 nm in UV-Visible spectroscopy, making it easily identifiable in various analytical procedures. Methylene blue's structural formula showcases the intricate arrangement of its atoms, which contributes to its stability and reactivity. The presence of the phenothiazine core with dimethylamine groups significantly influences its electronic properties, facilitating its interaction with light and making it a useful dye in multiple industries. This structure is also responsible for its strong adsorption properties, which are leveraged in wastewater treatment processes. In terms of its physical properties, methylene blue has a melting point of 180°C, and besides being highly soluble in water, it also dissolves in alcohol to a lesser extent, with a solubility of 10 g/L at 20°C. These properties are crucial for its application in different environments, where its solubility and stability are required for effective performance.

3.2.8.3 Usage of methylene blue

Methylene blue is widely used in the textile industry as one of the most common dyes for coloring fabrics such as silk, wool, cotton, and paper. Its strong affinity for adhering to the interstitial spaces of cotton fibers makes it a popular choice for providing permanent, vibrant colors that are resistant to fading from exposure to water, light, and other environmental factors. The extensive use of methylene blue in textile manufacturing, however, also contributes to

significant environmental concerns due to the discharge of dye-laden wastewater, which contains toxic and potentially carcinogenic compounds that can pollute water sources and harm aquatic life [14]. In the field of medicine, methylene blue has a diverse range of applications. It was the first synthetic antimalarial drug and continues to be used in the treatment of various medical conditions. Methylene blue is employed as a therapeutic agent for conditions such as methemoglobinemia, a blood disorder, and has shown promise in treating Alzheimer's disease and improving memory. Additionally, it is used in various diagnostic procedures, including the visualization of surgical sites, detection of neuroendocrine tumors, and as a photosensitizer in the photodynamic treatment of cancer and the inactivation of viruses like HIV and hepatitis in plasma [14] [15]. Methylene blue serves multiple purposes due to its chemical properties. It is used as a staining agent in microbiology for identifying bacteria and other microorganisms under the microscope. Furthermore, its role as a redox indicator in analytical chemistry allows for the detection of anionic surfactants and other compounds in trace analysis. Its fluorescence properties have also made it a valuable tool in near-infrared imaging for visualizing various biological structures during surgical procedures, highlighting its versatility and importance in scientific research and clinical diagnostics [14] [15].

Despite its wide range of uses, the toxicity and environmental impact of methylene blue cannot be overlooked. The textile industry, in particular, faces challenges in managing the dye's environmental footprint, necessitating the development of effective wastewater treatment methods. Meanwhile, in medical and laboratory contexts, the controlled application of methylene blue ensures patient safety and enhances its efficacy as a diagnostic and therapeutic agent. Continuous research and innovation are essential to maximize the benefits of methylene blue while minimizing its adverse effects on health and the environment [14] [15].

3.2.8.4 Effect on the environment

Methylene blue, a dye extensively used in the textile industry, poses significant environmental hazards. Its discharge into water bodies leads to a substantial increase in the chemical oxygen demand (COD) of the receiving waters, indicating a high level of pollution. This can cause a depletion of oxygen in the water, adversely affecting aquatic life. The dye's toxic effects on algae, which form the basis of aquatic ecosystems, are particularly concerning. Studies have shown that methylene blue inhibits the growth of microalgae such as Chlorella vulgaris and Spirulina platensis by disrupting their photosynthetic processes. This inhibition is primarily due to the reduced synthesis of chlorophyll pigments, which are essential for photosynthesis.

The dye's toxicity leads to metabolic disruptions in these algae, further exacerbating the decline in their populations [4]. The adverse impact of methylene blue on aquatic organisms extends beyond algae. Fish exposed to methylene blue exhibit significant physiological and histopathological changes. For instance, in species like Catla catla and Tilapia, the dye causes micronuclei formation and degeneration of gill structures, leading to impaired respiration and other vital functions. Additionally, the liver and muscle tissues of these fish show signs of hyperemia and necrosis when exposed to the dye. These effects not only threaten individual fish but also disrupt entire aquatic food webs, leading to long-term ecological imbalances [4]. Human exposure to methylene blue, although less direct than that of aquatic organisms, still poses health risks. The dye is known to release aromatic amines, such as benzidine, which are potential carcinogens. Long-term exposure to methylene blue can lead to various health issues, including respiratory problems and skin irritation. Moreover, workers in industries that use methylene blue are at a higher risk of developing these health conditions due to prolonged exposure. Effective measures to limit the release of methylene blue into the environment and protect workers from its harmful effects are therefore crucial [144] [3].

CHAPTER4: METHODS AND MATERIALS

4.1 Synthetic wastewater preparation and adsorbent preparation

4.1.1 Experimental set up

4.1.1.1 Apparatus

4.1.1.1.1 Electric Furnace

Figure 4.1: High temperature electrical furnace

4.1.1.1.2 Dehydration unit (Oven)

Figure 4.2: Isotherm Forced Convection Lab Oven

4.1.1.1.3 Analytical balance

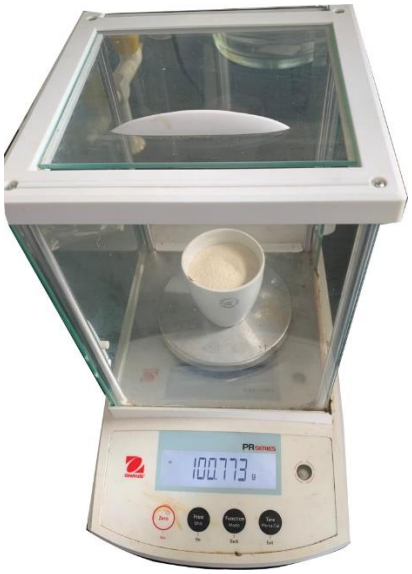

Figure 4.3: Analytical balance

4.1.1.1.4 UV- Spectrophotometer

Figure 4.4: Hach UV- Spectrophotometer Dr 6000

4.1.1.1.5 Fourier – Transform – Infrared Spectroscopy (FTIR)

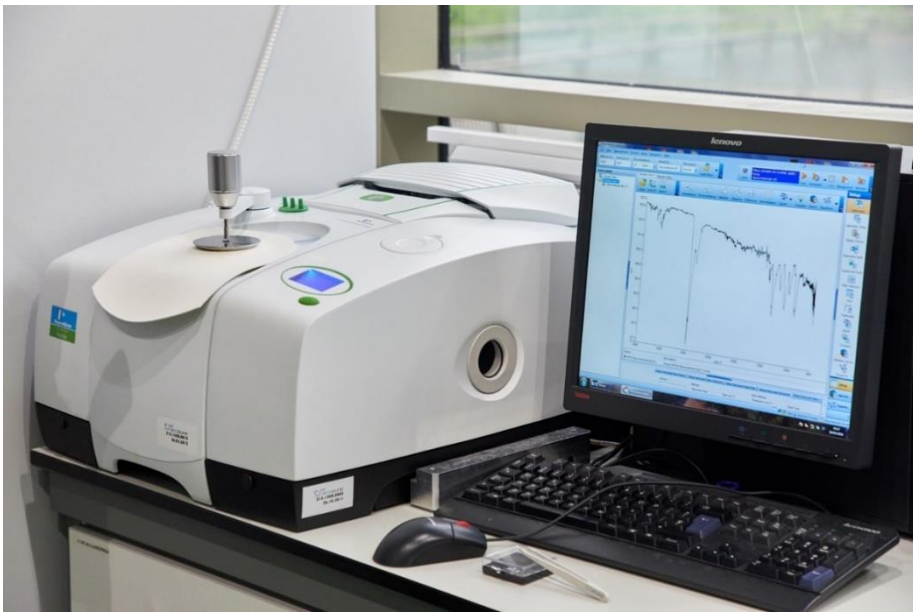

Figure 4.5: FTIR Spectrometer Perkinelmer Frontier

4.1.1.1.6 pH-meter (HACH HQ40d)

Figure 4.6: pH - meter (HACH HQ40d)

4.1.1.1.7 Platform Shaker

Figure 4.7: Orbimix-3010-Plateform-Shaker

4.2 Experimental Procedure

4.2.1 Raw materials preparation

To prepare the Sago seed powder (fig 4.9), we first harvested and collected the sago fruit from a sago palm in Mbeni – Comoros (a). The fruit was then split in two to collect the seeds (b) (c), which were dried in the sun for 5 to 6 days (d). After drying, the seeds were stored in a well-sealed carton for 45 days to complete the shelf life (e). Once this period was over, the seeds were cleaned and ground with a blender to obtain the raw Sago seed powder (f) [142].

Figure 4.8: (A) Sago fruit after harvest, (B) Sago seed in the drying process, (C) Obtained powder after grinding of dried sago seed

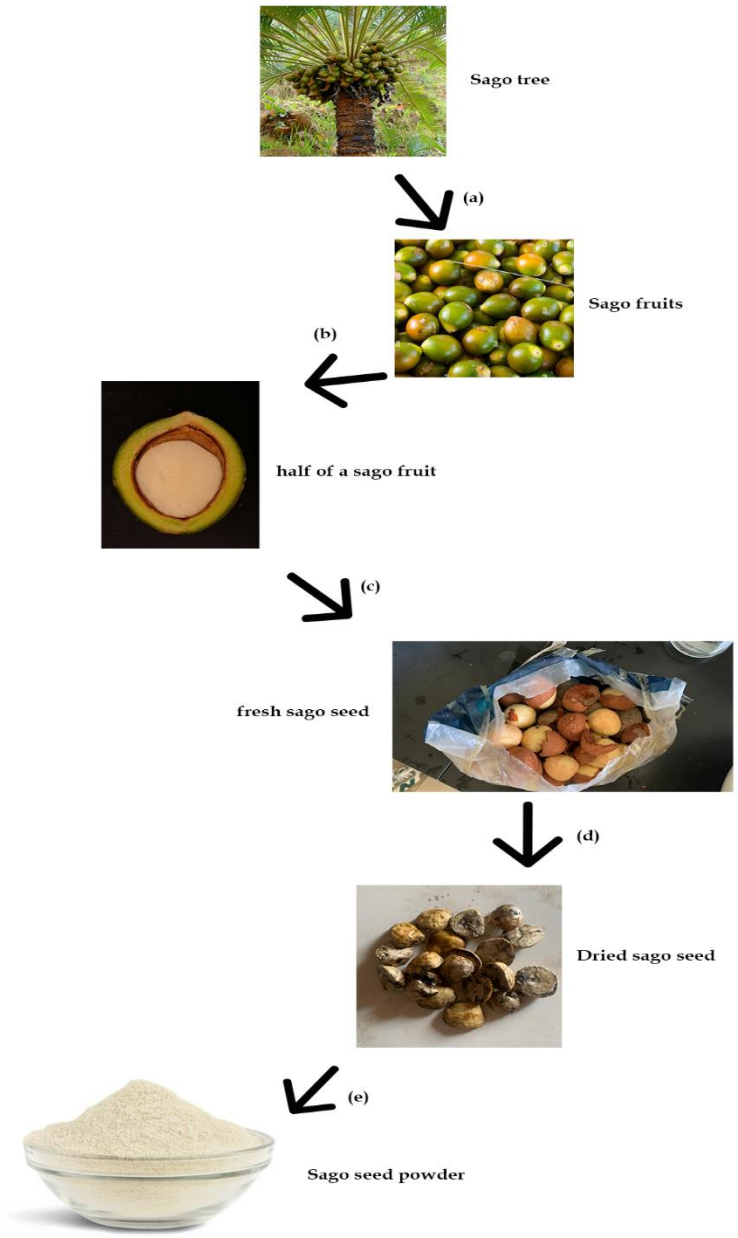

Figure 4.9: Sago seed powder production process

4.2.2 Carbonization

The starting raw material, Cycas thouarsii seed powder (Sago seed powder) was placed to 7 crucible and weighted then covered with aluminum foil and placed in a furnace.

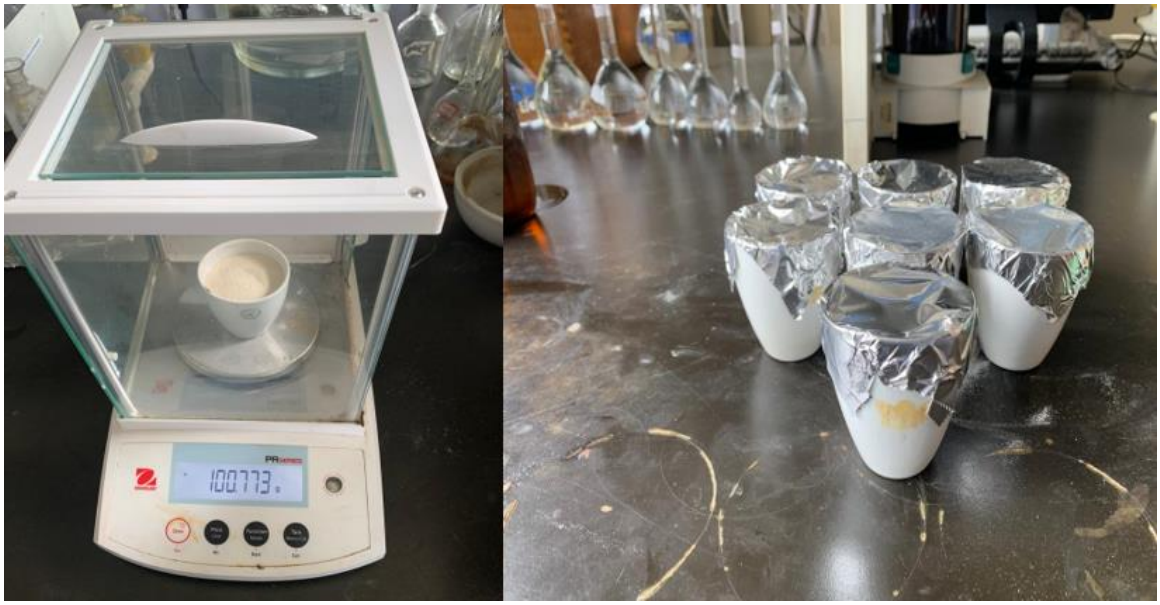

Figure 4.10: Preparation of raw material for carbonization

The samples were heated at 500°C for a period of 3 h.

Figure 4.11: Process of carbonization of raw material in a furnace

After the carbonization, the carbonized sample (residual char) was allowed to cool.

Figure 4.12: colling after carbonization

4.2.3 Carbon Activation

The Purpose of carbon activation is to increase the surface area and porosity of carbon materials, enhancing their ability to adsorb contaminants, gases, or impurities [145]. To prepare phosphoric acid (H_3PO_4) for the activation of sago seed char, an initial quantity of 500 ml of 85% H_3PO_4 was measured and subsequently diluted with 350 ml of distilled water in a conical flask, resulting in a final volume of 850 ml of 50% H_3PO_4. For the subsequent decantation process, 100g of sago seed char was combined with 200 ml of the aforementioned 50% H_3PO_4 solution in a beaker and left undisturbed for a duration of 48 hours [146]. At the conclusion of this designated timeframe, the mixture underwent filtration using filtration paper, thereby allowing for the collection of the char. The filtered char was subsequently transferred to a crucible, covered with aluminum foil, and subjected to pyrolysis by heating it in a furnace set at a temperature of 500°C for a period of 3 hours [132]. After the pyrolysis a 500 ml solution of 1M NaOH was prepared and used to wash the char with deionized water to get a pH equals to 7.95. The char was then dried at an oven with 110°C in a period of 3hours [147].

4.2.4 Methylene blue synthetized solution

For this study MB powder obtained from Sulfo Rwanda industries laboratory was used as the adsorbate molecule in adsorption experiments.

4.2.4.1 Procedure

1g of methylene blue powder was weighted and placed to a 1000 ml conical flask. Then distilled water was added up to the mark to obtain a solution of 1000 ppm (fig 4.13) [3] [148].

Figure 4.14: Methylene blue powder

Figure 4.13: Methylene blue Stock solution

4.2.4.2 Calibration Curve

To prepare a solution with a concentration of 50 ppm, 12.5 ml of the 1000 ppm stock solution was pipetted into a conical flask and then diluted to a final volume of 250 ml with distilled water. A 0.01 ppm solution was prepared from this solution. Additionally, a 0.5, 1, 1.5 ppm solution was also prepared (fig 4.15). Subsequently, the solutions with different concentrations were tested using a UV spectrophotometer at a wavelength of 665 nm, with distilled water used

as the reference sample. The absorbances obtained for each solution were then used to construct a calibration curve by plotting the absorbance against the concentration [147].

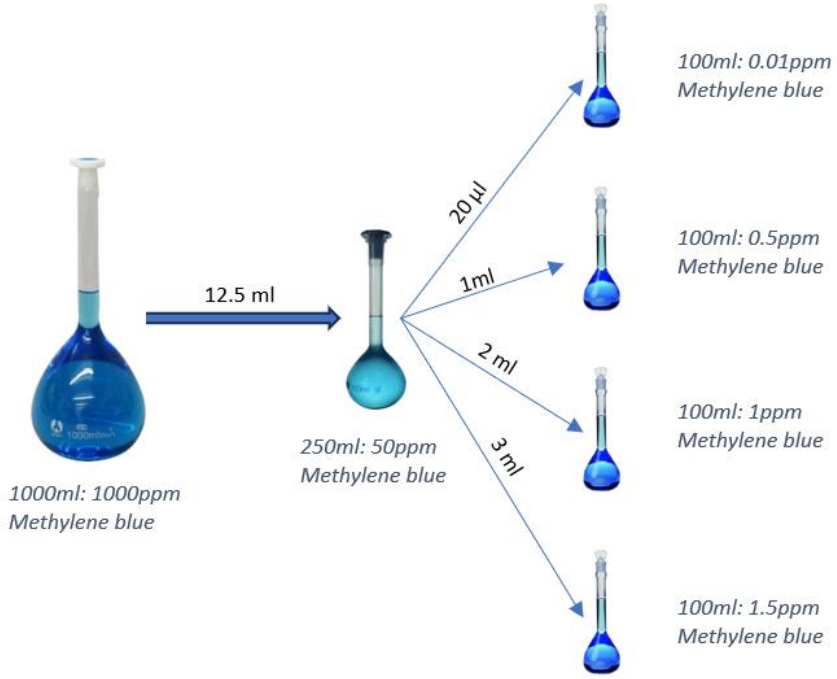

Figure 4.15: Methylene blue calibration procedure

Table 4.1: Methylene blue standard curve concentration (ppm) and absorption data

Concentration(ppm)	Absorption
0	0
0.01	0.002
0.5	0.094
1	0.177
1.5	0.291

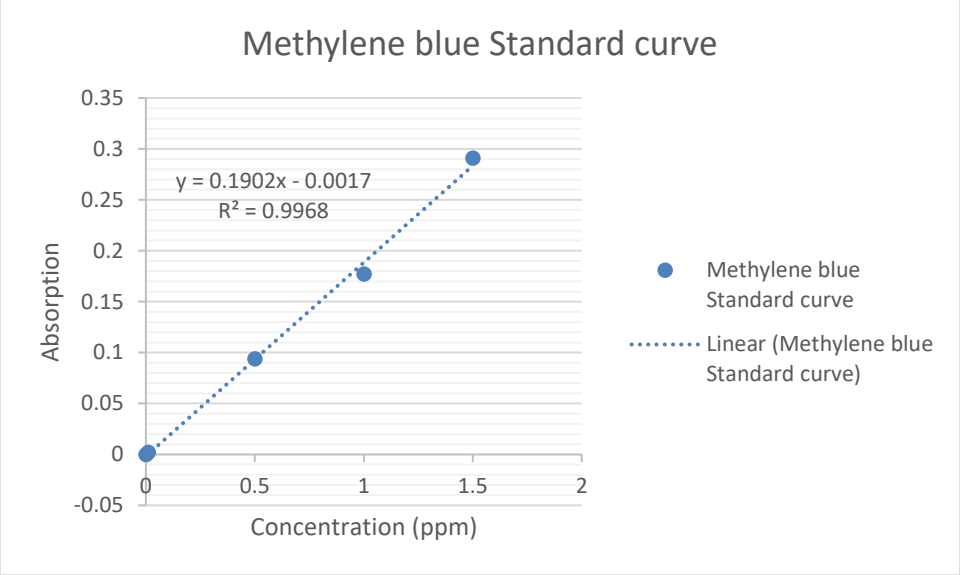

Figure 4.16: Methylene blue standard curve

A calibration curve with the equation:

$$y = 0.1902x - 0.0017 \quad \text{(eq 4.1)}$$

and an R^2 value of 0.9968 was obtained and we used the equation to determine the concentration of methylene blue remaining in a solution by measuring its absorbance. The high R^2 value indicates that the relationship between absorbance (y) and concentration (x) is very linear, meaning that absorbance can be accurately used to predict the concentration of methylene blue in the solution. By measuring the absorbance of a sample using UV-Spectrophotometer, the concentration of methylene blue was calculated using this calibration curve.

4.2.5 Effect of Activation temperature on carbon yield

To analyze the effect of activation temperature on carbon yield. 10g of impregnated sago seed char was placed in a crucible and weighted. The sample was then labeled to it proper activation temperature and the process was repeated for the 6 samples (500,600,700,800,900,1000°C). The samples were then placed in a furnace and each specific temperature was set for a period time of 3hours and after that weighted.

The formula that was used to determine the yield of carbon was the following [77]:

$$\text{Yield of Carbon} = \frac{Weight\ of\ sample\ after}{Weight\ of\ sample\ before} * 100 \quad \text{(eq 4.2)}$$

4.2.6 Characterization of sago seed activated carbon

4.2.6.1 XRF analysis

The procedure for analyzing the chemical composition of Sago seed samples using X-ray fluorescence (XRF) spectrometry involved several steps. Initially, two types of Sago seed samples were prepared: Sago seed powder raw material and Sago seed activated carbon. Each type of sample was divided into two separate tubes, resulting in a total of four tubes for the analysis. The materials required for this procedure included the X-MET8000 handheld XRF device, which was specifically designed for such analytical tasks.

Figure 4.18: X-MET8000 handheld XRF for analysis

Figure 4.17: 4 tubes with 2 samples (Sago seed powder raw material (Black) and Sago seed Activated carbon (white))

Before starting the analysis, it was ensured that the X-MET8000 handheld XRF device was properly calibrated and functioning. Calibration was essential for obtaining accurate and reliable results. Each of the four tubes containing the Sago seed samples was then individually subjected to the XRF analysis. The handheld XRF device was used to scan the samples, and it emitted X-rays that interacted with the elements in the samples, causing them to fluoresce. This fluorescence was detected and measured by the device, providing data on the chemical composition of the samples.

Figure 4.19: XRF analysis on samples

During the analysis, the manufacturer's guidelines for operating the XRF device, including settings and exposure times, were followed to ensure consistent and accurate results. The device's software processed the detected fluorescence data and generated a detailed excel report of the elements present in each sample. This report typically included information on the concentrations of various elements (%), which was crucial for comparing the chemical composition of the raw Sago seed material and the activated carbon.

The results from the XRF analysis were then interpreted to understand the differences between the raw and activated Sago seed samples. Activated carbon was expected to show a different elemental composition compared to the raw material due to the activation process, which typically involved treatments that altered the chemical structure and composition. These differences were analyzed to evaluate the effectiveness of the activation process and to assess the suitability of the activated carbon for its intended applications, such as adsorption processes in water purification.

4.2.6.2 Functional groupement analysis

The analysis of sago seed samples by (FTIR) involved several steps to ensure accurate results. Three small portion samples were prepared: sago seed powder as the raw material, sago seed activated carbon before adsorption, and sago seed activated carbon after adsorption. Each of these samples was carefully prepared to maintain their integrity throughout the analysis process.

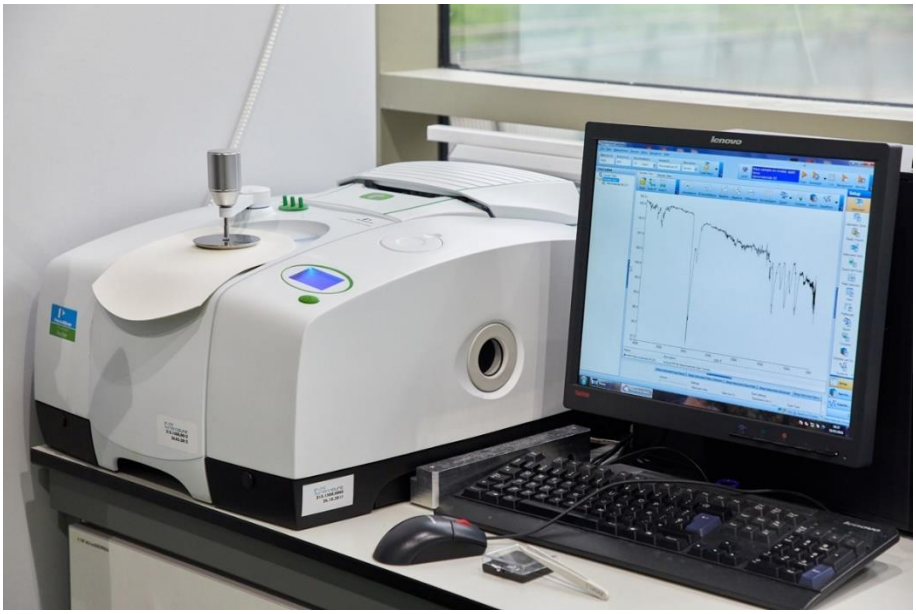

Figure 4.20: FTIR Spectrometer PerkinElmer Frontier

Using the FTIR Spectrometer PerkinElmer Frontier, the chemical functional groups of the three samples were analyzed. The spectrometer provided detailed insights into the molecular structure and composition of the sago seed materials. Each sample underwent rigorous examination to identify any changes in the functional groups resulting from the activation and adsorption processes.

During the FTIR analysis, the spectrometer recorded the absorption spectra of the samples. This data was crucial in understanding how the chemical composition of the sago seed materials changed. The differences in the spectra between the raw material, the activated carbon before adsorption, and the activated carbon after adsorption were analyzed to determine the effectiveness of the adsorption process.

4.2.7 Batch adsorption experiment

During the batch adsorption experimentation, the removal and adsorption capacity at a specific concentration or time was calculated by using the equation as follows:

$$\textbf{(Q}_e\textbf{) Adsorption Capacity (mg/g)} = \frac{C_o - C_e}{M} * V \qquad \text{(eq 4.3)}$$

$$\textbf{(R) Removal Rate (\%)} = \frac{C_o - C_e}{C_o} * 100 \qquad \text{(eq 4.4)}$$

Where: %R is the MB removal percentage, Q_e is the amount of MB adsorbed per unit mass of the adsorbent (mg/g), Co is the initial MB concentration (mg/L), Ce is the concentration of MB at equilibrium (mg/L), V is the volume of the aqueous solution (mL) and M is the AC mass (g) [29].

4.2.7.1 Optimization of operating parameters

4.2.7.1.1 Effect of contact time

Adsorption process is highly impacted by the contact time between the polluted solution and the adsorbent. In this research, to study the influence of contact time, and to get the optimum time for MB removal from the wastewater, 0. 25g of adsorbent was added to each six samples of wastewater containing 90 mg/L of MB. The samples were subjected to agitation at 120 rpm for different time durations, namely 30, 40, 50, 60, 70, 80 min. This speed was chosen based on preliminary tests to optimize the contact between methylene blue and the activated carbon particles [148]. Sample were removed from the shaker after their set time. Each sample was allowed to settle for 10 minutes after agitation. This settling period was critical to allow the activated carbon to adsorb the methylene blue effectively. After the settling time, the samples were filtered to separate the activated carbon from the solution. The filtration process was carried out using a standard filtration paper to ensure consistency across all samples. To measure the concentration of methylene blue remaining in the solution after adsorption, a spectrophotometer was used. The absorbance of the filtered solutions was measured at a wavelength of 665 nm, which corresponds to the maximum absorbance of methylene blue. Calibration curves were prepared using known concentrations of methylene blue to quantify the residual concentration in the samples. All experiments were conducted at room temperature. The data collected from the spectrophotometer readings were used to determine the equilibrium concentration after adsorption (Ct (mg/l)). This was done by using calibration curve equation (eq 4.1), the initial and final concentrations of methylene blue in the solution. The adsorption removal rate was then plotted against contact time to determine the suitable contact time of the adsorption process.

4.2.7.1.2 Effect of Dosage

The experimental setup for analyzing the dosage of sago seed activated carbon on the adsorption of methylene blue was meticulously organized to ensure accurate and reproducible results. Six samples were prepared, each with a different dosage of activated carbon (0.01, 0.05, 0.1, 0.15, 0.20, and 0.25g). The procedure followed a consistent methodology across all samples to maintain uniformity in the experiment. Firstly, 100 ml of solution was used for each sample. This volume was chosen to provide sufficient liquid for thorough mixing and

adsorption while being manageable within the experimental apparatus. Each sample solution contained a methylene blue concentration of 90 mg/l, a value selected to ensure a significant interaction between the dye and the activated carbon, thereby allowing the measurement of adsorption efficiency. The samples were agitated at a speed of 120 revolutions per minute (rpm). This agitation speed was critical to ensure that the activated carbon was evenly dispersed throughout the solution, promoting consistent contact between the methylene blue molecules and the carbon particles. The uniform agitation minimized the potential for settling or clumping of the activated carbon, which could affect the adsorption process. After agitation, a settling time of 10 minutes allowed the activated carbon to adsorb the methylene blue. This period was optimized through preliminary trials to ensure that sufficient adsorption occurred while preventing over-settling, which could complicate the separation of the carbon from the solution. The setup involved using identical flask for all samples to avoid variations in the adsorption due to differences in container material or geometry. Each flask was marked with the respective dosage of activated carbon to prevent any mix-up during the experiment. Variations in temperature could influence the adsorption capacity of activated carbon, so the experiments were conducted at room temperature. Samples were collected at the end of the settling period for analysis. The concentration of methylene blue remaining in the solution was measured using a spectrophotometer. This device provided precise readings of the dye concentration, which were then compared to the initial concentration to determine the amount adsorbed by the activated carbon. Each sample's data were recorded meticulously, noting the initial and final concentrations of methylene blue, the dosage of activated carbon used, and any observations during the experiment. This data collection was essential for analyzing trends and the effectiveness of different dosages of activated carbon.

4.2.7.1.3 Effect of initial concentration

The experimental setup for analyzing the initial concentration of methylene blue on its adsorption through activated carbon was meticulously organized to ensure accurate and reproducible results. Six samples were prepared, each with a different initial concentration of methylene blue (40, 65, 90, 115, 140, and 165 mg/L). The procedure followed a consistent methodology across all samples to maintain uniformity in the experiment. Firstly, 100 ml of solution was used for each sample. This volume was chosen to provide sufficient liquid for thorough mixing and adsorption while being manageable within the experimental apparatus. Each sample solution was carefully measured to ensure precision in the experimental

conditions, which is crucial for reliable data. The samples were mixed with 0.25 grams of activated carbon. This specific mass of activated carbon was selected based on the result of the effect of dosage preliminary experimented to ensure a significant interaction between the dye and the activated carbon, thereby allowing the measurement of adsorption efficiency. The mass was accurately weighed using an analytical balance to maintain consistency across all samples.

The samples were agitated at a speed of 120 revolutions per minute (rpm). This agitation speed was critical to ensure that the activated carbon was evenly dispersed throughout the solution, promoting consistent contact between the methylene blue molecules and the carbon particles.. After agitation, a settling time of 10 minutes was allowed for the activated carbon to adsorb the methylene blue. The setup involved using identical flask for all samples to avoid errors. Each flask was marked with the respective initial concentration of methylene blue to prevent any mix-up during the experiment. This ensured that each sample was treated under identical conditions. The experiments were conducted at room temperature to avoid any variations in temperature that could influence the adsorption capacity of activated carbon. Samples were collected at the end of the settling period for analysis. The concentration of methylene blue remaining in the solution was measured using a spectrophotometer. A device that provided precise readings of the dye concentration, which were then compared to the initial concentration to determine the amount adsorbed by the activated carbon. Each sample's data were recorded meticulously, noting the initial and final concentrations of methylene blue, the mass of activated carbon used, and any observations during the experiment. This data collection was essential for analyzing trends and the effectiveness of different initial concentrations of methylene blue on its adsorption.

4.2.7.1.4 Effect of pH

To analyze the effect of pH on the adsorption of methylene blue, the experiment was set up with six samples at different pH levels (2, 4, 6, 8, 10, and 12). The preparation involved creating a blank for UV-spectrophotometer analysis for each pH level. This was done by adjusting the pH of each sample using 1M HCl and 1M NaOH solutions. The blanks were prepared separately for each sample to ensure accurate pH adjustment and reliable spectrophotometric readings. Each sample had a volume of 100 ml with a concentration of 90 mg/L. To prepare these samples, 0.25 grams of activated carbon was added to each. The used concentration was selected based on the preliminary test on the initial concentration effect that indicated complete removal for the sample with 90 mg/l. The contact time for the methylene blue with the

adsorbent was set at 60 minutes. This duration was chosen based previous experiment to ensure sufficient interaction time between the methylene blue molecules and the adsorbent material, allowing for a measurable degree of adsorption. During this period, the samples were subjected to constant agitation to maintain uniform suspension and maximize contact efficiency. The agitation speed was maintained at 120 rpm throughout the contact time. This speed was optimized to ensure adequate mixing of the methylene blue solution with the adsorbent particles, preventing settling and promoting uniform interaction. It was crucial to avoid speeds that might cause shear forces strong enough to disrupt the adsorbent particles.

After the contact time, a settling period of 10 minutes was allowed. This period enabled the solid adsorbent particles to settle, making it easier to separate the supernatant for analysis. The settling time was optimized to balance between efficient settling and minimizing the time the samples remained undisturbed. The pH of each sample was continuously monitored and adjusted as needed during the preparation and contact phases. The use of 1M HCl and 1M NaOH facilitated precise pH adjustments, ensuring that each sample maintained its designated pH level throughout the experiment. Accurate pH control was critical as pH variations could significantly influence the adsorption capacity of the adsorbent. For each sample, the UV-spectrophotometer was calibrated using the prepared blanks to establish a baseline for absorbance readings. This calibration was essential to correct for any background absorbance caused by the pH adjustments and to ensure the accuracy of the subsequent methylene blue concentration measurements. The UV-spectrophotometric analysis involved measuring the absorbance of each sample at the maximum wavelength specific to methylene blue (665nm). The absorbance readings were then used to calculate the remaining concentration of methylene blue in the solution, allowing for the determination of the adsorption efficiency at different pH levels. After completing the measurements for all samples, the data were analyzed to evaluate the effect of pH on the adsorption of methylene blue. The results provided insights into the optimal pH conditions for maximum adsorption efficiency, contributing to the understanding of the adsorption mechanisms involved.

4.2.7.1.5 Effect of Agitation speed

The experimental setup for analyzing the effect of agitation speed on the adsorption of methylene blue was meticulously organized to ensure accurate and reproducible results. Four samples were prepared, each subjected to a different agitation speed (28, 50, 75, and 120 revolutions per minute (rpm)). The procedure followed a consistent methodology across all

samples to maintain uniformity in the experiment. Firstly, 100 ml of solution was used for each sample. This volume was chosen to provide sufficient liquid for thorough mixing and adsorption while being manageable within the experimental apparatus. Each sample solution contained a methylene blue concentration of 90 mg/l, a value selected based to previous experiment to ensure a maximum interaction between the dye and the activated carbon, thereby allowing the measurement of adsorption efficiency. For the adsorbent, 0.25 grams of activated carbon was used in each sample. This consistent mass ensured that any differences in adsorption efficiency could be attributed to the variations in agitation speed rather than differences in the amount of activated carbon. The samples were agitated at their respective speeds using a mechanical shaker. This agitation was critical to ensure that the activated carbon was evenly dispersed throughout the solution, promoting consistent contact between the methylene blue molecules and the carbon particles. Uniform agitation minimized the potential for settling or clumping of the activated carbon, which could affect the adsorption process.

After the 60-minute agitation period, a settling time of 10 minutes was allowed for the activated carbon to adsorb the methylene blue. This period was optimized through preliminary trials to ensure sufficient adsorption occurred while preventing over-settling, which could complicate the separation of the carbon from the solution. The setup involved using identical flask for all samples to avoid variations in adsorption due to differences in container material or geometry. Each flask was marked with the respective agitation speed to prevent any mix-up during the experiment. Variations in temperature could influence the adsorption capacity of activated carbon, so the experiments were conducted at room temperature. Samples were collected at the end of the settling period for analysis. The concentration of methylene blue remaining in the solution was measured using a spectrophotometer. This device provided precise readings of the dye concentration, which were then compared to the initial concentration to determine the amount adsorbed by the activated carbon. Each sample's data were recorded meticulously, noting the initial and final concentrations of methylene blue, the agitation speed used, and any observations during the experiment. This data collection was essential for analyzing trends and the effectiveness of different agitation speeds on adsorption efficiency.

4.2.7.2 Adsorption isotherm and kinetics

4.2.7.2.1 Isotherm models fitting

4.2.7.2.1.1 Langmuir isotherm model

The Langmuir isotherm model fitting procedure begins by utilizing experimental data obtained from studying the effect of initial concentration on the adsorption of methylene blue onto sago seed activated carbon. This data is essential as it provides the necessary values for initial concentration (Ce) and the amount of adsorbate per unit mass of adsorbent at equilibrium (q_e). These values are critical inputs for the Langmuir isotherm model, which is a common model used to describe adsorption processes. To facilitate the data analysis, two software programs are employed: Excel and Origin Pro 8.5. Excel is used for initial data handling and calculation, while Origin Pro 8.5 is utilized for plotting and performing linear fitting of the data (eq 3.8). The first step in the fitting procedure involves using Excel to calculate the values of $\frac{Ce}{q_e}$ for each pair of Ce and q_e obtained from the experimental data. This calculation is straightforward and involves dividing each equilibrium concentration by the corresponding adsorption capacity. These calculated values are then used for the next step of the process.

Once the $\frac{Ce}{q_e}$ values are calculated, they are plotted against Ce in Origin Pro 8.5. Specifically, Ce is placed on the X-axis, and $\frac{Ce}{q_e}$ is placed on the Y-axis. This plotting helps visualize the data and allows for linear fitting. The linear fitting is crucial because the Langmuir isotherm model can be transformed into a linear form, which simplifies the process of determining the model parameters. After plotting the data in Origin Pro 8.5, a linear fit is performed. The software generates a table containing the results of the linear fitting, including the intercept, slope, and the coefficient of determination (R^2). These values are essential for calculating the Langmuir isotherm parameters. The intercept of the linear plot corresponds to $\frac{1}{q_{max}}$, while the slope corresponds to $\frac{1}{K_L * q_{max}}$. Using the intercept obtained from the linear fit, the maximum adsorption capacity q_{max} can be calculated as:

$$q_{max} = \frac{1}{intercept} \qquad \text{(eq 4.5)}$$

Similarly, the Langmuir constant K_L is calculated using the slope and the previously determined q_{max} value:

$$K_L = \frac{1}{Slope * q_{max}} \quad \text{(eq 4.6)}$$

With q_{max} and K_L known, the next step involves calculating the separation factor R_L , which indicates the favorability of the adsorption process. The separation factor is given by the equation:

$$R_L = \frac{1}{1+Ci*K_L} \quad \text{(eq 4.7)}$$

where Ci is the initial concentration related to the maximum equilibrium concentration, which in this case is 90 mg/L. The separation factor R_L provides insight into the nature of the adsorption process R_L values between 0 and 1 indicate a favorable adsorption.

The entire procedure emphasizes the importance of accurate data handling and the use of software tools to derive meaningful parameters from experimental data.

4.2.7.2.1.2 Freundlich isotherm model

The procedure for fitting the Freundlich isotherm model involves several steps, utilizing both experimental data and software tools such as Excel and Origin Pro 8.5. This process is applied specifically to the data obtained from experiments examining the effect of initial concentration on the adsorption of methylene blue onto sago seed activated carbon. The Freundlich isotherm model is represented by the linear equation (eq 3.6). The primary aim was to determine the constants associated with the Freundlich isotherm model, which describes adsorption characteristics in heterogeneous systems. The experimental data consists of measurements of initial concentrations and corresponding adsorption capacities. These values are denoted as Ce (equilibrium concentration) and q_e (amount adsorbed per unit mass of adsorbent). To begin the fitting process, the natural logarithms of these values need to be calculated. Using Excel, log Ce is computed from the equilibrium concentration data (Ce), and log q_e is computed from the adsorption capacity data (q_e). After calculating the logarithmic values, these data points are plotted on a graph with log Ce on the x-axis and log q_e on the y-axis. This plotting is done using Origin Pro 8.5 software, which allows for precise and efficient data visualization and analysis. Once the data points are plotted, a linear fitting procedure is carried out. This fitting generated a straight line that best represents the relationship between log Ce and log q_e. The linear fitting

results in a table provided by Origin Pro 8.5, which includes important statistical values such as the slope, intercept, and the coefficient of determination (R^2). These values were critical for determining the constants of the Freundlich isotherm. The slope of the linear plot corresponds to the constant $\frac{1}{n}$, while the intercept can be used to calculate the constant K_f. To find these constants, the following formulas are used: $\frac{1}{n}$ is directly taken as the slope from the linear fit, and K_f is calculated as 10 raised to the power of the intercept ($K_f = 10^{intercept}$). These calculations yield the final values of the Freundlich constants, which can then be used to describe the adsorption process under study. The procedure demonstrated the importance of software tools in scientific data analysis. Excel is used for preliminary data manipulation, ensuring that the raw experimental data is transformed into a usable format. Origin Pro 8.5 provided advanced capabilities for plotting and fitting, allowing for the accurate determination of model parameters. Through this method, the adsorption characteristics of methylene blue onto sago seed activated carbon are quantitatively described by the Freundlich isotherm model. This model fitting is crucial for understanding the efficiency and capacity of the adsorbent material under different conditions. The constants obtained can help predict how the adsorbent will behave in various scenarios, aiding in the optimization of adsorption processes for practical applications. Moreover, the R^2 value obtained from the linear fit provided an indication of how well the model described the experimental data. A high R^2 value suggests that the Freundlich model is a good fit for the data, while a lower R^2 might indicate the need for a different model or further refinement of the experimental conditions. Overall, the Freundlich isotherm model fitting procedure was a systematic approach that combines experimental data with computational tools to derive meaningful insights into adsorption phenomena. This methodology was not only applicable to the specific case of methylene blue and sago seed activated carbon but could also be adapted to other systems and adsorbates, making it a versatile tool in the field of adsorption studies.

4.2.7.2.1.3 Temkin isotherm model

The Temkin isotherm model fitting method involves the use of experimental data to analyze the adsorption of methylene blue onto sago seed activated carbon. The initial step in this process was to gather data from the experiments focused on how the initial concentration of methylene blue affects its adsorption onto the activated carbon. This data included measurements of the equilibrium concentration of methylene blue (Ce) and the amount of methylene blue adsorbed per unit mass of activated carbon (q_e). To begin the fitting procedure,

the data obtained from these experiments were processed using Excel and Origin Pro 8.5 software. In Excel, the natural logarithm of the equilibrium concentration (ln Ce) is calculated from the experimental Ce values. Additionally, the corresponding q_e values from the experiment are organized for further analysis. This step ensured that the data was appropriately formatted for subsequent plotting and fitting. Next, the processed data was imported into Origin Pro 8.5, where a plot is created with ln Ce on the X-axis and q_e on the Y-axis. A linear fitting was then performed on this plot to establish a relationship between these two variables. The linear fitting process in Origin Pro 8.5 yields a table containing the intercept, slope, and the coefficient of determination (R^2) values. These values were crucial for determining the parameters of the Temkin isotherm model. Using the results from the linear fitting, the slope of the line was directly equated to the parameter B_T. The intercept obtained from the fitting was then used to calculate the parameter K_T. This calculation involved taking the exponential of the intercept divided by B_T, using the formula $K_T = \exp^{(\text{intercept}/BT)}$. These parameters, B_T and K_T, were essential components of the Temkin isotherm equation and helped in understanding the adsorption characteristics of the methylene blue onto the sago seed activated carbon.

The entire fitting procedure was crucial for deriving the Temkin isotherm model parameters, which provided insights into the adsorption process. The model assumed that the heat of adsorption decreases linearly with the coverage due to adsorbent-adsorbate interactions. This assumption was reflected in the Temkin isotherm linear equation, which is expressed as follow [76]:

$$q_e = \frac{R_T}{b_T} \ln A_T + \left(\frac{R_T}{b_T}\right) \ln C_e \qquad \text{(eq 4.8)}$$

where R_T is the universal gas constant multiplied by the temperature. By fitting the experimental data to this model, we could validate whether the Temkin isotherm accurately describes the adsorption process for the system under study. The values of B_T and K_T obtained from the fitting procedure helped quantify the adsorption capacity and the nature of the interactions between the methylene blue molecules and the activated carbon surface. The fitting process also involves verifying the quality of the fit by examining the R^2 value. A high R^2 value indicated that the linear model fits the experimental data well, suggesting that the Temkin isotherm is an appropriate model for describing the adsorption process. Conversely, a low R^2 value may implied that the model does not adequately capture the adsorption behavior, necessitating the consideration of alternative models or additional experimental data. Overall, the Temkin isotherm model fitting procedure was a systematic approach that combined

experimental data processing, plotting, and linear fitting to derive meaningful parameters that described the adsorption process. This procedure not only helped in understanding the adsorption characteristics but also aids in optimizing the use of adsorbents for practical applications such as wastewater treatment and pollutant removal. The Temkin isotherm model fitting method provided a robust framework for analyzing adsorption data. By following the detailed steps of data processing, plotting, and fitting, we could extract valuable information about the adsorption behavior and interactions within the system. The calculated parameters B_T and K_T offered insights into the adsorption capacity and the nature of the adsorbent-adsorbate interactions.

4.2.7.2.2 Kinetics models fitting

4.2.7.2.2.1 Pseudo First order kinetic model

The procedure for fitting a pseudo first order kinetic model involved using experimental data obtained from the adsorption of methylene blue onto sago seed activated carbon. This data specifically related to the effect of contact time on the adsorption process. To fit this data into the pseudo first order kinetic model linear equation (eq 3.2). Initially, the data from the experiment is processed using Excel to compute the values of ln ($q_e - q_t$). In this context, q_e is predetermined as 36 mg/g from prior experiments concerning the effect of initial concentration on the adsorption. The qt values, which represent the adsorption capacity at various time points, are used to calculate ln ($q_e - q_t$). After calculating these values, the data is plotted using Origin Pro 8.5 software. In this plot, the time t is represented on the X-axis, and ln ($q_e - q_t$) is plotted on the Y-axis. This step is essential to visualize the relationship between these variables and to perform the linear fitting necessary for model fitting. The next step involves performing a linear fit on the plotted data in Origin Pro 8.5. This process yields a table of results that includes the intercept, slope, and R^2 values of the fitted line. The R^2 value, which indicates the goodness of fit, is crucial for assessing how well the model represents the experimental data. With the intercept and slope values obtained from the linear fitting, the equilibrium adsorption capacity q_e and the rate constant K_1 can be calculated. Specifically, q_e is determined by taking the exponential of the intercept value. This relationship arised because the intercept in the linear equation corresponds to ln (q_e). To find the rate constant K_1, the slope value from the linear fit is used directly. Since the pseudo first order kinetic model equation is derived from integrating a first order rate equation, the slope of the linear plot represents $-K_1$. Hence, the rate constant K_1 is computed directly from the slope value. The entire process relied heavily on accurate data

handling and precise linear fitting, ensuring that the experimental observations align well with the theoretical model. It was important to use consistent and correct values throughout the procedure to avoid errors in the final kinetic parameters. The suitability of a contact time of 60 minutes is also considered in this procedure. This time frame was established from previous experiments that examined the effect of contact time on adsorption. By using this optimized contact time, the derived kinetic parameters are more reliable and relevant for the specific system under study.

4.2.7.2.2.2 Pseudo Second order kinetic model

The procedure described focuses on fitting a pseudo-second-order kinetic model to data obtained from an experiment on the adsorption of methylene blue onto sago seed activated carbon. The process utilized both Excel and Origin Pro 8.5 software for data manipulation and analysis. The goal was to determine the kinetic parameters that described the adsorption process. Initially, data from the experiment, specifically the effect of contact time on the adsorption of methylene blue, was used. The pseudo-second-order kinetic model was represented by the linear equation (eq 3.4). The fitting procedure starts with calculating $\frac{t}{q_t}$ for each time point using Excel. This involves dividing the contact time (in minutes) by the amount adsorbed (q_t) at each corresponding time point. Once the $\frac{t}{q_t}$ values are computed, they were plotted against time t using Origin Pro 8.5. In this plot, time t was on the x-axis and $\frac{t}{q_t}$ on the y-axis. A linear regression was then performed on this data to obtain the slope and intercept of the linear fit, as well as the coefficient of determination (R_2), which indicated how well the model fits the experimental data. From the linear fit, the slope and intercept values were critical. The equilibrium adsorption capacity q_e was calculated using the slope of the line, where:

$$q_e = \frac{1}{Slope} \qquad \text{(eq 4.11)}$$

Next, the rate constant K_2 was determined using both the intercept and the previously calculated q_e. The formula used for this calculation was:

$$K_2 = \frac{1}{intercept * q_e 2} \qquad \text{(eq 4.12)}$$

To ensure accuracy, q_e^2 (the square of q_e) was used in the calculation of K_2. These steps summarize the fitting procedure and calculations necessary to fit a pseudo-second-order kinetic

model to the experimental data. Throughout this process, it was essential to meticulously follow each step to avoid errors. For instance, correct plotting and accurate linear regression were crucial to obtaining reliable slope and intercept values. The use of software like Origin Pro 8.5 helped streamline these tasks and provided precise results. Moreover, the coefficient of determination (R_2) was a valuable indicator of the goodness of fit. A value close to 1 implied a good fit of the model to the data, reinforcing the reliability of the calculated kinetic parameters. This methodical approach allowed us to understand the kinetics of the adsorption process better. The derived parameters, q_e and K_2, were essential for modeling and predicting adsorption behavior under different conditions, facilitating the design and optimization of adsorption systems.

4.2.7.2.2.3 Elovich kinetic model

The Elovich kinetic model fitting method involves a systematic approach to analyze the adsorption data obtained from experiments. In this specific procedure, the focus is on the adsorption of methylene blue onto sago seed activated carbon. The primary goal was to determine the parameters of the Elovich kinetic model, which were the primary rate of adsorption (α) and the desorption constant (β). This is achieved using data processing software such as Excel and Origin Pro 8.5. The Elovich kinetic model is described by the equation[76]:

$$q_t = \frac{1}{\beta}\ln(\alpha\beta) + \frac{1}{\beta}\ln t \qquad \text{(eq 4.13)}$$

where q_t is the amount of adsorbate adsorbed at time t, α is the initial adsorption rate, and β is related to the extent of surface coverage and activation energy for chemisorption. The fitting procedure begins with the collection of experimental data on the effect of contact time in the adsorption process. Firstly, the experimental data, specifically the time (in minutes) and q_t values, are recorded. Using Excel, the natural logarithm of time (ln t) was calculated for each data point. These transformed data points were then plotted with ln t on the X-axis and q_t on the Y-axis using Origin Pro 8.5 software. Once the data was plotted, a linear fitting was performed. The linear fitting process in Origin Pro 8.5 generated a table of results that included the slope, intercept, and the coefficient of determination (R^2 value). These values were critical for determining the parameters of the Elovich model. The slope obtained from the linear fit was used to calculate β by taking the reciprocal of the slope:

$$\left(\beta = \frac{1}{Slope}\right) \qquad \text{(eq 4.14)}$$

This step was crucial as β represents the desorption constant in the model. Following this, the intercept of the linear fit was used in conjunction with β to determine α.

The intercept was initially given by:

$$\frac{1}{\beta}\ln(\alpha\beta) \qquad \text{(eq 4.15)}$$

By multiplying the intercept by β, the expression simplifies to ln(αβ). This could be further broken down to lnα+lnβ. Therefore, by isolating lnα, it could be calculated using the equation

$$\ln \alpha = (\text{intercept} \times \beta) - \ln \beta \qquad \text{(eq 4.16)}$$

To obtain α from lnα, the exponential function was applied, resulting in $\alpha = e^{\ln\alpha}$. This final calculation provided the primary rate of adsorption, completing the determination of both parameters of the Elovich isotherm model. The entire procedure relied heavily on the accuracy of the initial experimental data and the precision of the calculations performed using software tools. The quality of the linear fit, as indicated by the R^2 value, also plays a significant role in the reliability of the determined parameters.

4.2.8 Data analysis, presentations and dissemination methods

The study's findings were presented through tables and graphs. Furthermore, the adsorption test results were analyzed using both Excel and OriginPro 8.5 software. Linear fitting analysis was performed in OriginPro for linear analysis. The outcome of this study will be submitted to the University of Rwanda's Department of Civil, Environmental & Geomatic Engineering, shared with relevant parties, and published in an internationally peer-reviewed journal.

CHAPTER5: RESULTS, ANALYSIS AND DISCUSSION

5.1 Effect of Activation temperature on carbon yield

The results indicate a clear trend, as the activation temperature increases, the carbon yield decreases significantly. At 500°C, the carbon yield is extremely high, at 99.1%, suggesting minimal decomposition of the sago seed char at this relatively low temperature. This yield slightly decreases to 97.9% at 600°C, indicating a minor increase in decomposition but still maintaining a high level of carbon retention. These temperatures suggest the initial stages of thermal degradation, where most of the biomass's structural integrity is preserved.

A more drastic reduction in yield is observed at 700°C, where the carbon yield plummets to 36%. This substantial drop signifies a significant breakdown of the organic material, transitioning from a predominantly solid state to more volatile compounds. This temperature marks the onset of more intense pyrolytic reactions, where the biomass undergoes substantial structural decomposition, resulting in a significant loss of mass.

At 800°C, the yield further decreases to 8.5%, demonstrating an almost complete decomposition of the original biomass material. By this temperature, the majority of the organic compounds have been converted into gases or tar, leaving behind a minimal amount of solid residue. The negligible yield at this stage highlights the high efficiency of the pyrolysis process in breaking down the biomass.

Table 5.1: Results of effect of Activation temperature on carbon yield (Wi: initial weight and Wf: final weight)

Sago Seed			
Temperature (°C)	**Wi (g)**	**Wf(g)**	**Yield**
500	10	9.91	99.1
600	10	9.79	97.9
700	10	3.6	36
800	10	0.85	8.5
900	10	0	0
1000	10	0	0

Finally, at temperatures of 900°C and 1000°C, the carbon yield drops to zero, indicating complete volatilization of the sago seed biomass. At these extreme temperatures, all organic material was burned off, leaving no solid char behind. This suggests that the upper limit for efficient carbon yield from sago seeds lies below 900°C, as any higher temperature results in

total loss of solid carbon content. The common understanding is that while both temperature and chemical activator are crucial in the pyrolysis process, the best temperature for maximizing carbon yield appears to be around 500 - 600°C, where high carbon retention is achieved with minimal decomposition. This outcome is comparable to the investigation done by (Togibasa et al., 2021) where 500°C appears to be the best temperature set to achieve high value of carbon yield [149].

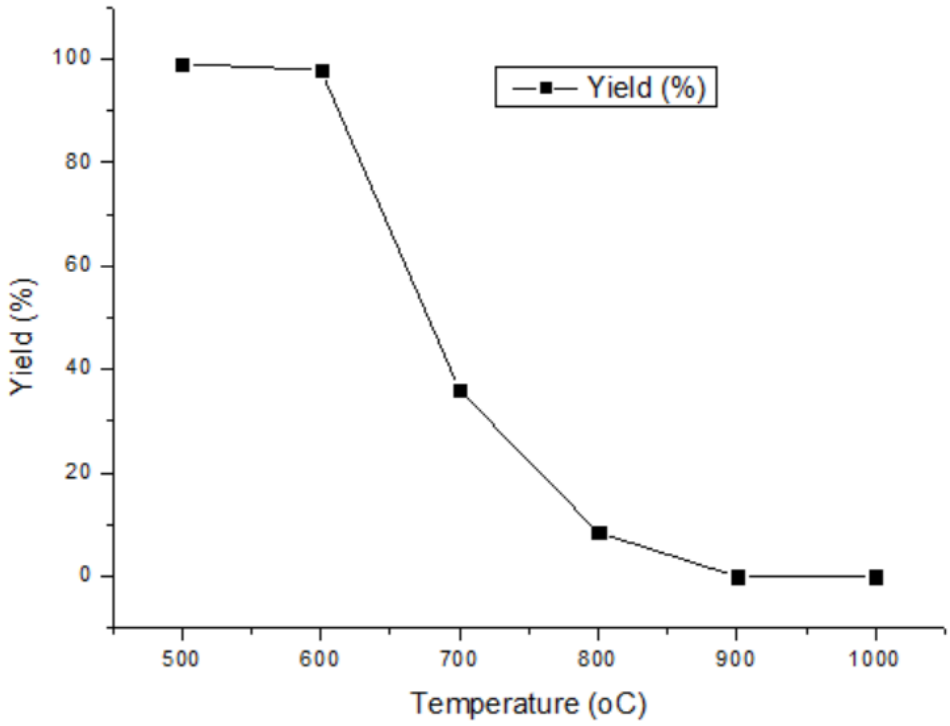

Figure 5.1: Effect of Activation temperature on carbon yield

5.2 Characterization of sago seed activated carbon

5.2.1 XRF analysis

The X-ray fluorescence (XRF) analysis of Sago seed raw material (SSRW) and Sago seed activated carbon (SSAC) offers comprehensive insights into the chemical composition changes induced by the activation process. The treatment of the raw sago seed material with phosphoric acid to produce activated carbon, significantly altering its elemental profile and enhanced its suitability for applications in adsorption.

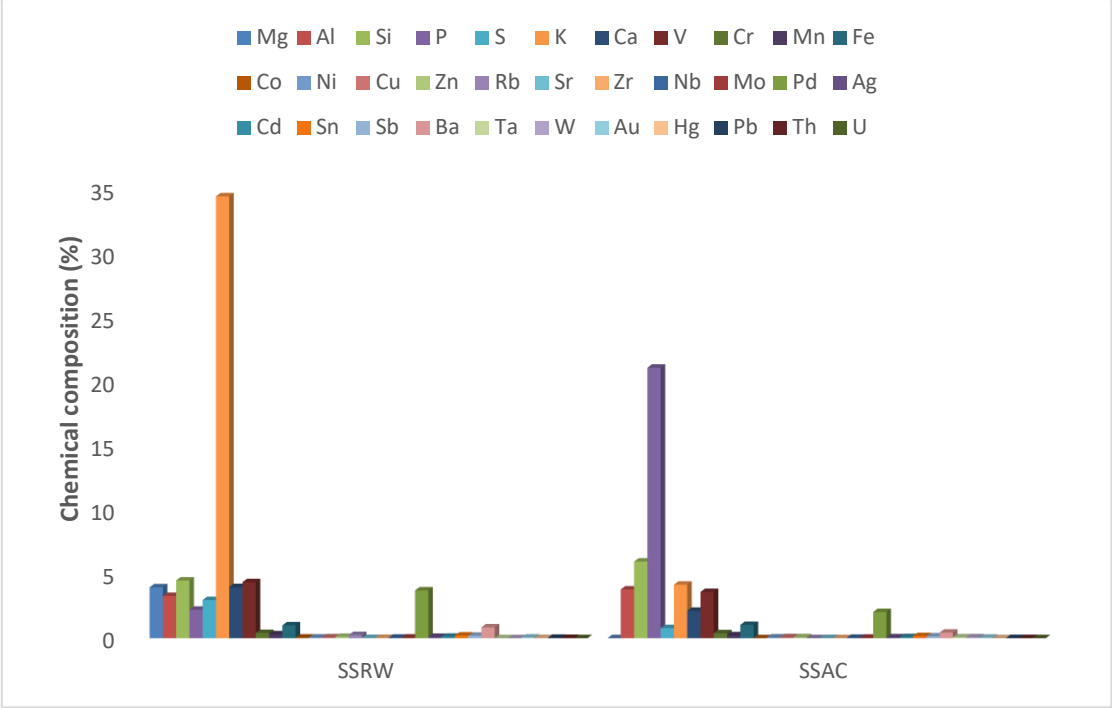

Figure 5.2: X- ray fluorescence (XRF) analysis of the chemical composition of Sago seed raw material (SSRW) and Sago seed Activated carbon (SSAC)

(Ni) and copper (Cu) show marginal increases, while others like cobalt (Co) and mercury (Hg) are completely eliminated in SSAC. For instance, cobalt and mercury are present in SSRW at 0.04% and 0.02%, respectively, but are undetectable in SSAC. This elimination is advantageous, particularly if these elements are considered undesirable contaminants. Moreover, trace elements such as vanadium (V), chromium (Cr), manganese (Mn), zinc (Zn), and others show various degrees of reduction or minor increases. Lead (Pb), for example, decreases from 0.03% in SSRW to 0.009% in SSAC, reflecting the purification effect of the activation process. Other elements like palladium (Pd), silver (Ag), and gold (Au) decrease after activation, likely due to partial volatilization or transformation during the high-temperature processes. The presence of rare earth and heavy metals in both raw and activated materials, albeit in trace amounts, is also notable. Elements such as cadmium (Cd), lead (Pb), and uranium (U) are present in reduced quantities in the activated carbon, underscoring the effectiveness of the activation and washing processes in reducing potential contaminants. Overall, the XRF analysis demonstrates that activating sago seeds with phosphoric acid significantly modifies their chemical composition. The process removes certain elements while introducing phosphorus 21.09%. A similar investigation conducted by (Xie et al., 2009), on orange peels activated by H_3PO_4 resulted in a phosphorus percentage of 2.31% [150]. This comparison illustrates the high capacity of sago seeds to incorporate phosphorus in high

concentrations, thereby enhancing their properties as an adsorbent. The changes observed in the analysis of sago seeds suggest that the produced activated carbon is more suitable for applications requiring high purity and specific elemental characteristics, such as water purification. The stability of elements like aluminum and silicon further indicates their role in maintaining the structural integrity of the activated carbon.

5.2.2 functional group analysis

5.2.2.1 FTIR spectra of Sago Seed powder (Raw material)

The FTIR spectrum of the sago seed raw material shows distinct peaks at 3274.52 cm^{-1}, 2920.74 cm^{-1}, 1638.98 cm^{-1}, 1536.52 cm^{-1}, 1242.66 cm^{-1}, and 1147.93 cm^{-1}. The broad peak at 3274.52 cm^{-1} is indicative of O-H stretching vibrations, typically associated with hydroxyl groups from water or alcohols. The peak at 2920.74 cm^{-1} corresponds to C-H stretching, signifying the presence of aliphatic hydrocarbons. The peaks at 1638.98 cm^{-1} and 1536.52 cm^{-1} suggest the presence of carbonyl (C=O) and amide (N-H) groups, respectively, hinting at the presence of proteins or other nitrogen-containing compounds. Lastly, the peaks around 1242.66 cm^{-1} and 1147.93 cm^{-1} are attributed to C-O stretching vibrations, pointing to alcohols, ethers, or esters within the material.

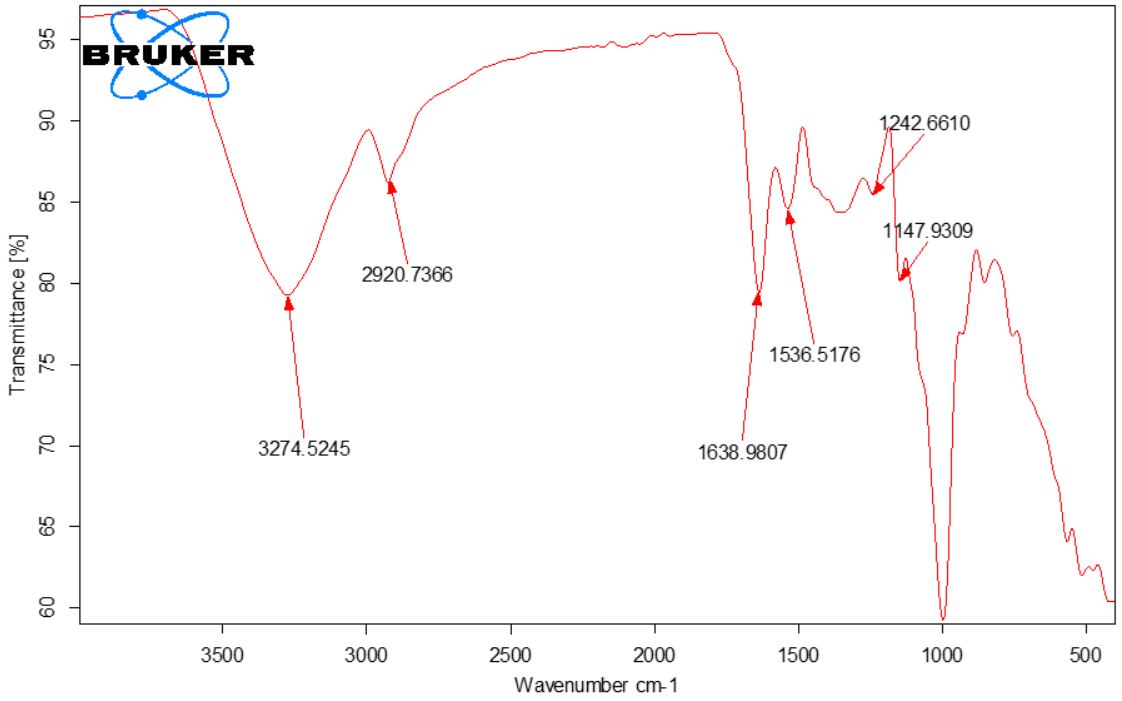

Figure 5.3: FTIR spectra of Sago Seed powder (Raw material)

5.2.2.2 FTIR spectra of Sago Seed Activated carbon before adsorption

The activated carbon derived from sago seeds before adsorption exhibits significant peaks at 1563.58 cm^{-1}, 1157.60 cm^{-1}, 1064.80 cm^{-1}, 1994.70 cm^{-1}, and 2323.36 cm^{-1}. The peak at 1563.58 cm^{-1} continues to reflect the N-H bending vibrations, indicating that some nitrogenous components remain post-activation. The C-O stretching vibrations persist in the peaks at 1157.60cm^{-1} and 1064.80 cm^{-1}. The new peaks at 1994.70 cm^{-1} and 2323.36 cm^{-1} suggest the formation of conjugated carbonyl or nitrile groups, which are characteristic of more structured carbon materials formed during the activation process. These changes indicate that activation modifies the raw material's chemical structure, enhancing its adsorption properties.

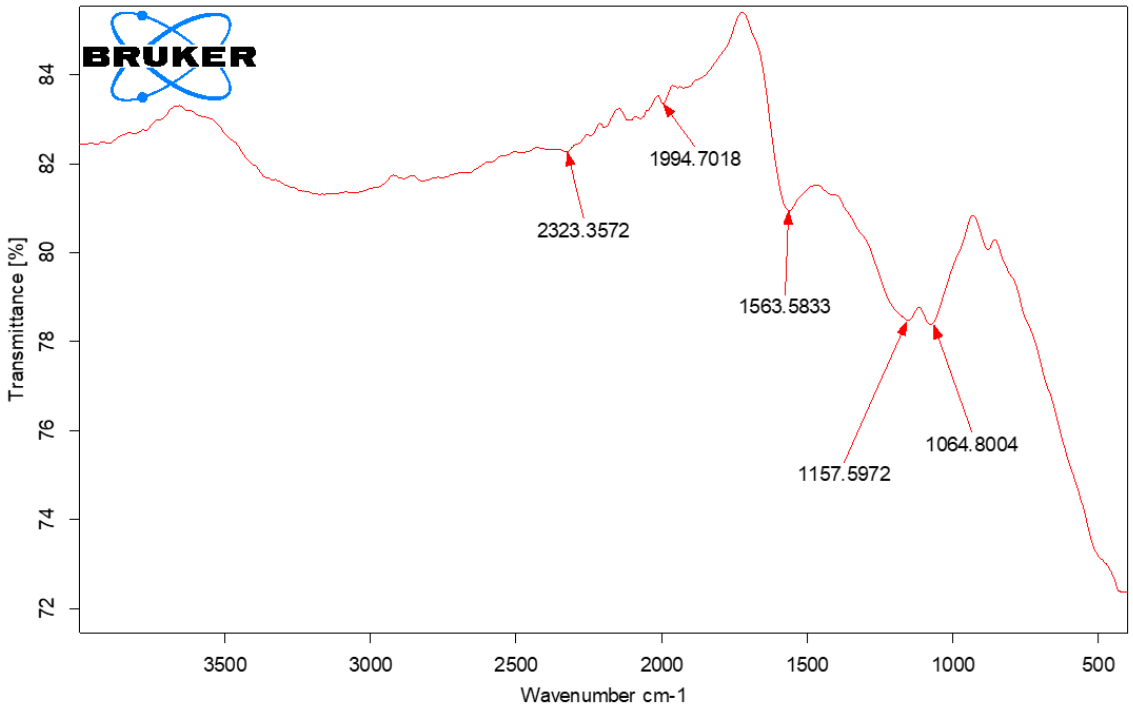

Figure 5.4: FTIR spectra of Sago Seed Activated carbon before adsorption

5.2.2.3 FTIR spectra of Sago Seed Activated carbon after adsorption

After adsorption, the FTIR spectrum of the activated carbon shows peaks at 1565.52 cm^{-1}, 1144.06 cm^{-1}, 1064.80 cm^{-1}, 1312.26 cm^{-1}, 1383.79 cm^{-1}, and 2329.16 cm^{-1}. The peak at 1565.52 cm^{-1}, similar to that before adsorption, suggests that N-H bending vibrations remain,

indicating that some nitrogenous compounds persist even after adsorption. The peaks at 1144.06 cm^{-1} and 1064.80 cm^{-1} reflect the ongoing presence of C-O stretching vibrations. New peaks at 1312.26 cm^{-1} and 1383.79 cm^{-1} indicate changes in the chemical environment or the formation of new functional groups due to adsorption, which might result from interactions between the adsorbent and adsorbate. The persistence of the peak at 2329.16 cm^{-1} points to stable functional groups that have not been significantly altered by the adsorption process.

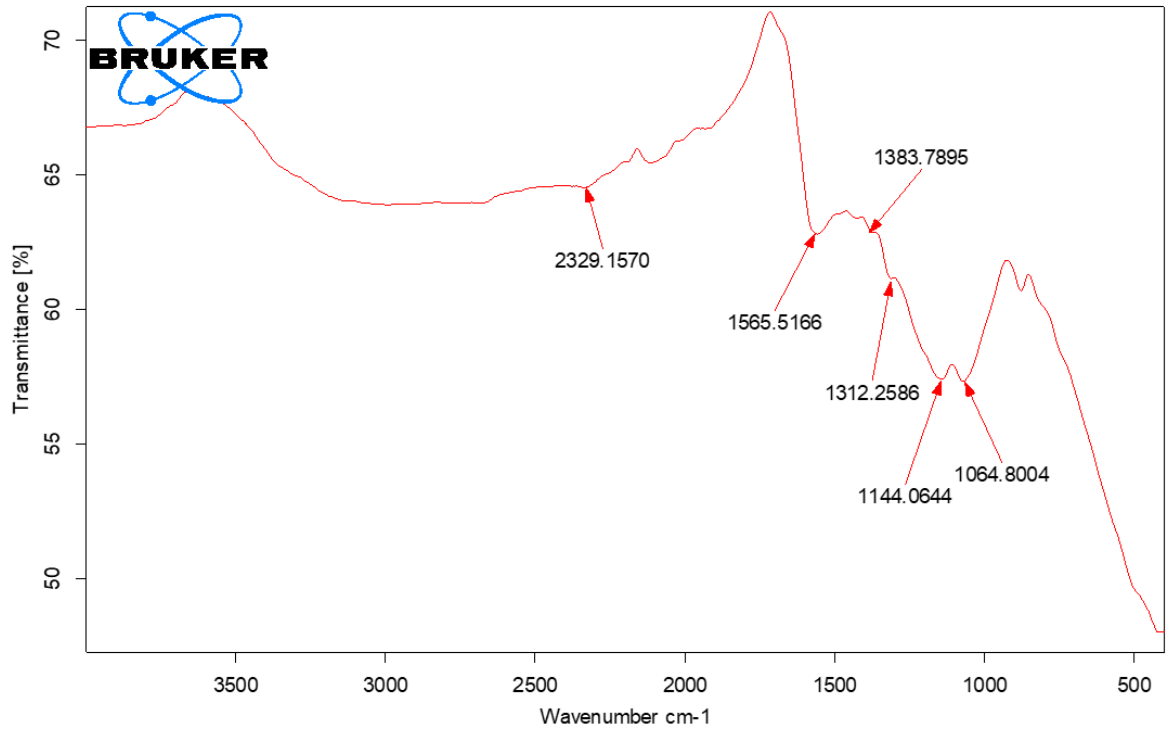

Figure 5.5: FTIR spectra of Sago Seed Activated carbon after adsorption

5.3 Effect of contact time

In terms of methodology, the research involved the preparation of activated carbon from sago seeds followed by its exposure to methylene blue solutions. Measurements were taken at various time intervals, ranging from 30 to 80 minutes, to evaluate the dye removal efficiency. Key parameters such as absorbance, dye concentration (Ct), adsorption capacity (qt), and removal rate (%) were meticulously recorded, providing a comprehensive dataset for analysis.

The initial phase of adsorption reveals a rapid decrease in absorbance from 0.18 to 0.10 within the first 30 minutes, indicating a substantial reduction in dye concentration from 0.96 mg/l to

0.51 mg/l. This suggests that the activated carbon exhibits a high initial adsorption rate, effectively capturing a significant amount of dye molecules from the solution in a short period.

Table 5.2: The Effect of Contact time on the percentage removal of Methylene Blue by Sago seed activated carbon data

Time (min)	Absorbance	Ct (mg/l)	qt (mg/g)	Removal rate (%)
30	0.18	0.96	35.61	88.93
40	0.10	0.51	35.79	89.43
50	0.01	0.07	35.97	89.92
60	0.002	0.02	35.99	89.98
70	0.009	0.06	35.98	89.94
80	0.007	0.04	35.98	89.95

As the contact time extends beyond 50 minutes, the data indicates a plateau in the removal rate and adsorption capacity. The removal rate increases only marginally from 89.43% at 40 minutes to 89.95% at 80 minutes, and the adsorption capacity stabilizes around 35.97 mg/g. This plateau suggests that the adsorption sites on the activated carbon are nearing saturation, and additional contact time yields diminishing improvements in dye removal.

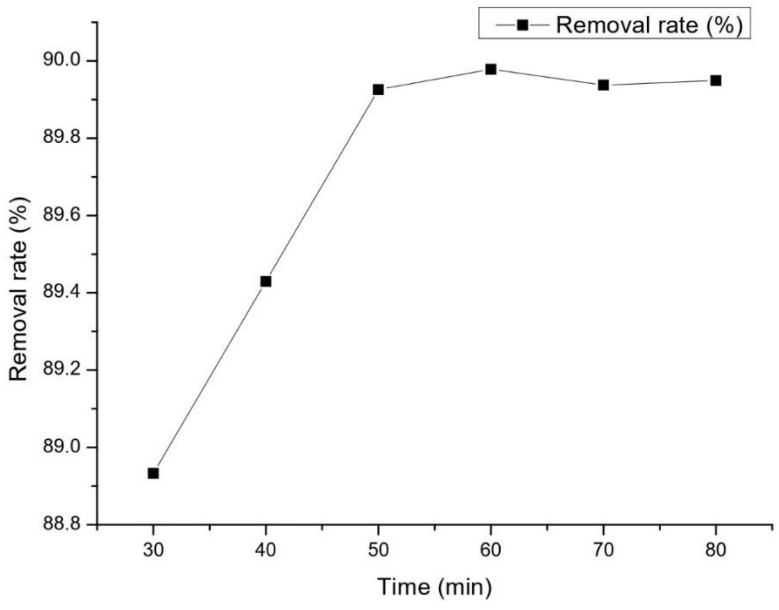

Figure 5.6: The Effect of Contact time on the percentage removal of Methylene Blue by Sago seed activated carbon

The identification of 50 minutes as the optimal contact time is a critical finding. At this point, the removal rate is nearly maximal, and the adsorption capacity has reached a stable level. A similar work was done by (Mulushewa et al., 2021) using Kaolin and Zeolite X as adsorbent for methylene blue removal from textile wastewater in Ethiopia and they found an optimal contact time of 60 min for zeolite-X achieving equilibrium faster than kaolin which is 80 min [3]. The mechanisms underlying the adsorption process likely include physical adsorption and potential chemical interactions between the dye molecules and the functional groups on the activated carbon surface. The rapid initial adsorption phase can be attributed to the high surface area and pore volume of the sago seed activated carbon, facilitating swift dye uptake.

5.4 Effect of initial concentration

The initial concentrations tested range from 40 mg/L to 165 mg/L, with corresponding removal rates, adsorption capacities, and equilibrium concentrations. Notably, the removal rates are exceptionally high across all tested concentrations, peaking at 99.95% for an initial concentration of 65 mg/L. This high removal efficiency underscores the potential of SSAC as a highly effective adsorbent for methylene blue, capable of achieving near-complete removal under optimal conditions.

Table 5.3: The Effect of initial concentration on the percentage removal of Methylene Blue by Sago seed activated carbon data

Initial concentration (mg/l)	Absorbance	Ce (mg/l)	qe (mg/g)	Removal rate (%)
40	0.006	0.04	15.98	99.90
65	0.005	0.03	25.98	99.94
90	0.10	0.52	35.79	99.42
115	0.13	0.72	45.71	99.37
140	0.60	3.17	54.73	97.73
165	1.90	10.02	61.99	93.92

The adsorption capacity (q_e) of SSAC increases with the initial concentration, starting from 15.98 mg/g at 40 mg/L and reaching 61.99 mg/g at 165 mg/L. This trend suggests that higher initial concentrations provide a greater driving force for mass transfer, leading to increased adsorption, which aligned with the same results obtained by (Fito et al., 2023) in their investigation on the adsorption of methylene blue from textile industrial wastewater using activated carbon developed from Rumex abyssinicus plant [144]. As the concentration of methylene blue rises, more dye molecules are available to interact with the adsorption sites on

SSAC, thereby enhancing the adsorption capacity. The equilibrium concentration (Ce), which represents the residual dye concentration in the solution after adsorption, also increases with the initial concentration. This indicates that at higher initial concentrations, the SSAC becomes saturated more quickly, leaving a higher residual concentration of methylene blue in the solution. This saturation effect is a common characteristic of adsorbents and highlights the importance of optimizing initial concentrations for effective adsorption.

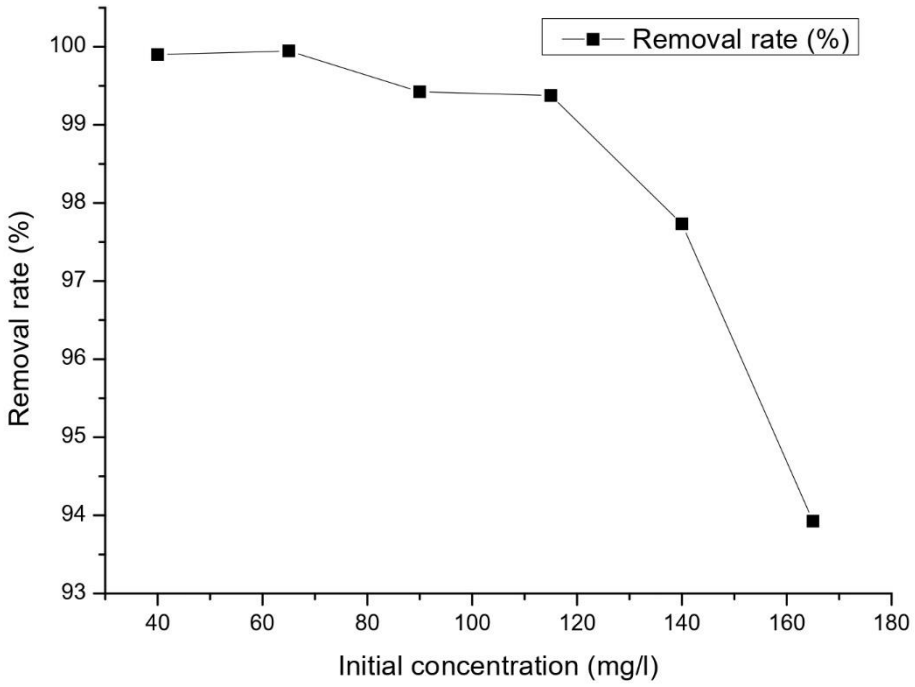

Figure 5.7: The Effect of initial concentration on the percentage removal of Methylene Blue by Sago seed activated carbon

The high removal efficiency across all initial concentrations demonstrates the robustness of SSAC in adsorbing methylene blue. This effectiveness can be attributed to the high surface area and porosity of the activated carbon, which provides numerous active sites for adsorption. The consistent performance of SSAC across varying concentrations suggests that it can be a reliable adsorbent in different settings, particularly in wastewater treatment applications where dye pollutants are prevalent.

5.5 Effect of adsorbent dosage

The experimentation results on the effect of Dosage on the removal of methylene blue by sago seed activated carbon provides an insightful analysis of how varying the dosage of sago seed activated carbon affects the removal efficiency of methylene blue from aqueous solutions. Firstly, the data demonstrates a clear inverse relationship between the dosage of activated carbon and the absorbance of methylene blue (Table 8). As the dosage increases from 0.01g to 0.25g, the absorbance decreases significantly from 3.23 to 0.01. This reduction in absorbance indicates that higher dosages of sago seed activated carbon are more effective in removing methylene blue from the solution, suggesting increased adsorption efficiency.

Table 5.4: The Effect of Dosage on the percentage removal of Methylene Blue by Sago seed activated carbon data

Dosage (g)	Absorbance	Ce (mg/l)	qe (mg/g)	Removal rate (%)
0.01	3.23	16.98	730.16	81.13
0.05	2.97	15.59	148.81	82.67
0.1	1.60	8.42	81.57	90.64
0.15	0.29	1.54	58.97	98.29
0.2	0.02	0.08	899.14	99.90
0.25	0.01	0.04	899.56	99.95

Moreover, the equilibrium concentration (Ce) of methylene blue in the solution decreases as the dosage of activated carbon increases. At the lowest dosage of 0.01g, Ce is 16.98 mg/l, whereas at the highest dosage of 0.25g, (Ce) drops drastically to 0.04 mg/l. This trend highlights the enhanced capability of sago seed activated carbon to lower the concentration of methylene blue in the solution at higher dosages, thus achieving better purification. The adsorption capacity (q_e), defined as the amount of dye adsorbed per unit mass of the adsorbent, exhibits a more complex pattern. At the lowest dosage, q_e is extremely high (730.16 mg/g), but it decreases initially as the dosage increases, reaching 81.58 mg/g at a dosage of 0.1g. Interestingly, at higher dosages, q_e increases again, peaking at 899.56 mg/g at the highest dosage of 0.25g. This pattern suggests an optimal dosage range where the adsorption efficiency is maximized before potential aggregation effects at very high dosages. In comparison to a study where methylene blue is removed by using ZnO nanoparticles. The result shown a higher removal efficiency at lower dosage, but the adsorption capacity decreases as the dosage increases [151]. Despite the difference range of adsorbent studied [0.01 - 0.25] g/l for sago

seeds and [0.1 – 5] g/l for ZnO nanoparticles. The SSAC demonstrate a near complete removal of MB even at lower quantities, while ZnO nanoparticules could achieve a removal efficiency up to 93 %.

Another critical parameter is the removal rate of methylene blue, which increases consistently with higher dosages of activated carbon. Starting from 81.13 % at 0.01g, the removal rate climbs to 99.95 % at 0.25g. This near-complete removal at higher dosages underscores the effectiveness of sago seed activated carbon as an adsorbent for methylene blue.

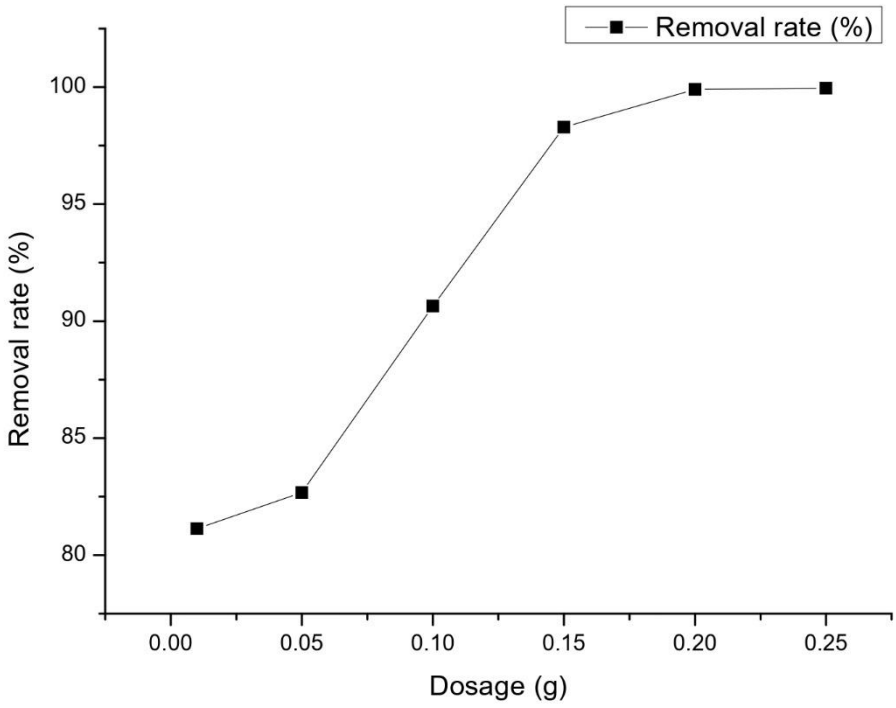

Figure 5.8: The Effect of Dosage on the percentage removal of Methylene Blue by Sago seed activated carbon

The most appropriate dosage of sago seed activated carbon for the removal of methylene blue, based on the obtained results, appears to be 0.2 g. This dosage achieves a near-complete removal rate of 99.90 %, with the equilibrium concentration (Ce) of methylene blue dropping to 0.08 mg/l and the adsorption capacity (q_e) reaching 899.14 mg/g. This dosage provides a balance between high removal efficiency and effective utilization of the activated carbon, without significant overuse that might lead to diminishing returns or unnecessary cost increases. The results give also an idea about the underlying mechanisms contributing to these observed trends. Typically, increased dosages of activated carbon provide a larger surface area

and more active sites for adsorption, which directly contributes to the enhanced removal rates and decreased equilibrium concentrations observed. However, at very high dosages, the adsorption capacity per unit mass may vary due to factors such as particle aggregation and saturation of active sites.

5.6 Effect of pH

In this stage of the study, the experiment focused on evaluating the effect of pH on the adsorption efficiency of methylene blue by the activated carbon derived from sago seeds. By varying the pH levels from 2 to 12, we aimed to determine how changes in pH influence the absorbance, equilibrium concentration (Ce), amount adsorbed at equilibrium (q_e), and overall removal rate of methylene blue. The results indicated a significant dependence of the adsorption process on the pH level, with an increasing trend in the removal rate observed as the pH was raised.

Table 5.5: The Effect of pH on the percentage removal of Methylene Blue by Sago seed activated carbon data

pH	Absorbance	Ce (mg/l)	qe (mg/g)	Removal rate (%)
2	1.90	10.02	31.99	88.87
4	0.80	4.24	34.30	95.29
6	0.29	1.56	35.38	98.27
8	0.11	0.61	35.75	99.32
10	0.01	0.06	35.97	99.93
12	0	0.009	36	99.99

At pH 2, the absorbance of methylene blue was measured at 1.90, leading to an equilibrium concentration (Ce) of 10.02 mg/l and an adsorption capacity (q_e) of 31.99 mg/g. The removal rate at this acidic pH was 88.87 %, suggesting a moderate adsorption efficiency of the activated carbon under these conditions. Increasing the pH to 4 resulted in a slight decrease in absorbance to 0.80 and a corresponding reduction in Ce to 4.24 mg/l. Consequently, the q_e slightly increased to 34.30 mg/g, and the removal rate improved marginally to 95.29 %. As the pH was further increased to 6, a more noticeable decrease in absorbance to 0.29 was recorded, along with a reduction in Ce to 1.56 mg/l. This led to a q_e of 35.38 mg/l and a further improvement in the removal rate to 98.27 %. At pH 8, the absorbance continued to drop to 0.11, with a corresponding Ce of 0.61 mg/l. The q_e remained high at 35.75 mg/l, and the removal rate increased to 99.32 %, indicating enhanced adsorption efficiency at this pH level. When the pH

was raised to 10, the absorbance was minimal at 0.01, resulting in a very low Ce of 0.06 mg/l. The q_e was 35.97 mg/l, and the removal rate reached an almost perfect 99.93 %. At the highest pH level tested, pH 12, the absorbance dropped to zero, indicating complete adsorption of methylene blue. The Ce was recorded at 0.008 mg/l, with a q_e of 35.99 mg/g, and the removal rate peaked at 99.99 %, demonstrating the highest adsorption efficiency.

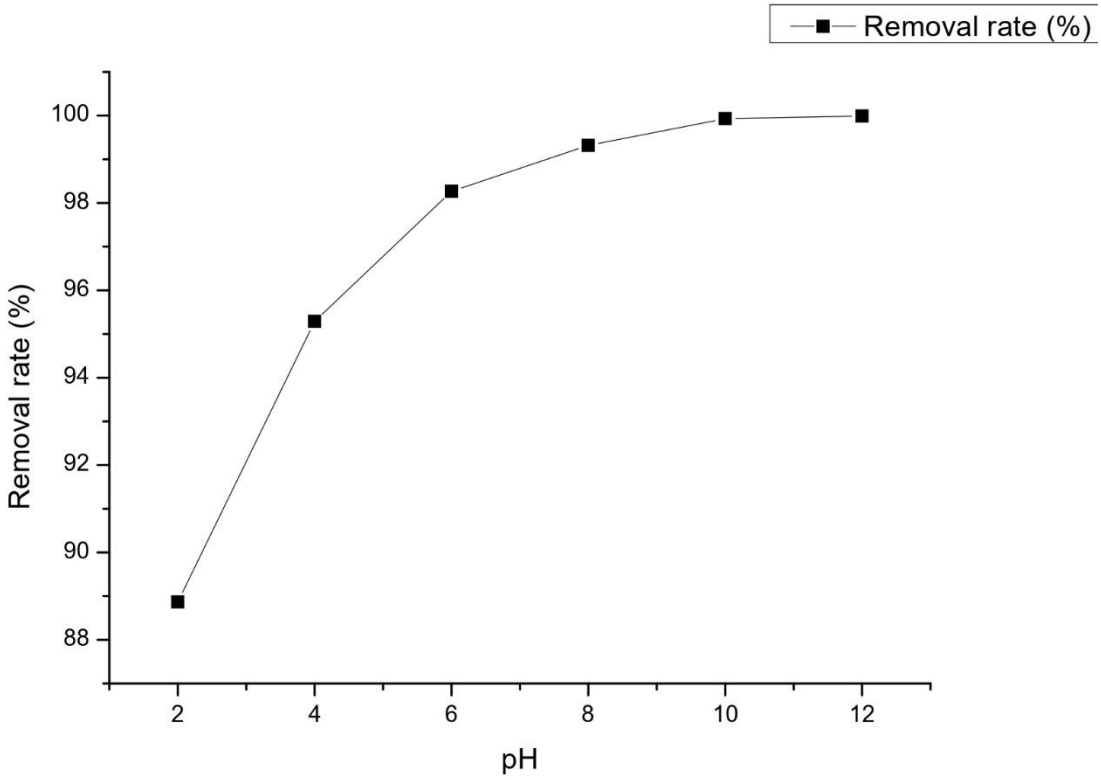

Figure 5.9: The Effect of pH on the percentage removal of Methylene Blue by Sago seed activated carbon

The data indicate that the adsorption capacity and removal efficiency of methylene blue by sago seed activated carbon are highly pH-dependent. The most effective removal rates were observed at basic pH levels, particularly between pH 8 and 12. Related observation have been reported in literature for the adsorption of MB on different adsorbent [152]. This suggests that the ionization state of both the activated carbon and the dye molecules plays a crucial role in the adsorption process, with higher pH levels favoring the removal of methylene blue. The increasing removal rate with rising pH can be attributed to the enhanced negative charge on the surface of the activated carbon at higher pH levels. This increased negative charge promotes greater electrostatic attraction between the negatively charged sites on the carbon and the cationic dye molecules. This electrostatic interaction is a key mechanism in the adsorption

process, significantly improving the efficiency as the pH increases. In comparison to the work done by (Manna et al., 2017), where it was found that most of the MB adsorbed by biosorbent derived from Lignocellulosic matter grafted with neem oil-phenolic resin were desorbed with acidic pH solution [153]. These findings imply that sago seed activated carbon is a highly effective adsorbent for methylene blue, particularly at higher pH levels. The research suggests potential applications in wastewater treatment, where controlling the pH could enhance the removal of dye pollutants. The study highlights the importance of pH as a critical parameter in the adsorption process and suggests that manipulating pH levels could be a simple yet effective strategy to enhance the performance of activated carbon adsorbents.

5.7 Effect of agitation speed

The effect of agitation speed on the removal of methylene blue by sago seed activated carbon (SSAC) was studied across various speeds, specifically 28, 50, 75, and 120 rpm. The removal rates, adsorption capacities, and equilibrium concentrations were analyzed to determine the optimal conditions for dye adsorption. The removal rates were high across all tested agitation speeds, with a peak removal rate of 99.97 % at 120 rpm (fig 5.10). This high removal efficiency underscores the potential of SSAC as a highly effective adsorbent for methylene blue, capable of achieving near-complete removal under optimal conditions.

Table 5.6: The Effect of Agitation speed on the percentage removal of Methylene Blue by Sago seed activated carbon data

Agitation speed (rpm)	Absorbance	Ce (mg/l)	qe (mg/g)	Removal rate (%)
28	0.75	3.93	34.43	95.63
50	0.25	1.30	35.48	98.55
75	0.10	0.49	35.80	99.45
120	0.007	0.028	35.99	99.97

The adsorption capacity (q_e) of SSAC shows a slight increase with agitation speed, starting from 34.43 mg/g at 28 rpm and reaching 35.99 mg/g at 120 rpm (Table 5.6). This trend suggests that higher agitation speeds provide a greater driving force for mass transfer, leading to increased adsorption. As the agitation speed increases, more dye molecules are available to interact with the adsorption sites on SSAC, thereby enhancing the adsorption capacity. The equilibrium concentration (Ce), which represents the residual dye concentration in the solution after adsorption, decreases significantly with increasing agitation speed. The Ce values drop from 3.93 mg/L at 28 rpm to a minimal 0.03 mg/L at 120 rpm. This indicates that at higher

agitation speeds, the SSAC becomes saturated more effectively, leaving a lower residual concentration of methylene blue in the solution. A similar result was observed in another study conducted by (Alam et al., 2022) where MB was absorbed using local adsorbents. The speed was adjusted from 150 rpm to 350 rpm at five different levels. It was noticed that the removal rate rose significantly to approximately 64% at 150 rpm. Nevertheless, the rate of dye removal decreased as the mixing speed increased further. The maximum removal rate, approximately 75%, was seen at a speed of 350 rpm. At these higher speeds, the trend line showed essentially little change [154]. This saturation effect is a common characteristic of adsorbents and highlights the importance of optimizing agitation speed for effective adsorption.

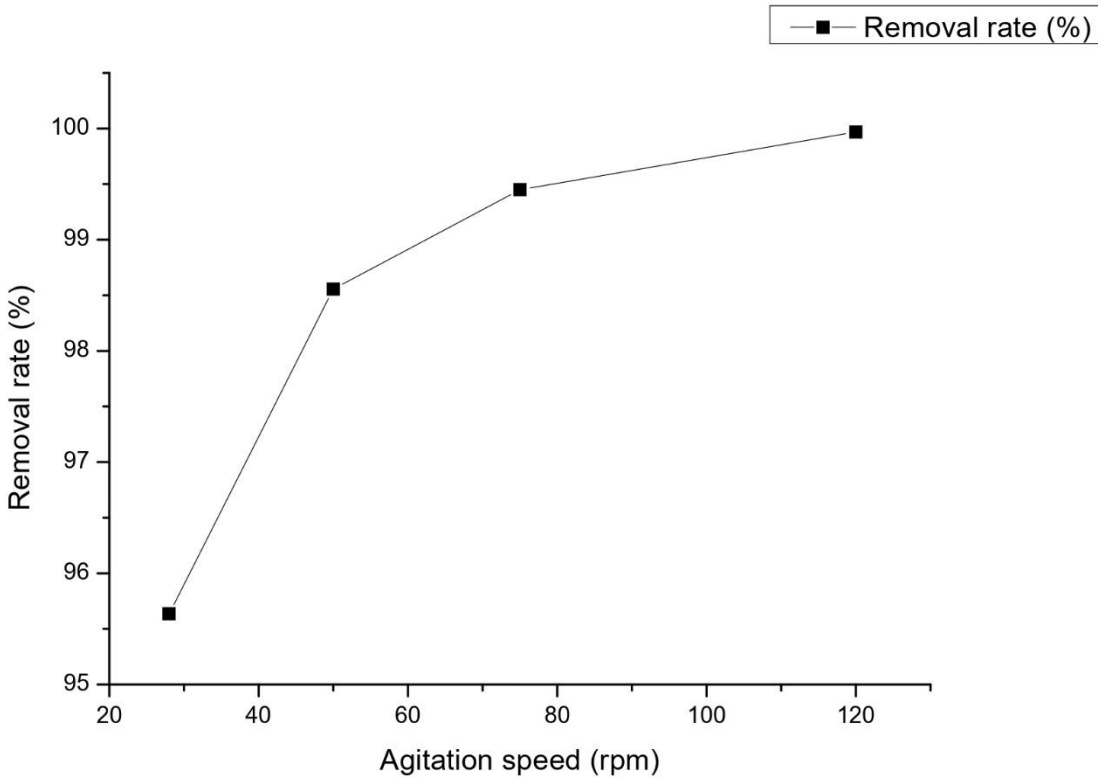

Figure 5.10: The Effect of Agitation speed on the percentage removal of Methylene Blue by Sago seed activated carbon

5.8 Adsorption isotherms

5.8.1 Langmuir isotherm model

The Langmuir isotherm model is a widely applied theoretical framework used to describe adsorption processes, particularly for understanding how molecules like dyes interact with adsorbent materials. In this context of removing Methylene Blue dye using sago seed activated carbon. The result of the Langmuir model provides critical insights into the adsorption capacity and efficiency of the adsorbent. The Langmuir isotherm assumes monolayer adsorption on a homogeneous surface with a finite number of identical sites. This means that once a dye molecule occupies a site, no further adsorption can occur at that site. The model is characterized by its ability to define the maximum adsorption capacity, which is particularly useful in designing and optimizing treatment processes. Key parameters in the Langmuir isotherm include q_{max} (the maximum adsorption capacity) and K_L (the Langmuir constant related to the affinity of binding sites). For the sago seed activated carbon, the maximum adsorption capacity q_{max} was found to be 203.67 mg/g, indicating a high capacity for removing Methylene Blue dye compared to the results obtained by (Mulushewa et al., 2021) (Faical et al., 2018) [3] [155]. This high capacity suggests that sago seed activated carbon is a highly effective adsorbent for this purpose.

Table 5.7: Langmuir isotherm model on the removal of Methylene Blue by Sago seed activated carbon data

Initial concentration (mg/l)	**Ce (mg/l)**	**qe (mg/g)**	**Ce/qe**
40	0.04	15.98	0.0025
90	0.52	35.79	0.014
115	0.72	45.71	0.016
140	3.17	54.73	0.058
165	10.02	61.99	0.16

The data shows various initial concentrations of Methylene Blue and their corresponding equilibrium concentrations (*Ce*) and adsorption capacities (q_e). The values of q_e increased with higher initial concentrations, demonstrating that the adsorbent becomes more saturated as more dye is introduced. This trend aligns with the Langmuir model's prediction of monolayer adsorption until saturation is reached. The ratio ($\frac{Ce}{qe}$) (Table 5.7) reflects the efficiency of the

adsorption process at different concentrations. Lower values of ($\frac{Ce}{qe}$) indicate higher efficiency, as less residual dye remains in the solution relative to the amount adsorbed. For instance, at the lowest initial concentration of 40 mg/l, the ($\frac{Ce}{qe}$) value is 0.0025, showing very high adsorption efficiency. The Langmuir constant K_L and the dimensionless separation factor R_L are also crucial for evaluating the adsorption process. The value of K_L was determined to be 0.31, which signifies the affinity between the dye molecules and the sago seed activated carbon. The separation factor R_L, which indicates the favorability of the adsorption process, was calculated to be 0.03, suggesting that the adsorption is highly favorable. The outcome was comparable to the previous investigation done by (Al-Saeedi et al., 2023)in the investigation of methylene blue elimination onto 5% Mn_3O_4/Bi_2O_3 which the R_L value was found to be equal to 0.0004 [156].

Table 5.8: Langmuir parameters

intercept	**Slop**	**qmax (mg/g)**	**K_L**	**R_L**	**R^2**
0.0049	0.016	203.66	0.31	0.03	0.99

A high correlation coefficient (R^2) of 0.99 supports the suitability of the Langmuir isotherm model for describing the adsorption of Methylene Blue on sago seed activated carbon. Most of literatures that shows materials used for MB removal in water describes a best fitting with the Langmuir isotherm[157][158][144]. This high R^2 value implies that the experimental data fit well with the Langmuir model, confirming the reliability of the results and the effectiveness of the adsorption process.

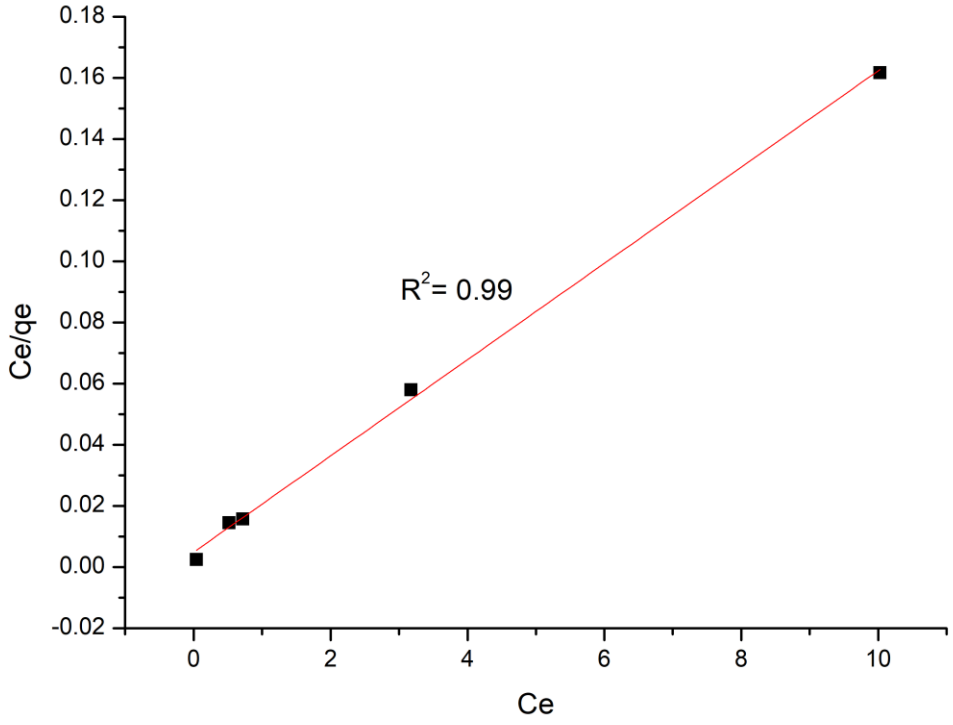

Figure 5.11: Langmuir isotherm model on the removal of Methylene Blue by Sago seed activated carbon

Analyzing the intercept and slope from the Langmuir plot, the intercept is directly related to $\frac{1}{q_{max}}$, and the slope to $\frac{1}{K_L * q_{max}}$. These values help in deriving the $q_{\max}$ and K_L, which are essential for understanding the adsorption capacity and the nature of the adsorbent-dye interaction. By having the values of Langmuir parameters (Table 5.8) we can determine the Adsorption capacity (qe) with a given concentration by using its linear equation (eq 3.8). The Langmuir isotherm model's applicability to this adsorption system suggests that the adsorption sites on the sago seed activated carbon are homogeneous and have a uniform affinity for the Methylene Blue dye. This homogeneity is a crucial assumption of the Langmuir model, which appears to hold true in this context.

5.8.2 Freundlich isotherm model

The Freundlich isotherm model is a widely used empirical equation that describes adsorption processes, particularly useful for heterogeneous surfaces. This model helps in understanding how adsorbates like Methylene Blue interact with adsorbents such as sago seed activated carbon. The application of the Freundlich isotherm model provides crucial insights into the

adsorption capacity and efficiency of the adsorbent in this study. The Freundlich isotherm is expressed by the equation (eq 3.5).

Table 5.9: Freundlich isotherm model on the removal of Methylene Blue by Sago seed activated carbon data

Initial concentration (mg/l)	**Ce (mg/l)**	**qe (mg/l)**	**LogCe**	**Logqe**
40	0.04	15.98	-1.39	1.20
90	0.52	35.79	-0.28	1.55
115	0.72	45.71	-0.14	1.66
140	3.17	54.73	0.50	1.74
165	10.02	61.99	1.0011	1.79

The data obtained (Table 5.9) details the initial concentration of Methylene Blue, its corresponding equilibrium concentration (Ce), adsorption capacity at equilibrium (q_e), and their logarithmic values (Log (Ce) and Log (q_e)). Initial concentrations of Methylene Blue range from 40 mg/l to 165 mg/l. Ce decreases with increased adsorption, while q_e increases with higher initial dye concentrations, indicating that the adsorbent becomes more saturated as more dye is introduced. From the data, the Freundlich constants were derived: K_f = 40.31, indicating a significant adsorption capacity of the sago seed activated carbon; 1/n = 0.25, suggesting favorable adsorption conditions as values between 0 and 1 indicate favorable adsorption; and R^2 = 0.90, which shows a good fit of the experimental data to the Freundlich isotherm model, validating its reliability.

Table 5.10: Freundlich parameters

intercept	**Slop**	**1/n**	**K_f**	**R^2**
1.60	0.25	4.018	40.32	0.90

The Freundlich isotherm model's application to the adsorption of Methylene Blue onto sago seed activated carbon suggests a heterogeneous surface with varying affinities for the adsorbate. The values of q_e increase with higher initial concentrations of Methylene Blue, showing that the adsorbent becomes more saturated as more dye is introduced. The linear plot of Log (q_e) against Log (Ce) confirms the suitability of the Freundlich isotherm model for this adsorption process. The slope (1/n) and intercept (Log K_f) from this plot provide essential parameters that help in understanding the adsorption dynamics.

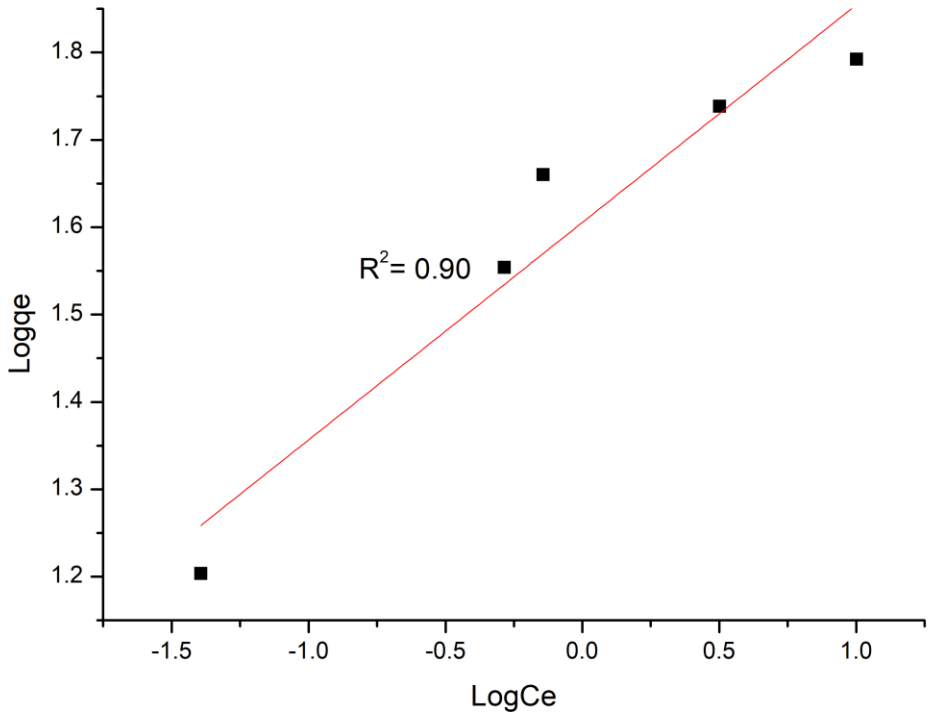

Figure 5.12: Freundlich isotherm model on the removal of Methylene Blue by Sago seed activated carbon

The Freundlich isotherm model effectively describes the adsorption of Methylene Blue onto sago seed activated carbon, highlighting its heterogeneous nature and high adsorption capacity. The values of K_f and 1/n indicate that the sago seed activated carbon is a highly effective adsorbent, with a significant capacity for dye removal under favorable adsorption conditions. The high correlation coefficient (R^2) further supports the model's applicability, confirming that the experimental data align well with the Freundlich isotherm model.

5.8.3 Temkin isotherm model

The Temkin isotherm model is used to analyze adsorption data and provides insights into the adsorption process, including the interactions between adsorbate and adsorbent.

Table 5.11: Temkin isotherm model on the removal of Methylene Blue by Sago seed activated carbon data

Initial concentration (mg/l)	Ce (mg/l)	qe (mg/g)	LnCe
40	0.04	15.98	-3.21
90	0.52	35.79	-0.65
115	0.72	45.71	-0.33
140	3.17	54.73	1.15
165	10.02	61.99	2.30

For an initial concentration of 40 mg/l, Ce yielded to 0.04 mg/l and a q_e of 15.98 mg/g. The natural logarithm of the equilibrium concentration (Ln Ce) was calculated as -3.21. As the initial concentration increased to 90 mg/l, the Ce rose to 0.52 mg/l and q_e of 35.79 mg/g. The Ln Ce for this concentration was -0.65. At an initial concentration of 115 mg/l, the Ce results to 0.72 mg/l and q_e of 45.71 mg/g. The Ln Ce was - 0.33. For 140 mg/l initial concentration, the absorbance significantly increased to 0.60, producing a Ce of 3.17 mg/l and q_e of 54.73 mg/g, with an Ln Ce of 1.15. Lastly, at the highest concentration tested, 165 mg/l, the absorbance reached 1.90, resulting in a Ce of 10.02 mg/l, a q_e of 61.99 mg/g, and an Ln Ce of 2.30. The Temkin isotherm model parameters were determined from the experimental data. The intercept of the linear plot was found to be 44.09, and the slope was 8.50. These values were used to calculate the Temkin constants B_T and K_T, which were 8.50 J mol-1 and 178.36 L mg-1, respectively. The correlation coefficient (R^2) for the model fit was 0.96 (Table 5.12), indicating a high degree of correlation between the experimental data and the model.

Table 5.12: Temkin parameters

intercept	Slop	B_T (J mol^{-1})	K_T (L mg^{-1})	R^2
44.09	8.50	8.50	178.36	0.96

Similar results was obtained by (Fito et al., 2023), where the Temkin isotherm presented an A_T and B_T equals to 5.67 L/g and 26.88 J/mol with an R^2 equals to 0.96 [144]. The Temkin isotherm model considers the effects of indirect adsorbate/adsorbent interactions and assumes that the heat of adsorption of all molecules in the layer decreases linearly with coverage due to these interactions.

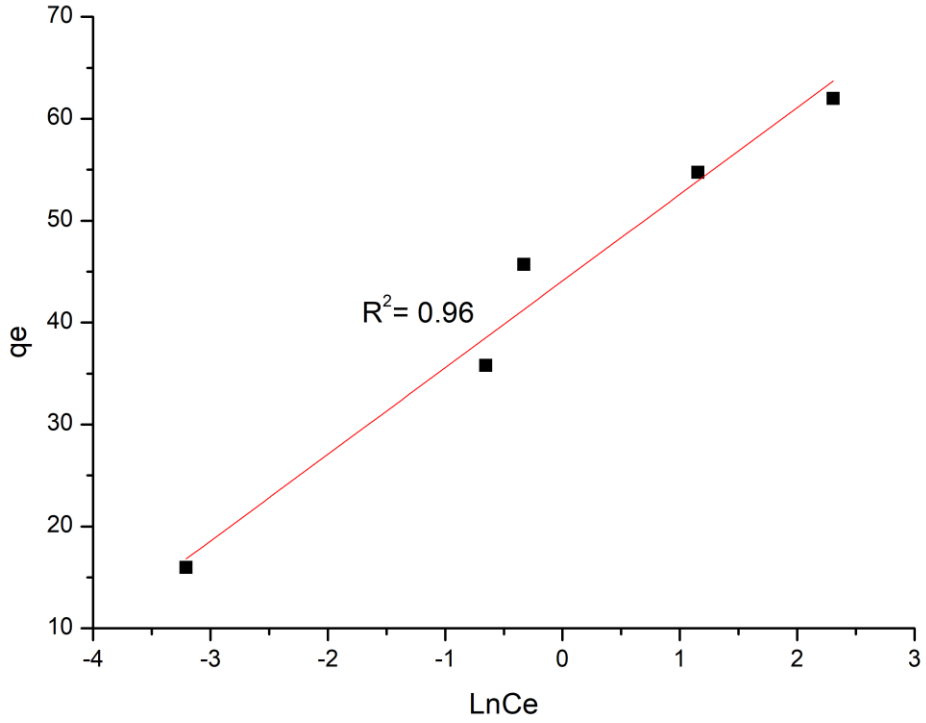

Figure 5.13: Temkin isotherm model on the removal of Methylene Blue by Sago seed activated carbon

The linear decrease in adsorption energy is characterized by the Temkin constants. The B_T constant reflects the heat of adsorption, and K_T is related to the equilibrium binding constant. The high R^2 value suggests that the Temkin isotherm model accurately describes the adsorption of Methylene Blue onto sago seed activated carbon. This implies that the adsorbent-adsorbate interactions are significant and that the heat of adsorption decreases as more Methylene Blue molecules are adsorbed. In practical terms, the study demonstrates the efficacy of sago seed activated carbon as an adsorbent for Methylene Blue removal from aqueous solutions. The findings could be useful in designing and optimizing adsorption systems for wastewater treatment, where controlling the concentration of pollutants like Methylene Blue is essential.

5.9 Adsorption kinetics modeling

5.9.1 Pseudo 1st order kinetic model

The study investigates the adsorption kinetics of methylene blue dye onto activated carbon using a pseudo-first-order kinetic model. The adsorption process was monitored by measuring the absorbance of methylene blue at different time intervals. The absorbance values were then

used to calculate the concentration of methylene blue in the solution (Ct), the amount of dye adsorbed per unit mass of activated carbon (qt), and the natural logarithm of the difference between the equilibrium concentration and the concentration at time t (ln (qe - qt)). The data collected at different time points (30, 40, 50, and 60 minutes) is tabulated in (Table 5.13), showing a decrease in absorbance and Ct over time, indicating the progressive adsorption of methylene blue onto the activated carbon.

Table 5.13: Pseudo -first- order kinetic model on the removal of Methylene Blue by Sago seed activated carbon data

Time (min)	**Ct (mg/l)**	**qt (mg/g)**	**ln(qe-qt)**
30	0.96	35.61	-0.96
40	0.51	35.79	-1.58
50	0.07	35.97	-3.62
60	0.02	35.99	-4.86

The study further presents a linear plot of ln (qe - qt) versus time, which is indicative of the pseudo-first-order kinetic model.

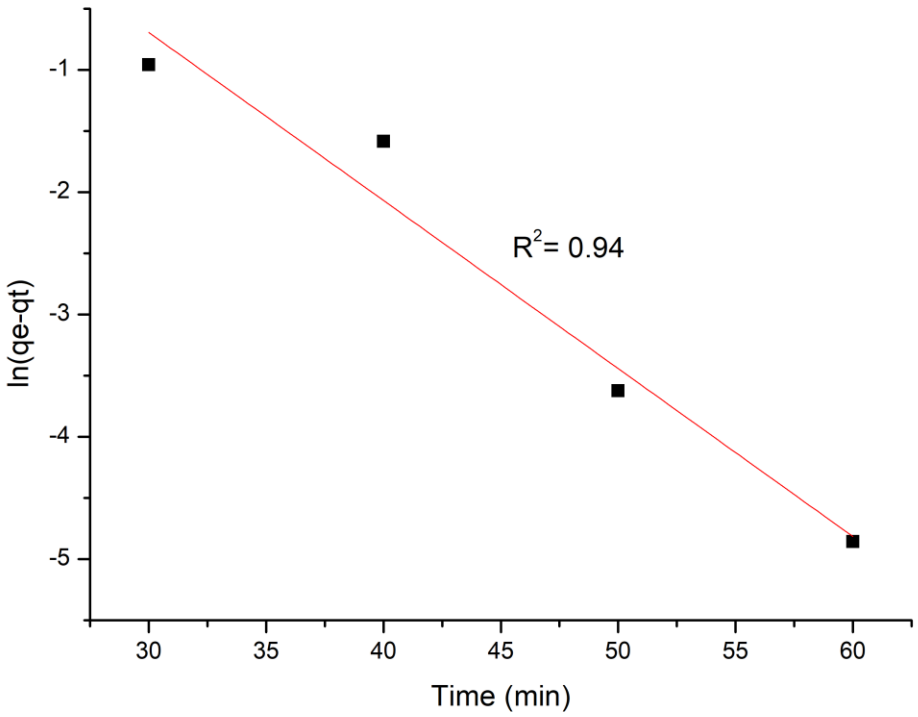

Figure 5.14: Pseudo - first - order kinetic model on the removal of Methylene Blue by Sago seed activated carbon

The slope and intercept of this plot were used to determine the rate constant (K_1) and the theoretical equilibrium adsorption capacity (q_e). The intercept and slope obtained from the plot are 3.43 and - 0.14, respectively. These values were used to calculate the qe, which was found to be 30.81 mg/g, and the rate constant K_1, which was - 0.0022 min^{-1}. The correlation coefficient (R^2) of the plot was 0.94, indicating a good fit to the pseudo-first-order kinetic model. Similarly, the removal of MB onto activated carbon derived from paulownia wood showed comparable values, at 25°C, qe was found to be 293.50 mg g^{-1} with a K_1 of 0.0017 min^{-1} and a correlation coefficient of $R^2 = 0.93$ [159].

Table 5.14: Pseudo - first - order kinetic model parameters

intercept	**Slop**	**qe (mg/g)**	**K_1**	**R^2**
3.43	- 0.14	30.81	- 0.0022	0.94

By having all values (Table 5.14), the Pseudo – first – order kinetic model linear equation (eq 3.2) can be rewrite as:

$$\ln (qe - qt) = \ln (30.81) + 0.0023t \quad \text{(eq 5.2)}$$

Therefore, at any given time the value of ln (qe - qt) can be determined. The results suggest that the adsorption of methylene blue onto activated carbon follows the pseudo-first-order kinetic model, which assumes that the rate of occupation of adsorption sites is proportional to the number of unoccupied sites. The high R^2 value supports the applicability of this model to the adsorption process under study. The negative value of the rate constant K_1 indicates that the adsorption process slows down over time, which is consistent with the decrease in qt values as the adsorption reaches equilibrium. The study also discusses the potential implications of these findings for practical applications in wastewater treatment. The adsorption capacity and rate constant are crucial parameters for designing and optimizing adsorption systems for dye removal. The pseudo-first-order kinetic model provides a simple yet effective means of predicting the adsorption behavior and can be used to estimate the time required to achieve a desired level of dye removal (eq 5.2). The study emphasizes the need for careful consideration of kinetic models in adsorption studies and highlights the usefulness of the pseudo-first-order model for the methylene blue-activated carbon system. Additionally, the study suggests that the activated carbon used in the experiments has a high adsorption capacity for methylene blue, making it a suitable adsorbent for dye removal applications. The negative rate constant indicates a decrease in adsorption rate over time, which is typical as the system approaches equilibrium. This information is crucial for understanding the dynamics of the adsorption process and for scaling up the system for industrial applications. The high adsorption capacity and the good fit of the kinetic model underscore the potential of SSAC as an effective adsorbent for dye removal from aqueous solutions.

5.9.2 Pseudo 2nd order kinetic model

The adsorption of methylene blue onto activated carbon was analyzed using the pseudo-second-order kinetic model. This model is useful for understanding the adsorption mechanisms and the interaction between adsorbate and adsorbent. The experiment measured the absorbance of methylene blue solution at different time intervals to determine the concentration of the dye in solution (Ct) and the amount of dye adsorbed per unit mass of activated carbon (Qt). The removal rate of methylene blue and the parameter t/Qt were also calculated at each time point.

The initial absorbance of the solution was recorded at 30 minutes corresponding to a dye concentration of 0.96 mg/l. At this time, the amount of dye adsorbed onto the activated carbon (Qt) was 35.61 mg/l. The value of t/Qt was found to be 0.84. As time progressed to 40 minutes, the results indicate a lower dye concentration of 0.51 mg/l. The corresponding Qt was 35.79 mg/l, with t/Qt increasing to 1.12. At 50 minutes, a dye concentration of 0.07 mg/l was obtained. The Qt at this point was 35.97 mg/l, while t/Qt increased to 1.39. Finally, at 60 minutes, the dye concentration dropped to 0.02 mg/l. The amount of dye adsorbed (Qt) was 35.99 mg/l, and t/Qt reached 1.67.

Table 5.15: Pseudo -Second- order kinetic model on the removal of Methylene Blue by Sago seed activated carbon data

Time (min)	**Ct (mg/l)**	**Qt (mg/l)**	**t/Qt**
30	0.96	35.61	0.84
40	0.51	35.79	1.12
50	0.07	35.97	1.39
60	0.02	35.99	1.67

The data from these measurements were then used to fit the pseudo-second-order kinetic model.

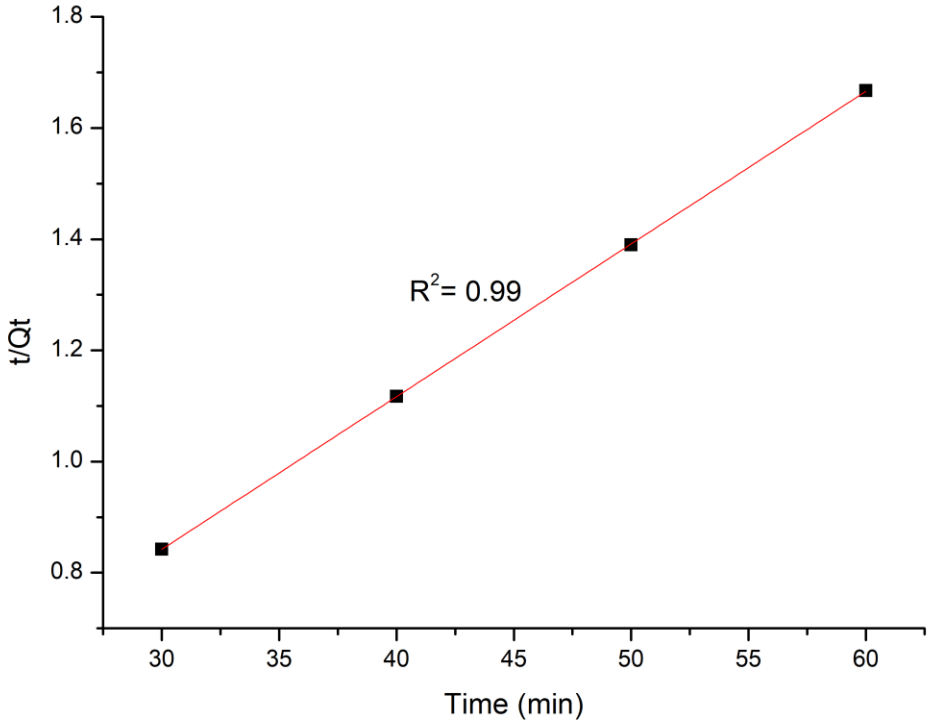

Figure 5.15: Pseudo - second- order kinetic model on the removal of Methylene Blue by Sago seed activated carbon

The model parameters, including the intercept, slope, equilibrium adsorption capacity (q_e), squared equilibrium adsorption capacity (q_e^2), rate constant (K_2), and the correlation coefficient (R^2), were determined.

Table 5.16: Pseudo - Second - order kinetic model parameters

intercept	**Slop**	**qe (mg/g)**	**qe^2 (mg/g)**	**K_2**	**R^2**
0.02	0.03	36.40	1325.20	0.04	0.99

The intercept value was found to be 0.02, and the slope was 0.03. The equilibrium adsorption capacity (q_e) was calculated to be 36.40 mg/g, while q_e^2 was 1325.20 mg/g. The rate constant (K_2) was 0.04, and the correlation coefficient (R^2) was very close to 1 at 0.99, indicating an excellent fit to the pseudo-second-order kinetic model. This high correlation coefficient suggests that the adsorption process of methylene blue onto activated carbon follows the pseudo-second-order kinetic model very closely. The model's accuracy implies that the adsorption mechanism involves chemisorption, where the rate-limiting step may be the sharing

or exchange of electrons between the adsorbate and adsorbent. A parallel result was found in a study on MB removal by activated carbon based of banana peels residue where the adsorption process is likely a chemisorption mechanism [155]. The calculated equilibrium adsorption capacity (q_e) also aligns well with the observed data, further confirming the validity of the model. The study successfully applied the pseudo-second-order kinetic model to analyze the adsorption of methylene blue onto activated carbon. The model parameters obtained from the experimental data indicated a high correlation, supporting the model's applicability. The high adsorption capacity and removal rate underscore the potential of activated carbon as a practical solution for dye removal in water treatment processes. This analysis contributes valuable insights into the adsorption mechanisms and can inform the development of optimized treatment strategies for dye-contaminated wastewater.

5.9.3 Elovich kinetic model

The Elovich isotherm model is a theoretical framework commonly used to describe adsorption processes, particularly useful for understanding how molecules such as dyes interact with adsorbent materials over time. In the context of removing Methylene Blue dye using sago seed activated carbon, the Elovich model provides significant insights into the adsorption kinetics and mechanisms involved. The Elovich model assumes that the adsorption sites increase exponentially with adsorption, making it suitable for heterogeneous systems where chemisorption is the primary mechanism. This model is characterized by its ability to describe the adsorption rate and capacity over time, which is crucial for optimizing treatment processes.

Table 5.17: Elovich kinetic model parameters

intercept	**Slope**	**β**	**lnβ**	**lnα**	**α ($mg.g^{-1}min^{-1}$)**	**R^2**
34.39	0.38	2.64	0.97	89.81	1.01E+39	0.76

Key parameters in the Elovich isotherm include the intercept and slope derived from the plot, which are used to calculate the Elovich constants β and α (Table 5.17). For the sago seed activated carbon, the intercept was found to be 34.39 and the slope 0.38. These values help determine the constants β and α, which represent the number of available sites and the initial adsorption rate, respectively. The value of β was calculated to be 2.64, indicating the energy required for chemisorption, while α was found to be an exceptionally high 1.01E+39 (mg. $g^{-1}min^{-1}$), suggesting a very rapid initial adsorption rate. In comparison to a research where

methylene blue was eliminated using natural Algerian goethite, The value of β was found to be 15.87 g/mg and α equals to 6.47 with a high correlation coefficient ($R^2 = 0.96$) [160].

Table 5.18: Elovich kinetic model on the removal of Methylene Blue by Sago seed activated carbon

Time (min)	**Ct (mg/l)**	**qt (mg/g)**	**lnt**
30	0.96	35.61	3.40
40	0.51	35.79	3.69
50	0.07	35.97	3.91
60	0.02	35.99	4.09
70	0.06	35.98	4.25
80	0.04	35.98	4.38

The data shows various time intervals and their corresponding concentrations (Ct), adsorption capacities (qt), and natural logarithm of time (lnt). The adsorption capacity (qt) remained relatively stable, starting at 35.61 mg/g at 30 minutes and increasing slightly to 35.98 mg/g at 80 minutes (Table 5.18), indicating that the adsorbent reaches near saturation quickly. This stability in qt values reflects the high efficiency of sago seed activated carbon in adsorbing Methylene Blue dye. The Elovich constants β and α are critical for evaluating the adsorption process. The lower β value suggests a higher rate of chemisorption initially, while the high α value indicates a rapid initial adsorption rate. These constants, along with the intercept and slope, provide a comprehensive understanding of the adsorption kinetics.

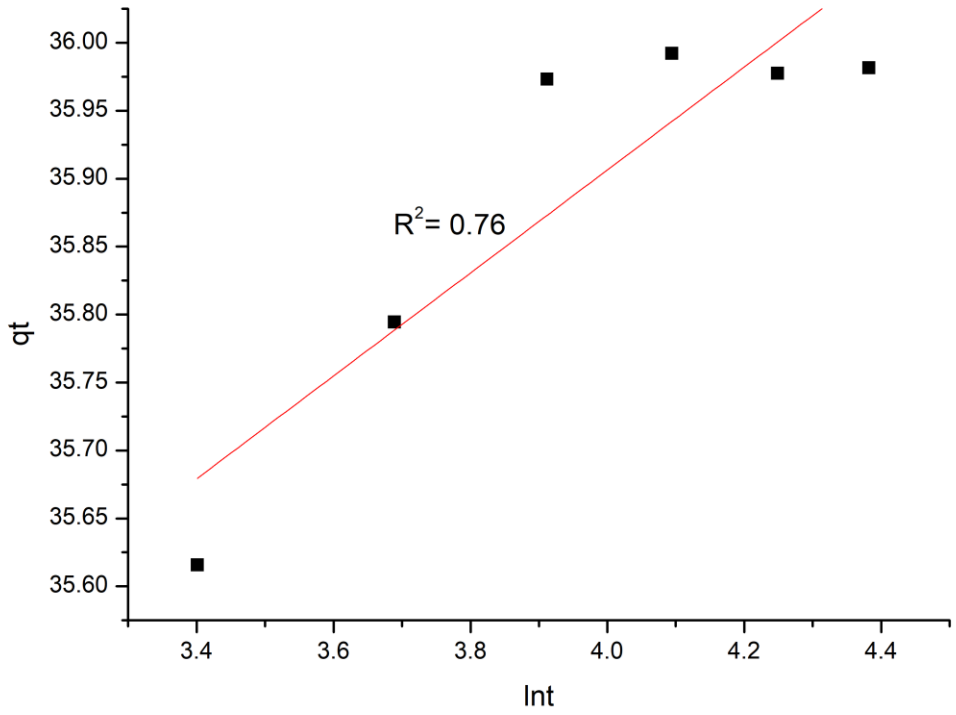

Figure 5.16: Elovich kinetic model on the removal of Methylene Blue by Sago seed activated carbon

The correlation coefficient (R^2) was found to be 0.76, indicating a moderate fit of the experimental data to the Elovich model. While not perfect, this R^2 value suggests that the Elovich model can reasonably describe the adsorption kinetics for this system, although the previous models offer a better fit. The Elovich isotherm model's applicability to this adsorption system suggests that the adsorption process is initially rapid and becomes more stable over time. The exponential increase in adsorption sites aligns well with the heterogeneous nature of the sago seed activated carbon, supporting the model's assumptions. This analysis highlights the effectiveness of sago seed activated carbon in removing Methylene Blue dye, providing valuable insights for optimizing dye removal processes.

CHAPITER6: CONCLUSION

This study was conducted to examine the adsorption of methylene blue from synthetic wastewater using activated carbon derived from Sago seeds. The experimental investigation was performed at the College of Science and Technology, University of Rwanda, on a laboratory scale. The activated carbon was derived from Sago seeds sourced from Comoros, specifically from Grand Comoros. Following the preparation of the synthetic wastewater and the adsorbent, the activated carbon obtained was subjected to characterizations. XRF and FTIR analyses of SSAC demonstrated that the incorporation of phosphorus altered its chemical structure, enhancing its porosity, surface area, and the development of more organized carbon structures during activation. The percentage of Methylene blue removal decreased with higher initial dye concentrations due to the formation of a monolayer of dye molecules on the SSAC surface. The optimal concentration for maximum dye removal was determined to be 115 ppm. The removal efficiency increased with contact time, with the optimal contact time being 50 minutes. Additionally, higher adsorbent doses improved dye removal, with the optimal dose being 0.2 g/L. At lower pH levels, positively charged hydrogen ions on the adsorbent surface caused electrostatic repulsion with the cationic Methylene blue dye, reducing adsorption. Conversely, at pH 8, adsorption was significantly higher due to electrostatic attraction. The concentration of methylene blue in the solution decreases with high agitation speed effectively saturating the SSAC and the optimum agitation speed has been determined to be 75 rpm. The adsorption data were then examined using several isotherm models in order to comprehend the adsorption mechanism. The Langmuir isotherm model yielded the most accurate match for the experimental data, indicating that the adsorption of methylene blue onto sago seed activated carbon occurred as a monolayer over a uniform surface. The study also analyzed the rate at which the adsorption process occurs, and found that the pseudo-second-order kinetic model had the highest level of agreement with the experimental results. These findings indicate that chemisorption, which involves the sharing or exchange of electrons between the adsorbent and adsorbate, was the primary process at play. Hence, the study conclusively showed that sago seed activated carbon is a highly promising and effective adsorbent for the elimination of methylene blue from water-based solutions. The effective implementation of SSAC in a simulated wastewater demonstrates its potential for wider application in the treatment of industrial wastewater. Future research should investigate the regeneration and reutilization of SSAC, as well as its efficacy against additional contaminants, in order to improve its economic and environmental sustainability.

RECOMMENDATION

Based on the findings of this study, the following recommendations are proposed:

- This study demonstrates that the Sago seed plant has a satisfactory sorption capacity, which is important considering the imminent threat of habitat destruction. Therefore, it is advisable to undertake conservation efforts and promote the cultivation of Sago plant in various locations.
- The efficiency of activated carbon derived from Sago seeds in sequestering methylene blue from synthetic wastewater was found to be commendable. However, further investigation is needed to determine its effectiveness in removing methylene blue and other pollutants from actual textile industry effluents, which often contain competing ions.
- Additional research should be conducted to explore the potential for regeneration and reusability of Sago seed activated carbon.
- It is crucial to evaluate the efficacy of Sago seed-derived activated carbon under different environmental conditions and to scale up the production process for industrial applications. These studies will help determine the long-term viability and economic feasibility of using Sago seed-derived activated carbon for wastewater treatment.

REFERENCES

[1] X. D. Crystallography, "Wastewater engineering_Advanced wastewater treatment systems," pp. 1–23, 2016.

[2] D. K. Hingane, "WASTEWATER MANAGEMENT AND ITS CHALLENGES," pp. 105–109, 2022, [Online]. Available: www.ijaar.co.in

[3] Z. Mulushewa, W. T. Dinbore, and Y. Ayele, "Removal of methylene blue from textile waste water using kaolin and zeolite-x synthesized from Ethiopian kaolin," *Environ. Anal. Heal. Toxicol.*, vol. 36, no. 1, pp. 1–13, 2021, doi: 10.5620/eaht.2021007.

[4] A. Krishna Moorthy, B. Govindarajan Rathi, S. P. Shukla, K. Kumar, and V. Shree Bharti, "Acute toxicity of textile dye Methylene blue on growth and metabolism of selected freshwater microalgae," *Environ. Toxicol. Pharmacol.*, vol. 82, no. November 2020, p. 103552, 2021, doi: 10.1016/j.etap.2020.103552.

[5] R. Of, T. H. E. Urban, W. Treatment, and Q. Directive, "Legislative train 01.2024 1," no. October 2021, pp. 2023–2025, 2024.

[6] A. Tariq and A. Mushtaq, "Untreated Wastewater Reasons and Causes: A Review of Most Affected Areas and Cities," *Int. J. Chem. Biochem. Sci.*, vol. 23, no. 1, pp. 121–143, 2023.

[7] M. Ravina *et al.*, “Urban wastewater treatment in african countries: Evidence from the hydroaid initiative,” *Sustain.*, vol. 13, no. 22, pp. 1–21, 2021, doi: 10.3390/su132212828.

[8] REMA, “Water Quality Management Plan for Rwanda TECHNICAL ASSISTANCE IN ENVIRONMENT AND NATURAL RESOURCES MANAGEMENT Water Quality Management Plan for Rwanda 30/06/2020 Water Quality Management Plan for Rwanda (Final),” 2020.

[9] J. Brown, S. Cairncross, and J. H. J. Ensink, “Water, sanitation, hygiene and enteric infections in children,” *Arch. Dis. Child.*, vol. 98, no. 8, pp. 629–634, 2013, doi: 10.1136/archdischild-2011-301528.

[10] R. B. Johnston, “THE 2030 AGENDA FOR SUSTAINABLE DEVELOPMENT,” *Arsen. Res. Glob. Sustain. - Proc. 6th Int. Congr. Arsen. Environ. AS 2016*, pp. 12–14, 2016, doi: 10.1201/b20466-7.

[11] F. Wang *et al.*, “Emerging contaminants: A One Health perspective,” *Innovation*, vol. 5, no. 4, p. 100612, 2024, doi: 10.1016/j.xinn.2024.100612.

[12] Y.-L. Cheng *et al.*, “Structure and Properties of Dyes and Pigments,” *Intech*, vol. 11, no. tourism, p. 13, 2016, [Online]. Available: https://www.intechopen.com/books/advanced-biometric-technologies/liveness-detection-in-biometrics

[13] A. Tebeje, Z. Worku, T. T. I. Nkambule, and J. Fito, “Adsorption of chemical oxygen demand from textile industrial wastewater through locally prepared bentonite adsorbent,” *Int. J. Environ. Sci. Technol.*, vol. 19, no. 3, pp. 1893–1906, 2022, doi: 10.1007/s13762-021-03230-4.

[14] I. Khan *et al.*, “Review on Methylene Blue: Its Properties, Uses, Toxicity and Photodegradation,” *Water (Switzerland)*, vol. 14, no. 2, 2022, doi: 10.3390/w14020242.

[15] T. Cwalinski *et al.*, “Methylene blue—current knowledge, fluorescent properties, and its future use,” *J. Clin. Med.*, vol. 9, no. 11, pp. 1–12, 2020, doi: 10.3390/jcm9113538.

[16] P. O. Oladoye, T. O. Ajiboye, E. O. Omotola, and O. J. Oyewola, “Methylene blue dye: Toxicity and potential elimination technology from wastewater,” *Results Eng.*, vol. 16, no. August, p. 100678, 2022, doi: 10.1016/j.rineng.2022.100678.

[17] S. Ben Salah, M. Missaoui, A. Attia, G. Lesage, M. Heran, and R. Ben Amar, “Treatment of real textile effluent containing indigo blue dye by hybrid system combining adsorption and membrane processes,” *Front. Membr. Sci. Technol.*, vol. 3, no. March, pp. 1–14, 2024, doi: 10.3389/frmst.2024.1348992.

[18] N. Malatji *et al.*, “Removal of methylene blue from wastewater using hydrogel nanocomposites: A review,” *Nanomater. Nanotechnol.*, vol. 11, pp. 1–27, 2021, doi: 10.1177/18479804211039425.

[19] K. Hab Alrman, S. Alhariri, and I. Al- Bakri, “Ultrafiltration membrane based on chitosan/adipic acid: Synthesis, characterization and performance on separation of methylene blue and reactive yellow-145 from aqueous phase,” *Heliyon*, vol. 10, no. 11, p. e31055, 2024, doi: 10.1016/j.heliyon.2024.e31055.

[20] N. C. Homem, N. U. Yamaguchi, M. F. Vieira, M. T. S. P. Amorim, and R.

Bergamasco, “Surface modification of microfiltration membrane with GO nanosheets for dyes removal from aqueous solutions,” *Chem. Eng. Trans.*, vol. 60, no. September 2018, pp. 259–264, 2017, doi: 10.3303/CET1760044.

[21] H. Raval, R. Sharma, and A. Srivastava, “Novel protocol for fouling detection of reverse osmosis membrane based on methylene blue colorimetric method by image processing technique,” *Water Sci. Technol.*, vol. 89, no. 3, pp. 513–528, 2024, doi: 10.2166/wst.2023.425.

[22] P. Moradihamedani, “Recent advances in dye removal from wastewater by membrane technology: a review,” *Polym. Bull.*, vol. 79, no. 4, pp. 2603–2631, 2022, doi: 10.1007/s00289-021-03603-2.

[23] C. Zaharia, C. P. Musteret, and M. A. Afrasinei, “The Use of Coagulation–Flocculation for Industrial Colored Wastewater Treatment—(I) The Application of Hybrid Materials,” *Appl. Sci.*, vol. 14, no. 5, 2024, doi: 10.3390/app14052184.

[24] Susilawati *et al.*, “Fe3O4/SiO2 composite derived from rice husk ash to enhance methylene blue removal efficiency in wastewater treatment,” *Case Stud. Chem. Environ. Eng.*, vol. 9, no. April, p. 100762, 2024, doi: 10.1016/j.cscee.2024.100762.

[25] Z. Bedlovičová, “Green synthesis of silver nanoparticles using actinomycetes,” *Green Synth. Silver Nanomater.*, pp. 547–569, 2022, doi: 10.1016/B978-0-12-824508-8.00001-0.

[26] C. Waghmare *et al.*, “Adsorption of methylene blue dye onto phosphoric acid-treated pomegranate peel adsorbent: Kinetic and thermodynamic studies,” *Desalin. Water Treat.*, vol. 318, no. April, p. 100406, 2024, doi: 10.1016/j.dwt.2024.100406.

[27] S. Ce, E. Aboshaloa, N. Ageel, and A. Albashini, “Faculty Science-Sirte Alhdad GM , Scientific Efficient Removal of Methylene Blue Dyes from Aqueous Solutions Using Various Charcoal Adsorbents : A Comparative Thermodynamic and Isotherm Study of Olive , Pine , and Commercial Activated Carbon”, doi: 10.37375/issn.2789-858X.

[28] E. Santoso, R. Ediati, Y. Kusumawati, H. Bahruji, D. O. Sulistiono, and D. Prasetyoko, “Review on recent advances of carbon based adsorbent for methylene blue removal from waste water,” *Mater. Today Chem.*, vol. 16, p. 100233, 2020, doi: 10.1016/j.mtchem.2019.100233.

[29] M. Abbas, “Removal of methylene blue pollutant from the textile industry by adsorption onto Zeolithe: Kinetic and thermodynamic study,” *J. Eng. Fiber. Fabr.*, vol. 17, 2022, doi: 10.1177/1558925021993692.

[30] N. Hamri *et al.*, “Enhanced Adsorption Capacity of Methylene Blue Dye onto Kaolin through Acid Treatment: Batch Adsorption and Machine Learning Studies,” *Water (Switzerland)*, vol. 16, no. 2, pp. 1–23, 2024, doi: 10.3390/w16020243.

[31] A. K. Roy Choudhury, *Environmental impacts of the textile industry and its assessment through life cycle assessment. In Roadmap to Sustainable Textiles and Clothing, Environmental and Social Aspects of Textiles and Clothing Supply Chain*, no. July 2014. 2014. doi: 10.1007/978-981-287-110-7.

[32] A. K. R. Choudhury, *Sustainable chemical technologies for textile production*. Elsevier Ltd, 2017. doi: 10.1016/B978-0-08-102041-8.00010-X.

[33] R. B. Benjamin Manirakiza, Lanre Anthony Gbadegesin, Antoine Nsabimana,

"Review on trends of wastewater pollution and treatment system challenges: A case study of Rwanda, East Africa," vol. 1, no. 1, pp. 11–20, 2017.

[34] M. O. F. Lands, "Republic of Rwanda Ministry of Lands , Resettlement and Environment " Rwanda Environmental Policy "," 2003.

[35] REMA, CoEB, and University of Rwanda, "Guidelines for Water Quality Management in Rwanda," p. 71, 2020.

[36] A. Gadabu, "North American Academic Research," vol. 3, no. April, pp. 413–429, 2020, doi: 10.5281/zenodo.3732795.

[37] A. Mittal, "Adsorption Technology for the Treatment of Waste Water." 2010. [Online]. Available: https://m.youtube.com/watch?v=LPjzfGChGlE#

[38] M. Von Sperling, *Wastewater Characteristics, Treatment and Disposal*, vol. 6, no. 0. 2015. doi: 10.2166/9781780402086.

[39] P. Ranjit, V. Jhansi, and K. V. Reddy, *Conventional Wastewater Treatment Processes BT - Advances in the Domain of Environmental Biotechnology: Microbiological Developments in Industries, Wastewater Treatment and Agriculture*. 2021. [Online]. Available: https://doi.org/10.1007/978-981-15-8999-7_17

[40] M. von Sperling, *Activated Sludge and Aerobic Biofilm Reactors*, vol. 5, no. August. Brazil, 2018.

[41] A. di Biase, M. S. Kowalski, T. R. Devlin, and J. A. Oleszkiewicz, "Moving bed biofilm reactor technology in municipal wastewater treatment: A review," *J. Environ. Manage.*, vol. 247, no. June, pp. 849–866, 2019, doi: 10.1016/j.jenvman.2019.06.053.

[42] S. Waqas *et al.*, "Recent progress in integrated fixed-film activated sludge process for wastewater treatment: A review," *J. Environ. Manage.*, vol. 268, no. December 2019, p. 110718, 2020, doi: 10.1016/j.jenvman.2020.110718.

[43] D. Di Trapani, M. Christensson, M. Torregrossa, G. Viviani, and H. Ødegaard, "Performance of a hybrid activated sludge/biofilm process for wastewater treatment in a cold climate region: Influence of operating conditions," *Biochem. Eng. J.*, vol. 77, pp. 214–219, 2013, doi: 10.1016/j.bej.2013.06.013.

[44] S. Al-Asheh, M. Bagheri, and A. Aidan, "Membrane bioreactor for wastewater treatment: A review," *Case Stud. Chem. Environ. Eng.*, vol. 4, no. April, 2021, doi: 10.1016/j.cscee.2021.100109.

[45] K. Samal, S. Mahapatra, and M. Hibzur Ali, "Pharmaceutical wastewater as Emerging Contaminants (EC): Treatment technologies, impact on environment and human health," *Energy Nexus*, vol. 6, no. April, p. 100076, 2022, doi: 10.1016/j.nexus.2022.100076.

[46] P. V. C. Srivastava, *Physico-chemical processes for wastewater treatment*, IIT Roorke. India: National program on technology enhanced learning (NPTL), 2022. [Online]. Available: https://nptel.ac.in/courses/103107212

[47] F. M. YASIN, "Physical separation processes (Adsorption)," 2004.

[48] R. Yousef, H. Qiblawey, and M. H. El-Naas, "Adsorption as a process for produced water treatment: A review," *Processes*, vol. 8, no. 12, pp. 1–22, 2020, doi:

10.3390/pr8121657.

[49] S. Dutta, B. Gupta, S. K. Srivastava, and A. K. Gupta, “Recent advances on the removal of dyes from wastewater using various adsorbents: A critical review,” *Mater. Adv.*, vol. 2, no. 14, pp. 4497–4531, 2021, doi: 10.1039/d1ma00354b.

[50] S. S. Ray, R. Gusain, and N. Kumar, *Adsorption in the context of water purification*. 2020. doi: 10.1016/b978-0-12-821959-1.00004-0.

[51] S. Singh, N.B., Nagpal, G. and Agrawal, “Water purification by using adsorbents: A review,” *Environ. Technol. Innov.*, vol. 11, pp. 187–240, 2018.

[52] S. De Gisi, G. Lofrano, M. Grassi, and M. Notarnicola, “Characteristics and adsorption capacities of low-cost sorbents for wastewater treatment: A review,” *Sustain. Mater. Technol.*, vol. 9, pp. 10–40, 2016, doi: 10.1016/j.susmat.2016.06.002.

[53] M. Alaqarbeh, P. Al, and H. Bin Abdullah, “Adsorption Phenomena: Definition, Mechanisms, and Adsorption Types: Short Review,” *RHAZES Green Appl. Chem.*, vol. 13, no. September, pp. 43–51, 2021, doi: 10.48419/IMIST.PRSM/rhazes-v13.28283.

[54] K. Wang, Y. Zhang, R. Qi, M. Yang, and R. Deng, “Effects of activated carbon surface chemistry and pore structure on adsorption of HAAs from water,” *Huagong Xuebao/Journal Chem. Ind. Eng.*, vol. 57, no. 7, pp. 1659–1663, 2006.

[55] Z. Hasan and S. H. Jhung, “Removal of hazardous organics from water using metal-organic frameworks (MOFs): Plausible mechanisms for selective adsorptions,” *J. Hazard. Mater.*, vol. 283, pp. 329–339, 2015, doi: 10.1016/j.jhazmat.2014.09.046.

[56] A. El Jery *et al.*, “Isotherms, kinetics and thermodynamic mechanism of methylene blue dye adsorption on synthesized activated carbon,” *Sci. Rep.*, vol. 14, no. 1, pp. 1–12, 2024, doi: 10.1038/s41598-023-50937-0.

[57] M. El Gamal, H. A. Mousa, M. H. El-Naas, R. Zacharia, and S. Judd, “Bio-regeneration of activated carbon: A comprehensive review,” *Sep. Purif. Technol.*, vol. 197, no. August 2017, pp. 345–359, 2018, doi: 10.1016/j.seppur.2018.01.015.

[58] K. S. Knaebel, “ADSORBENT SELECTION Dublin , Ohio 43016.,” 2004.

[59] R. Ganjoo, S. Sharma, A. Kumar, and M. M. A. Daouda, “Activated Carbon: Fundamentals, Classification, and Properties,” *Act. Carbon*, no. May, pp. 1–22, 2023, doi: 10.1039/bk9781839169861-00001.

[60] J. O. Ighalo, F. O. Omoarukhe, V. E. Ojukwu, K. O. Iwuozor, and C. A. Igwegbe, “Cost of adsorbent preparation and usage in wastewater treatment: A review,” *Clean. Chem. Eng.*, vol. 3, no. June, p. 100042, 2022, doi: 10.1016/j.clce.2022.100042.

[61] Musa Abubakar Tadda *et al.*, “A review on activated carbon: process, application and prospects,” *J. Adv. Civ. Eng. Pract. Res.*, vol. 2, no. 1, pp. 7–13, 2016.

[62] B. D. Zdravkov, J. J. Čermák, M. Šefara, and J. Janků, “Pore classification in the characterization of porous materials: A perspective,” *Cent. Eur. J. Chem.*, vol. 5, no. 2, pp. 385–395, 2007, doi: 10.2478/s11532-007-0017-9.

[63] M. M. Dubinin, “A STUDY OF THE POROUS STRUCTURE OF ACTIVE CARBONS USING A VARIETY OF METHODS,” *Acad. Sci. /Moscow*, pp. 101–114,

1955.

[64] U. Teknologi, “Characteristic Adsorbents,” vol. 1, no. c, pp. 1–12, 1987.

[65] S. Iftekhar, D. L. Ramasamy, V. Srivastava, M. B. Asif, and M. Sillanpää, “Understanding the factors affecting the adsorption of Lanthanum using different adsorbents: A critical review,” *Chemosphere*, vol. 204, pp. 413–430, 2018, doi: 10.1016/j.chemosphere.2018.04.053.

[66] M. T. Yagub, T. K. Sen, S. Afroze, and H. M. Ang, “Dye and its removal from aqueous solution by adsorption: A review,” *Adv. Colloid Interface Sci.*, vol. 209, pp. 172–184, 2014, doi: 10.1016/j.cis.2014.04.002.

[67] M. A. Olatunji, M. U. Khandaker, H. N. M. E. Mahmud, and Y. M. Amin, “Influence of adsorption parameters on cesium uptake from aqueous solutions- a brief review,” *RSC Adv.*, vol. 5, no. 88, pp. 71658–71683, 2015, doi: 10.1039/c5ra10598f.

[68] V. K. Saini and A. Shankar, *How to Improve Selectivity of a Material for Adsorptive Separation Applications*. 2019. doi: 10.1007/978-3-319-73645-7_43.

[69] E. Fitzer, K. H. Köchling, H. P. Böhm, and H. Marsh, “Recommended Terminology for the Description of Carbon as a Solid (© 1995 IUPAC),” *Ind. Carbon Graph. Mater. Raw Mater. Prod. Appl. Vol. 1 2*, vol. 1–2, no. 3, pp. 45–87, 2021, doi: 10.1002/9783527674046.ch4.

[70] Chemistry Topics, “Physical adsorption and chemical adsorption,” Medium. [Online]. Available: https://pandakajal42.medium.com/physical-adsorption-and-chemical-adsorption-8f4d67434ca9

[71] P. M. ARMENANTE, “Adsorption,” *Adsorpt. J. Int. Adsorpt. Soc.*.

[72] T. S. Jakubov, O. N. Kabanova, and V. V. Serpinsky, “Temperature dependence of adsorption,” *J. Colloid Interface Sci.*, vol. 79, no. 1, pp. 170–177, 1981, doi: 10.1016/0021-9797(81)90060-6.

[73] G. K. Latinwo and S. E. Agarry, “Removal of Phenol from Paint Wastewater by Adsorption onto Phosphoric Acid Activated Carbon Produced from Coconut Shell: Isothermal and Kinetic Modelling Studies,” *Chem. Mater. Res.*, vol. 7, no. 5, pp. 123–137, 2015, [Online]. Available: https://www.iiste.org/Journals/index.php/CMR/article/view/22876

[74] V. Yadav, J. Ali, and M. C. Garg, “Biosorption of Methylene Blue Dye from Textile-Industry Wastewater onto Sugarcane Bagasse: Response Surface Modeling, Isotherms, Kinetic and Thermodynamic Modeling,” *J. Hazardous, Toxic, Radioact. Waste*, vol. 25, no. 1, pp. 1–9, 2021, doi: 10.1061/(asce)hz.2153-5515.0000572.

[75] S. E. Agarry, C. N. Owabor, and A. O. Ajani, “Modified Plantain Peel As Cellulose-Based Low-Cost Adsorbent for the Removal of 2,6-Dichlorophenol From Aqueous Solution: Adsorption Isotherms, Kinetic Modeling, and Thermodynamic Studies,” *Chem. Eng. Commun.*, vol. 200, no. 8, pp. 1121–1147, 2013, doi: 10.1080/00986445.2012.740534.

[76] Y. Sukmono, R. A. Kristanti, B. V. Foo, and T. Hadibarata, “Adsorption of Fe and Pb from Aqueous Solution using Coconut Shell Activated Carbon,” *Biointerface Res. Appl. Chem.*, vol. 14, no. 2, pp. 1–14, 2024, doi: 10.33263/BRIAC142.030.

[77] M. Soleimani and T. Kaghazchi, “Agricultural waste conversion to activated carbon by chemical activation with phosphoric acid,” *Chem. Eng. Technol.*, vol. 30, no. 5, pp. 649–654, 2007, doi: 10.1002/ceat.200600325.

[78] J. Spisak, “The Discovery And History Of Activated Carbon,” *Multimedia Learning Stations*. Abhi Ro Water Purifier, pp. 119–130, 2024. doi: 10.5040/9798400688317.0012.

[79] A. M. Metwaly *et al.*, “Traditional ancient Egyptian medicine: A review,” *Saudi J. Biol. Sci.*, vol. 28, no. 10, pp. 5823–5832, 2021, doi: 10.1016/j.sjbs.2021.06.044.

[80] CAMFIL, “HISTORIC JOURNEY OF ACTIVATED CARBON AND BREAKTHROUGHS.” [Online]. Available: https://www.camfil.com/en/insights/innovation-technology-and-research/journey-of-activated-carbon

[81] Z. Heidarinejad, M. H. Dehghani, M. Heidari, G. Javedan, I. Ali, and M. Sillanpää, “Methods for preparation and activation of activated carbon: a review,” *Environ. Chem. Lett.*, vol. 18, no. 2, pp. 393–415, 2020, doi: 10.1007/s10311-019-00955-0.

[82] R. Baby, B. Saifullah, and M. Z. Hussein, “Carbon Nanomaterials for the Treatment of Heavy Metal-Contaminated Water and Environmental Remediation,” *Nanoscale Res. Lett.*, vol. 14, no. 1, 2019, doi: 10.1186/s11671-019-3167-8.

[83] A. W. P. Fung, A. M. Rao, K. Kuriyama, M. S. Dresselhaus, G. Dresseliiaus, and M. Endot, “Characterization of Activated Carbon Fibers,” *MRS Proc.*, vol. 209, 1990, doi: 10.1557/proc-209-335.

[84] Sadashiv Bubanale and M Shivashankar, “History, Method of Production, Structure and Applications of Activated Carbon,” *Int. J. Eng. Res.*, vol. V6, no. 06, 2017, doi: 10.17577/ijertv6is060277.

[85] T. Gupta, “Carbon: The black, the gray and the transparent,” *Carbon Black, Gray Transparent*, pp. 1–319, 2017, doi: 10.1007/978-3-319-66405-7.

[86] A. Swiatkowski, “Adsorption and its Applications in Industry and Environmental Protection Studies in,” *Surf. Sci. Catal.*, vol. 120, pp. 69–94, 1998.

[87] D. Jr, “Activated Carbon-Lect 11,” 1989.

[88] U. S. Army Corps of Engineers, “Chapter 2. principles of operation and theory,” *Eng. Des. Adsorpt. Des. Guid.*, no. Design Guide No. 1110-1-2, p. 99, 2001.

[89] WQA, “Granular Activated Carbon (GAC) Fact Sheet,” 2013.

[90] Z. K. Chowdhury, R. S. Summers, G. P. Westerhoff, B. J. Leto, K. O. Nowack, and C. J. Corwin, *Activated Carbon*, vol. 3, no. 8. 1955. doi: 10.1021/jf60054a617.

[91] Pureflow, “Activated Carbon.” [Online]. Available: https://pureflowinc.com/activated-carbon/

[92] N. Byamba-Ochir, B. Buyankhishig, N. Byambasuren, and E. Surenjav, “Characterization of silver loaded activated carbon prepared under supercritical water condition,” *Solid State Phenom.*, vol. 288, no. March, pp. 59–64, 2019, doi: 10.4028/www.scientific.net/SSP.288.59.

[93] I. Isik-Gulsac, “Investigation of impregnated activated carbon properties used in

hydrogen sulfide fine removal," *Brazilian J. Chem. Eng.*, vol. 33, no. 4, pp. 1021–1030, 2016, doi: 10.1590/0104-6632.20160334s20150164.

[94] M. Ates and A. S. Sarac, "Conducting polymer coated carbon surfaces and biosensor applications," *Prog. Org. Coatings*, vol. 66, no. 4, pp. 337–358, 2009, doi: 10.1016/j.porgcoat.2009.08.014.

[95] C. Donau, "Activated Carbon and its Applications," *Donau Carbon*, vol. 4, no. 4, pp. 81–94, 2010, [Online]. Available: https://www.donau-carbon.com/getattachment/76f78828-2139-496f-9b80-6b6b9bdc6acc/aktivkohle.aspx%0Ahttps://pdfs.semanticscholar.org/4d8c/b2cbc834c17949fd5e24ffb46d864cd84a15.pdf%0Ahttps://mospace.umsystem.edu/xmlui/bitstream/handle/10355/8078/research.pdf?

[96] E. Sangotayo, E. Olukunle, A. Kasali, and L. Oluwatosin, "Characterization of Activated Carbons Produced from Some Agricultural Residues Available online www.jsaer.com Journal of Scientific and Engineering Research , 2017 , 4 (6): 132-140 Characterization of Activated Carbons Produced from Some Agricultural Re," no. January, 2017.

[97] P. Sreenivasa, S. Asridh, P. Sreejith, B. Firoz, A. Akash, and P. P. Deepak, "Design and Fabrication of Activated Carbon Manufacturing Machine and Experimental Investigation of Saw Dust Activated Carbon," 2018.

[98] R. H. Gumus and I. Okpeku, "Production of Activated Carbon and Characterization from Snail Shell Waste (<i>Helix</i> <i>pomatia</i>)," *Adv. Chem. Eng. Sci.*, vol. 05, no. 01, pp. 51–61, 2015, doi: 10.4236/aces.2015.51006.

[99] S. V. Mikhalovsky and V. G. Nikolaev, "Chapter 11 Activated carbons as medical adsorbents," *Interface Sci. Technol.*, vol. 7, no. C, pp. 529–561, 2006, doi: 10.1016/S1573-4285(06)80020-7.

[100] M. A. Al Jumaan, "The Role of Activated Charcoal in Prehospital Care," *Med. Arch. (Sarajevo, Bosnia Herzegovina)*, vol. 77, no. 1, pp. 64–69, 2023, doi: 10.5455/medarh.2023.77.64-69.

[101] M. W. Shannon, "A General Approach to Poisoning," *Haddad Winchester's Clin. Manag. Poisoning Drug Overdose*, no. January, pp. 13–61, 2020.

[102] R. Derlet and T. E. Albertson, "Cl iniclt Review," no. May, 2014.

[103] M. D. Adams, "Influence of the Surface Chemistry and Structure of Activated Carbon on the Adsorption of Aurocyanide," *XVIII Int. Miner. Process. Congr.*, no. May 1993, pp. 1175–1188, 1993.

[104] J. Rogans, "Activated Carbon in Gold Recovery," *Kemix Ltd*, no. June, pp. 1–34, 2012.

[105] H. McLaughlin, "Understanding activated carbon reactivation and low-temperature regeneration technology," *Int. Sugar J.*, vol. 107, no. 1274, pp. 112–127, 2005.

[106] NOBEL, "ACTIVATED CARBON FILTERS." [Online]. Available: https://www.nobel.srl/en/technical-information/activated-carbon-filters/

[107] M. Atabaki, "Performance of activated carbon in water filters," no. January 2013, 2014.

[108] P. R. dos Santos and L. A. Daniel, “A review: organic matter and ammonia removal by biological activated carbon filtration for water and wastewater treatment,” *Int. J. Environ. Sci. Technol.*, vol. 17, no. 1, pp. 591–606, 2020, doi: 10.1007/s13762-019-02567-1.

[109] B. Zieliński, P. Miądlicki, and J. Przepiórski, “Development of activated carbon for removal of pesticides from water: case study,” *Sci. Rep.*, vol. 12, no. 1, pp. 1–14, 2022, doi: 10.1038/s41598-022-25247-6.

[110] E. Lember, K. Pachel, and E. Loigu, “Removal of heavy metals and total organic carbon from wastewater using powdered activated carbon,” *Proc. Est. Acad. Sci.*, vol. 68, no. 1, pp. 100–110, 2019, doi: 10.3176/proc.2019.1.10.

[111] І. Наумко, О. Пономаренко, Г. Занкович, В. Мороз, and Л. Проскурко, “Ізотопний склад карбону й оксигену кальциту прожилково-вкрапленої мінералізації породних комплексів північно-західної частини Кросненської зони Українських Карпат,” *Доповіді Нан України*, vol. 4, pp. 591–593, 2015.

[112] D. B. and F. D. Michael Kamrin, Nancy Hayden,Barry Christian, “Home Water Treatment Using Activated Carbon.” Purdue University. [Online]. Available: https://www.extension.purdue.edu/extmedia/WQ/WQ-13.html

[113] L. Piai, S. Mei, K. van Gijn, and A. Langenhoff, “Effects of organic matter in drinking water and wastewater on micropollutant adsorption to activated carbon,” *Int. J. Environ. Sci. Technol.*, vol. 21, no. 3, pp. 2547–2558, 2024, doi: 10.1007/s13762-023-05132-z.

[114] I. K. Tetteh, I. Issahaku, and A. Y. Tetteh, “Recent advances in synthesis, characterization, and environmental applications of activated carbons and other carbon derivatives,” *Carbon Trends*, vol. 14, no. February, p. 100328, 2024, doi: 10.1016/j.cartre.2024.100328.

[115] B. Sun and M. Sain, “Super activated renewable carbon (SARC) for elimination of gas-phase volatile organic compounds (VOCs) from low-carbon composites (LCCs),” *Ind. Crops Prod.*, vol. 211, no. February, p. 118173, 2024, doi: 10.1016/j.indcrop.2024.118173.

[116] A. U. Guinea *et al.*, “Adsorption and desorption processes of trihalomethanes on different granulated activated carbons in a full-scale advanced water treatment plant,” *Water Supply*, vol. 24, no. 1, pp. 1–10, 2024, doi: 10.2166/ws.2023.324.

[117] O. J. I. Kramer *et al.*, “Fluidisation characteristics of granular activated carbon in drinking water treatment applications,” *Adv. Powder Technol.*, vol. 32, no. 9, pp. 3174–3188, 2021, doi: 10.1016/j.apt.2021.06.017.

[118] P. Xia *et al.*, “Complex odor control based on ozonation/GAC advanced treatment: optimization and application in one full-scale water treatment plant,” *Environ. Sci. Eur.*, vol. 32, no. 1, 2020, doi: 10.1186/s12302-020-00313-w.

[119] H. K. Holden, “Activated Carbon Filter.” pp. 55–387, 1971. [Online]. Available: http://www.google.com/patents?hl=en&lr=&vid=USPAT3611678&id=3U4BAAAAEBAJ&oi=fnd&dq=activated+carbon+filter&printsec=abstract#v=onepage&q&f=false

[120] HUATAN, “Carbon Block Vs. Granular Activated Carbon: Which Is Better?” [Online]. Available: https://watfilter.com/carbon-block-vs-granular-activated-carbon/

[121] Y. Braslavska, V. Ponomarov, T. Mitchenko, Z. Maletskyi, and I. Kosogina, "Production Technology and Filtering Properties of Carbon Block Cartridges," *Water Water Purif. Technol. Sci. Tech. News*, vol. 33, no. 2, pp. 32–42, 2022, doi: 10.20535/2218-930022022255835.

[122] "carbon_block_5." [Online]. Available: https://www.octomarine.com/wp-content/uploads/2021/11/carbon_block_5.png

[123] J. Byrd, "What Is Catalytic Carbon Media in Water Treatment?," WaterFilterGuru.com. [Online]. Available: https://waterfilterguru.com/

[124] Homewater.com, "What Are the Benefits of Catalytic Carbon Filters?" [Online]. Available: https://www.homewater.com/blog/what-are-the-benefits-of-catalytic-carbon-filters

[125] "catalytic_carbon_single." [Online]. Available: https://www.chansonalkalinewater.com/cart/pub/media/catalog/product/cache/7e4740f09b8a445fa38973e9399a4a6f/c/a/catalytic_carbon_single.png

[126] WaterProfessionals, "Activated Carbon Filters." [Online]. Available: https://www.waterprofessionals.com/learning-center/activated-carbon-filters/y

[127] L. Sbardella, J. Comas, A. Fenu, I. Rodriguez-Roda, and M. Weemaes, "Advanced biological activated carbon filter for removing pharmaceutically active compounds from treated wastewater," *Sci. Total Environ.*, vol. 636, pp. 519–529, 2018, doi: 10.1016/j.scitotenv.2018.04.214.

[128] J. Byrd, "What are Volatile Organic Compounds (VOCs) in Water?," WaterFilterGuru.com. [Online]. Available: https://waterfilterguru.com/what-are-vocs-in-water/

[129] D. J. Smith, P. Pettit, and T. Schofield, "Activated carbon in water treatment," *Water Supply*, vol. 14, no. 2, pp. 85–98, 1996.

[130] Liza Corsillo, "The Best Water Filter Pitchers, According to Experts," The Strategist. [Online]. Available: https://nymag.com/strategist/article/best-water-filter-pitchers.html

[131] NSF, "Filtration Media Certification." [Online]. Available: https://www.nsf.org/water-systems/treatment-chemicals-media/filtration-media

[132] M. M. -, "Activated Carbon as an Adsorbent: A Review," *Int. J. Multidiscip. Res.*, vol. 5, no. 4, pp. 1–7, 2023, doi: 10.36948/ijfmr.2023.v05i04.5478.

[133] M. Molina-Sabio and F. Rodríguez-Reinoso, "Role of chemical activation in the development of carbon porosity," *Colloids Surfaces A Physicochem. Eng. Asp.*, vol. 241, no. 1–3, pp. 15–25, 2004, doi: 10.1016/j.colsurfa.2004.04.007.

[134] Y. Gao, Q. Yue, B. Gao, and A. Li, "Insight into activated carbon from different kinds of chemical activating agents: A review," *Sci. Total Environ.*, vol. 746, p. 141094, 2020, doi: 10.1016/j.scitotenv.2020.141094.

[135] C. Bouchelta, M. S. Medjram, O. Bertrand, and J. P. Bellat, "Preparation and characterization of activated carbon from date stones by physical activation with steam," *J. Anal. Appl. Pyrolysis*, vol. 82, no. 1, pp. 70–77, 2008, doi: 10.1016/j.jaap.2007.12.009.

[136] B. Sajjadi, W. Y. Chen, and N. O. Egiebor, “A comprehensive review on physical activation of biochar for energy and environmental applications,” *Rev. Chem. Eng.*, vol. 35, no. 6, pp. 735–776, 2019, doi: 10.1515/revce-2017-0113.

[137] J. Zhou, A. Luo, and Y. Zhao, “Preparation and characterisation of activated carbon from waste tea by physical activation using steam,” *J. Air Waste Manag. Assoc.*, vol. 68, no. 12, pp. 1269–1277, 2018, doi: 10.1080/10962247.2018.1460282.

[138] P. Nowicki, J. Kazmierczak, and R. Pietrzak, “Comparison of physicochemical and sorption properties of activated carbons prepared by physical and chemical activation of cherry stones,” *Powder Technol.*, vol. 269, pp. 312–319, 2015, doi: 10.1016/j.powtec.2014.09.023.

[139] L.-M. A. du Petit-Thouars, “Cycas thouarsii.” [Online]. Available: https://en.wikipedia.org/wiki/Cycas_thouarsii

[140] K. Hill, “Cycas thouarsii.” Royal Botanic Gardens Sydney, 1998.

[141] I. Walker, “Ntsambu, the foul smell of home: Food, commensality and identity in the comoros and in the diaspora1,” *Food Foodways*, vol. 20, no. 3–4, pp. 187–210, 2012, doi: 10.1080/07409710.2012.715962.

[142] F. De Sciences and B. P. Moroni, “Cycas (Cycadacea),” vol. 10, no. 2, pp. 394–408, 2014.

[143] S. M. Yakout and G. Sharaf El-Deen, “Characterization of activated carbon prepared by phosphoric acid activation of olive stones,” *Arab. J. Chem.*, vol. 9, pp. S1155–S1162, 2016, doi: 10.1016/j.arabjc.2011.12.002.

[144] J. Fito *et al.*, “Adsorption of methylene blue from textile industrial wastewater using activated carbon developed from Rumex abyssinicus plant,” *Sci. Rep.*, vol. 13, no. 1, pp. 1–17, 2023, doi: 10.1038/s41598-023-32341-w.

[145] R. Ganjoo, S. Sharma, A. Kumar, and M. M. A. Daouda, “Activated Carbon: Fundamentals, Classification, and Properties,” *Act. Carbon*, pp. 1–22, 2023, doi: 10.1039/bk9781839169861-00001.

[146] Z. Heidarinejad, M. H. Dehghani, M. Heidari, G. Javedan, I. Ali, and M. Sillanpää, “Methods for preparation and activation of activated carbon: a review,” *Environ. Chem. Lett.*, vol. 18, no. 2, pp. 393–415, 2020, doi: 10.1007/s10311-019-00955-0.

[147] R. Benard, K. Lemaro, and F. Angelo, “PREPARATION AND CHARACTERISATION OF ACTIVATED CARBON FROM LOCALLY AVAILABLE MATERIALS, VIZ. COCONUT SHELLS,” University of Nairobi, 2012.

[148] M. Muniyandi, P. Govindaraj, and G. Bharath Balji, “Potential removal of Methylene Blue dye from synthetic textile effluent using activated carbon derived from Palmyra (Palm) shell,” *Mater. Today Proc.*, vol. 47, no. xxxx, pp. 299–311, 2021, doi: 10.1016/j.matpr.2021.04.468.

[149] O. Togibasa, M. Mumfaijah, Y. K. Allo, K. Dahlan, and Y. O. Ansanay, “The effect of chemical activating agent on the properties of activated carbon from sago waste,” *Appl. Sci.*, vol. 11, no. 24, 2021, doi: 10.3390/app112411640.

[150] Z. G. Xie, F. Y. Ji, X. M. Qiu, and H. Huang, “Preparation and characterization of

mesoporous activated carbon from orange peel," *Gongneng Cailiao/Journal Funct. Mater.*, vol. 40, no. 4, pp. 645–649, 2009.

[151] H. Chemingui *et al.*, "Investigation of methylene blue adsorption from aqueous solution onto ZnO nanoparticles: equilibrium and Box-Behnken optimisation design," *Int. J. Environ. Anal. Chem.*, vol. 103, no. 12, pp. 2716–2741, 2023, doi: 10.1080/03067319.2021.1897121.

[152] G. F. Bitencourt *et al.*, "Acidic and Basic Functionalized Biochar from Licuri Nutshell for Methylene Blue Removal: A More Sustainable Solution for Wastewater Treatment," *J. Braz. Chem. Soc.*, vol. 35, no. 5, pp. 1–16, 2024, doi: 10.21577/0103-5053.20230182.

[153] S. Manna, D. Roy, P. Saha, D. Gopakumar, and S. Thomas, "Rapid methylene blue adsorption using modified lignocellulosic materials," *Process Saf. Environ. Prot.*, vol. 107, pp. 346–356, 2017, doi: 10.1016/j.psep.2017.03.008.

[154] M. Z. Alam, M. N. Bari, and S. Kawsari, "Statistical optimization of Methylene Blue dye removal from a synthetic textile wastewater using indigenous adsorbents," *Environ. Sustain. Indic.*, vol. 14, no. September 2021, p. 100176, 2022, doi: 10.1016/j.indic.2022.100176.

[155] M. Faical, R. Atmani, M. Talbi, and N. Amardo, "Adsorption of methylene blue in solution on activated carbon based of banana peels residue Projet volubilis View project Phosphate fertilizer View project," *Artic. Int. J. Sci. Eng. Res.*, no. November, 2018, [Online]. Available: https://www.researchgate.net/publication/328783332

[156] S. I. Al-Saeedi *et al.*, "Isotherm and kinetic studies for the adsorption of methylene blue onto a novel Mn3O4-Bi2O3 composite and their antifungal performance," *Front. Environ. Sci.*, vol. 11, no. May, pp. 1–16, 2023, doi: 10.3389/fenvs.2023.1156475.

[157] Y. Kuang, X. Zhang, and S. Zhou, "Adsorption of methylene blue in water onto activated carbon by surfactant modification," *Water (Switzerland)*, vol. 12, no. 2, pp. 1–19, 2020, doi: 10.3390/w12020587.

[158] W. A. Hammad, M. A. Darweesh, N. Zouli, S. M. Osman, B. Eweida, and M. H. A. Amr, "Adsorption of cationic dye onto Raphanus seeds: optimization, adsorption kinetics, thermodynamic studies," *Sci. Rep.*, vol. 14, no. 1, pp. 1–19, 2024, doi: 10.1038/s41598-024-66761-z.

[159] S. Yorgun, N. Karakehya, and D. Yıldız, "Adsorption of methylene blue onto activated carbon obtained from ZnCl2 activation of paulownia wood: Kinetic and equilibrium studies," *Desalin. Water Treat.*, vol. 58, no. January, pp. 274–284, 2017, doi: 10.5004/dwt.2017.0172.

[160] M. Larakeb, M. R. Remmache, M. M. Snoussi, A. Ziar, and L. Hadjeris, "Experimental study of methylene blue adsorption from aqueous solutions onto natural Algerian goethite," *Water Pract. Technol.*, vol. 00, no. 0, pp. 1–20, 2024, doi: 10.2166/wpt.2024.191.